Phosphatidylinositol 3-phosphate binding properties and autoinhibition mechanism of Phafin2

Tuoxian Tang

Dissertation submitted to the faculty of the Virginia Polytechnic Institute and State University in partial fulfillment of the requirements for the degree of

Doctor of Philosophy
in
Biological Sciences

Daniel G. S. Capelluto, Chair
Rana Ashkar
Peter J. Kennelly
Florian Schubot

April 26, 2021
Blacksburg, VA

Keywords: Phafin2, phosphatidylinositol 3-phosphate, PH domain, FYVE domain, protein-lipid interactions

Phosphatidylinositol 3-phosphate binding properties and autoinhibition mechanism of Phafin2

Tuoxian Tang

Academic Abstract

Phafin2 is a member of the Phafin protein family. Phafins are modular with an N-terminal PH (Pleckstrin Homology) domain followed by a central FYVE (Fab1, YOTB, Vac1, and EEA1) domain. Both the Phafin2 PH and FYVE domains bind phosphatidylinositol 3-phosphate [PtdIns(3)P], a phosphoinositide mainly found in endosomal and lysosomal membranes. Phafin2 acts as a PtdIns(3)P effector for endosomal cargo trafficking, macropinocytosis, apoptosis, and autophagy. The PtdIns(3)P binding activity is critical to the localization of Phafin2 on a specific membrane and, subsequently, helps the recruitment of other binding partners to the same membrane surface. However, there are no studies on the structural basis of PtdIns(3)P binding, the PtdIns(3)P-binding properties of each domain, and the apparent redundancy of two PtdIns(3)P binding domains in Phafin proteins.

In the present dissertation, different biochemical and biophysical techniques were utilized to investigate the structural features of Phafin2 and its lipid interactions. This dissertation shows that Phafin2 is a moderately elongated monomer with a predicted α/β structure and ~40% random coil content. Phafin2 binds lipid bilayer-embedded PtdIns(3)P with high affinity; its PH and FYVE domains display distinct PtdIns(3)P-binding properties. Unlike the PH domain, the Phafin2 FYVE domain binds both membrane-embedded PtdIns(3)P and water-soluble dibutanoyl PtdIns(3)P with similar affinity. An intramolecular autoinhibition mechanism is found in Phafin2, in which a conserved C-terminal aspartic acid-rich (polyD) motif inhibits the binding of Phafin2 PH domain to PtdIns(3)P. The polyD motif specifically interacts with the Phafin2 PH domain. Using negative-stain Transmission Electron Microscopy, Phafin2 was found to cause membrane tubulation in a PtdIns(3)P-dependent manner. In conclusion, this study provides the structural and functional basis of Phafin2 lipid interactions and evidence of an intramolecular autoinhibition mechanism for PtdIns(3)P binding to the Phafin2 PH domain, which is mediated by the C-terminal polyD. The distinct PtdIns(3)P binding properties of the

Phafin2 PH and FYVE domains may indicate that these two domains have different functions. Considering that the Phafin2 PH domain's PtdIns(3)P binding is intramolecularly regulated, cells may employ a unique mechanism to release the Phafin2 PH domain from the conserved C-terminal motif and control the functions of Phafin2 in PtdIns(3)P- and PH domain-dependent signaling pathways.

Phosphatidylinositol 3-phosphate binding properties and autoinhibition mechanism of Phafin2

Tuoxian Tang

General Audience Abstract

Living cells need to absorb extracellular materials to sustain their growth and achieve cellular homeostasis. When cells require an uptake of liquids, they employ pinocytosis ("cell drinking"); when cells uptake solid particles, they use phagocytosis ("cell eating"); and when cells are in nutrient starvation status, they exploit an evolutionarily conserved process to survive known as autophagy ("self-eating"). Cells coordinate these activities through complex biochemical signaling systems. In each of these activities, a specific pathway is used to transfer the extracellular materials into the intracellular compartments and regulate the intracellular communications. Protein-lipid interactions are critical to these signaling pathways. This study focuses on the interactions between Phafin2 and phosphatidylinositol 3-phosphate [PtdIns(3)P]. Phafin2 is a cytoplasmic protein involved in autophagy, and PtdIns(3)P is a transient lipid signaling molecule localized to a specific organelle. After cells trigger autophagic events, Phafin2 protein molecules are associated with PtdIns(3)P. Subsequently, Phafin2 will recruit other protein binding partners. In this research project, biochemical and biophysical approaches were employed to study the structural features and PtdIns(3)P binding properties of Phafin2. Phafin2 was found to have two distinct PtdIns(3)P-binding domains; however, one of them is intramolecularly regulated. The results of this study help us to understand why Phafin2 displays two PtdIns(3)P-binding domains with different properties and how this is regulated, information that might be instrumental to understanding the roles of Phafin2 in physiological and disease scenarios.

Dedication

This dissertation is dedicated to my wife Jing and my daughter Bella.

Acknowledgements

I would like to thank my advisor, Dr. Daniel Capelluto, for his guidance and help in the last six years. I feel lucky to choose Daniel as my Ph.D. advisor. Without his support, I could not achieve this degree. Daniel did everything he could to help me grow from a graduate student to an independent researcher. I am very grateful for Daniel's guidance in conducting experiments, giving presentations, and writing proposals.

I would like to thank my current and former committee members: Drs. Peter Kennelly, Florian Schubot, Rana Ashkar, and Zhiyong Cheng. Their insightful comments and suggestions were essential to the progression of my research project. Their questions during the committee meetings prompted me to think more about the biological relevance of my research and helped me prepare better presentations.

I would like to thank my current and former lab members: Dr. Xiaolin Zhao, Dr. Wen Xiong, Dr. Wei Song, Tiffany Roach, Evan Littleton, Robert Wallace, Phillip Choi, and Andrew Biscardi. I also want to thank my friends and other colleagues at Virginia Tech: Xianlin Zou, Dr. Zhixiong Sun, Dr. Xiguang Xu, Dr. Jingren Deng, Dr. Meng Cai, and Dr. Sha Ding. I appreciate all the help you provided me in my lab work and daily life.

I would like to thank the Department of Biological Sciences, especially the Graduate Director, Dr. Jeff Walters, the Graduate Coordinator, Rebecca Zimmerman, and the Teaching Assistant Coordinator, Wooram Lee. I also want to thank the Graduate School of Virginia Tech. I am thankful that the Department of Biological Sciences and the Graduate School of Virginia Tech provided me scholarships and fellowships to support my graduate studies. Many thanks to the Graduate School Selection Committee, which awarded me the Joseph Frank Hunkler Memorial Scholarship. Special thanks to the Center of Soft Matter and Biological Physics, which provided funds to attend the Virginia Academy of Sciences meeting.

Finally, I would like to thank my wife, Jing Sun, for her unconditional love and support.

Table of Contents

Abbreviations

ATG	Autophagy-related
AUC	Analytical ultracentrifugation
CD	Circular dichroism
DFCP1	Double FYVE-containing protein 1
EAPF	Endoplasmic reticulum-associated apoptosis-involved protein containing PH and FYVE domains
EEA1	Early endosomal antigen 1
EGFR	Epidermal growth factor receptor
ER	Endoplasmic reticulum
FYVE	Fab 1, YOTB, Vac1, and EEA1
GFP	Green fluorescent protein
InsR	Insulin receptor
ITC	Isothermal titration calorimetry
LAPF	Lysosome-associated apoptosis-inducing protein containing PH and FYVE domains
LAMP-2A	Lysosome-associated membrane protein type 2A
LBA	Liposome binding assay
LPOA	Lipid-protein overlay assay
mTOR	Mechanistic target of rapamycin
mTORC2	Mechanistic target of rapamycin complex 2
NMR	Nuclear magnetic resonance
PCD	Programmed cell death
PDK1	Phosphoinositide-dependent protein kinase 1
PH	Pleckstrin homology
Phafin	PH domain and FYVE domain-containing proteins
PI	Phosphoinositide
PI3K	Phosphoinositide 3-kinase
PKB	Protein kinase B
PLEKHF2	Pleckstrin homology and FYVE domain containing 2
PtdIns(3)P	Phosphatidylinositol 3-phosphate
PtdIns(4)P	Phosphatidylinositol 4-phosphate

PtdIns(5)P	Phosphatidylinositol 5-phosphate
PtdIns(3,4)P_2	Phosphatidylinositol (3,4)-bisphosphate
PtdIns(3,5)P_2	Phosphatidylinositol (3,5)-bisphosphate
PtdIns(4,5)P_2	Phosphatidylinositol (4,5)-bisphosphate
PtdIns(3,4,5)P_3	Phosphatidylinositol (3,4,5)-trisphosphate
SPR	Surface plasmon resonance
TEM	Transmission electron microscopy
TF	Tryptophan fluorescence
TNF-α	Tumor necrosis factor-alpha
WIPI	WD repeat domain phosphoinositide-interacting

Chapter 1 Introduction

1. Phafin proteins

Phafin proteins are PH (Pleckstrin Homology) domain and FYVE (Fab 1, YOTB, Vac1, and EEA1) domain-containing proteins. The Phafin protein family has fourteen proteins from various species. Sequence alignment and phylogenetic analysis showed that this protein family could be divided into two subfamilies: Phafin1 and Phafin2. [1]

1.1 Phafin1

Phafin1, also known as LAPF (a lysosome-associated apoptosis-inducing protein containing PH and FYVE domains) and PLEKHF1 (pleckstrin homology and FYVE domain containing 1), is a 279 amino acid protein (the modular organization of human Phafin1 protein is shown in Figure 1). The genomic data show that the human *Phafin1* gene is located on chromosome 19q12 (https://www.ncbi.nlm.nih.gov/gene/79156). RNA-seq experiments performed on tissue samples from 95 human individuals representing 27 different tissues indicated that the *Phafin1* gene is ubiquitously expressed in fat, spleen, and, to a lesser extent, in 25 other tissues. [2]

Phafin1 is a cytosolic protein that contains two PtdIns(3)P-binding domains, an N-terminal PH domain and a central FYVE domain (Figure 1). Phafin1 is a pro-apoptotic protein. After translocating to lysosomes, Phafin1 induces caspase-independent apoptosis through the lysosomal-mitochondrial pathway. [1] Phafin1 acts as an adaptor protein by recruiting phosphorylated p53 to lysosomes, triggering apoptosis. [3] Phafin1 also plays a role in autophagy. The Phafin1 protein is targeted to lysosomes by Rab7-dependent signaling, inducing autophagosome formation. In HEK293T cells, co-transfection of hLC3A (microtubule-associated protein light chain 3, an autophagosome marker) and Phafin1 is sufficient to induce autophagy. [4-5]

1.2 Phafin2

Phafin2, also known as EAPF (an endoplasmic reticulum-associated apoptosis-involved protein containing PH and FYVE domains) and PLEKHF2 (pleckstrin homology and FYVE domain containing 2), [6] is a 249 amino acid protein (the modular organization of human

Phafin2 protein is shown in **Figure 1**). The human *Phafin2* gene is located on chromosome 8q22 (https://www.ncbi.nlm.nih.gov/gene/79666). The quantitative transcriptomics analysis showed that the human *Phafin2* gene has broad expression in bone marrow, lymph node, and other tissues. [2] The overall expression level of human Phafin2 is higher than Phafin1 in different tissues. Like Phafin1, Phafin2 is a cytosolic protein that contains the PtdIns(3)P-binding PH and FYVE domains (**Figure 1**) [7]. Previous studies showed that Phafin2 is involved in endosomal cargo trafficking, apoptosis, macropinocytosis, and autophagy. The functional roles of Phafin2 in cell signaling pathways are summarized below.

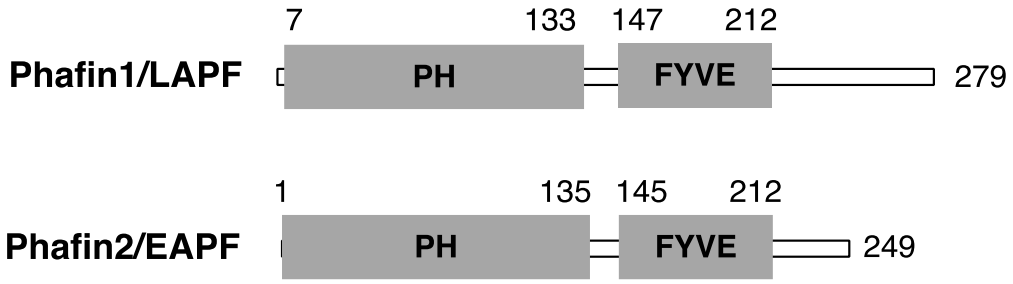

Figure 1. Modular organization of human Phafin1 and Phafin2.

2. The functional roles of Phafin2 in cell signaling pathways

2.1 Apoptosis

Apoptosis is a process of programmed cell death (PCD). The apoptotic pathway is characterized by various morphological changes, including cell shrinkage, chromatin condensation, plasma membrane blebbing, and apoptotic bodies. There are two main apoptotic pathways: the death receptor pathway ("extrinsic") and the mitochondrial pathway ("intrinsic"). [8-9] The tumor necrosis factor-alpha (TNF-α) can initiate the death receptor pathway directly and the mitochondrial pathway indirectly. Like Phafin1, Phafin2 is a pro-apoptotic protein. However, Phafin1 and Phafin2 use different pathways to facilitate cellular apoptosis. Phafin1 induces caspase-independent apoptosis via the lysosomal-mitochondrial pathway, whereas Phafin2 promotes TNF-α-induced cellular apoptosis through an endoplasmic reticulum-mitochondrial apoptotic pathway [6]. Overexpression of Phafin2 enhances cellular sensitivity to apoptosis induction and TNF-α-induced activity of caspase 3. Silencing of Phafin2 expression protects cells from TNF-α-mediated apoptosis induction. Both the Phafin2 PH and FYVE domains contribute to the translocation of Phafin2 to the endoplasmic reticulum. Two mutants of Phafin2, Phafin2ΔPH (deletion of the N-terminal PH

domain) and Phafin2ΔFYVE (deletion of the central FYVE domain), failed to colocalize with the endoplasmic reticulum (ER) after TNF-α treatment, suggesting that both domains are required for ER localization. Moreover, these two deletion mutants reduced the sensitivity of L929 cells to TNF-α-mediated apoptosis. [6]

2.2 Endosomal cargo trafficking

Cells in multicellular organisms communicate by means of a large number of extracellular signal molecules. The extracellular signal molecule usually binds to a receptor protein embedded in the plasma membrane of the target cell. Intracellular signaling pathways, which are comprised of intracellular signaling proteins, will process and distribute the signals to a specific target. There are three major types of cell-surface receptors: (a) ion-channel coupled receptors, (b) G-protein-coupled receptors, and (c) enzyme-coupled receptors. The epidermal growth factor receptor (EGFR) is an enzyme-coupled receptor. Activated, ligand-bound EGFR is internalized by endocytosis, which has been recognized as a cellular mechanism to terminate signaling through the degradation of activated receptor complexes, protecting the cells from excessive stimulation. [10-12] After internalization, EGFR molecules are ubiquitinated and incorporated into multivesicular endosomes. These intraluminal vesicles and receptor cargos are transported to lysosomes for degradation. [13]

Phafin2 mediates EGFR degradation by promoting endosome fusion, and it regulates the function of endosomes *via* association with other binding partners. [13] The yeast two-hybrid assay shows that it colocalizes strongly with the early endosomal antigen 1 (EEA1), an endosomal-tethering protein that mediates endosome fusion [13-14]. In Phafin2-depleted cells, degradation of EGFR is delayed, and the EGFR is accumulated in early endosomes. This suggests that Phafin2 regulates receptor trafficking through early endosomes by promoting endosome fusion. Besides its role in EGFR degradation, Phafin2 also modulates the density of insulin receptors (InsR) on the cell surface. [14] Overexpression of Phafin2 increases the amount of InsRs on plasma membranes but does not change the amount of EGFR. [14] The downregulation of Phafin2 expression by Phafin2 siRNA (small interference RNA) shows decreased InsRs on the cell surface. These results indicate that the upregulation of Phafin2 expression inhibits the internalization of InsR, resulting in the increased level of InsR at the plasma membrane. [13-14]

2.3 Macropinocytosis

Macropinocytosis is an actin-dependent endocytosis mechanism that cells use to ingest extracellular fluids and soluble macromolecules. These materials are internalized into large vesicles, called macropinosomes. [15-17] Under special conditions, macropinocytosis can facilitate the uptake of bacteria and viruses, causing their cell entry. Macropinocytosis has been receiving more attention because of its involvement in immune defense and removal of apoptotic bodies.

A recent study shows that Phafin2 is recruited to the newly formed macropinosomes through interactions between Phafin2 and PtdIns(3)P, which is transiently generated on these endocytic vesicles. On the vesicle surfaces, Phafin2 interacts with the actin cross-linking protein Filamin A, promoting the entry of macropinosomes through actin matrix and subsequent maturation. [18] Cellular Phafin2 depletion significantly reduces the number of macropinosomes. The same research group also reported that the motor binding protein JIP4 is recruited to the tubulating macropinosomes by Phafin2 in a PtdIns(3)P dependent manner. JIP4 is a coiled-coil protein that promotes the tubulation of macropinosomes. The Phafin2 PH domain, but not the FYVE domain, mediates the interaction between Phafin2 and JIP4. The depletion of Phafin2 or JIP4 and the disruption of PtdIns(3)P binding have a suppressive effect on tubulation. [19]

2.4 Autophagy

Autophagy is a cellular self-digestion mechanism by which damaged cytoplasmic components, including misfolded proteins and defective organelles, are sequestered in double-membrane vesicles, known as autophagosomes, and delivered to lysosomes for degradation. The metabolites produced by this degradation process can be recycled to build new cellular macromolecules and functional organelles. Autophagy is a highly conserved process occurring in eukaryotic cells. [20-23] Under normal growth conditions, autophagy is active at basal levels, maintaining cellular homeostasis. However, cellular stresses, such as nutrient starvation, growth factor deprivation, infection, and accumulation of misfolded proteins, may induce autophagy. The induced autophagic pathways can be selective (e.g.,

protein aggregates) or nonselective (sequestration of bulk cytoplasm), depending on the stimulus. [24-25]

Based on their different mechanisms and functions, there are three primary types of autophagy: microautophagy, macroautophagy, and chaperone-mediated autophagy. [26-27] In microautophagy, cytoplasmic components are directly engulfed into the lysosomes through invagination of the lysosomal membrane. In the case of macroautophagy (often referred to as autophagy; **Figure 2**), cargoes are sequestered by autophagosomes, and the fusion of autophagosomes with lysosomes results in the formation of autolysosomes. The lysosomal hydrolytic enzymes can digest the autolysosomal contents, and the resulting molecules are transported back to the cytosol through membrane permeases. The chaperone-mediated autophagy relies on the action of a cytosolic and lysosomal Hsc70 chaperone, which recognizes soluble cytosolic proteins carrying the pentapeptide KFERQ-like sequence [28]. The Hsc70 chaperone will associate with the integral membrane receptor LAMP-2A (lysosome-associated membrane protein type 2A), translocating the substrate proteins across the lysosomal membrane. [29] Autophagy plays a key role in cellular adaptation to changing environmental conditions, cellular remodeling during development and differentiation, and lifespan determination [30]. Autophagic dysfunction is associated with a plethora of human diseases, such as cancer [31-32], neurodegeneration [33], microbial infection [23], myopathies [34], and aging [35].

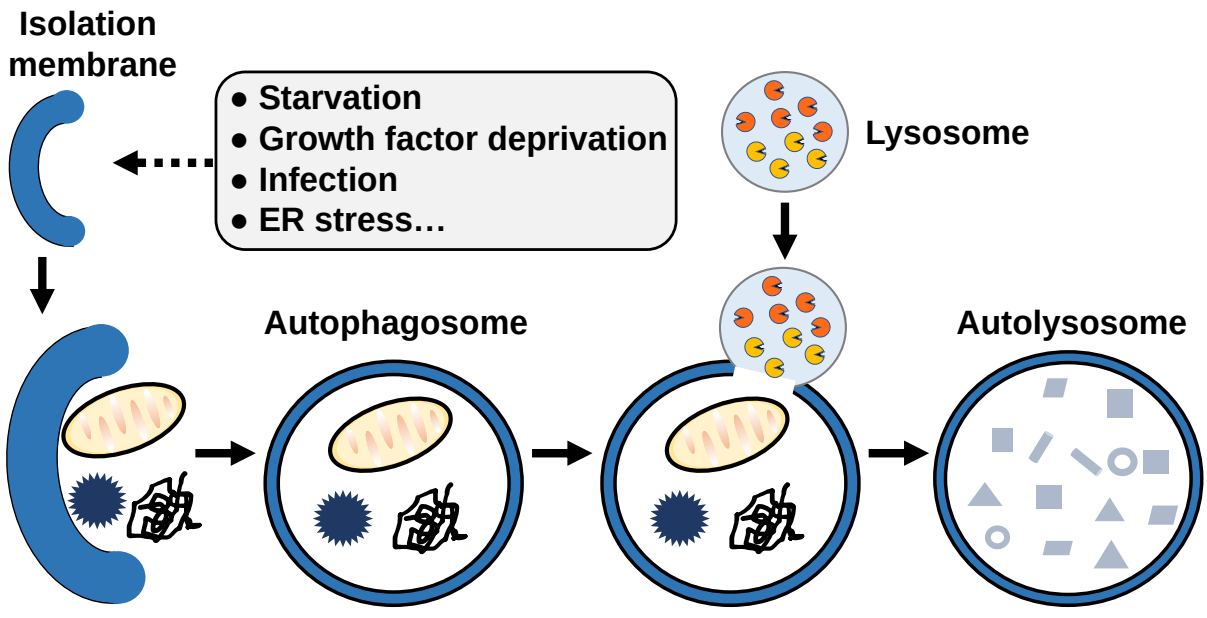

Figure 2. Schematic diagram of the autophagic pathway.

The molecular machinery of autophagy is conserved in yeasts and mammals. There are several distinct stages in the autophagic pathway: induction and vesicle nucleation (formation of isolation membrane), vesicle expansion, autophagosome-lysosome fusion (fusion of double-membraned autophagosomes with lysosomes to form autolysosomes), and autolysosomal degradation. [20] (**Figure 2**) A unique membrane structure, which is called isolation membrane or phagophore, emerges after autophagy induction. The isolation membrane expands and elongates to form the autophagosomes, double-membrane vesicles, which engulf cytosolic components. After maturation, autophagosomes fuse with lysosomes. The engulfed cargoes are degraded by the lysosomal hydrolases. [21-25] The knowledge on autophagy has been markedly expanded after identifying more than 20 different *ATG* (autophagy-related) genes from yeast genetic studies. These *ATG* genes encode evolutionarily conserved Atg proteins, which are essential to the autophagic machinery. For example, autophagosomal membrane expansion is mediated by two ubiquitin-like conjugation systems (Atg12 and Atg8). Many PtdIns(3)P binding proteins are involved in the autophagic process, such as DFCP1 (double FYVE-containing protein 1) and WIPI (WD repeat domain phosphoinositide-interacting) family proteins, which are critical to autophagosome formation. [23-25]

The ULK complex [Atg 1(ULK1/2), Atg 11, Atg 13, Atg 17, Atg 29, and Atg 31] is indispensable to the induction of autophagy. After autophagy induction, this complex translocates to the early autophagic machinery. [23] Previous studies showed that PtdIns(3)P is indispensable to autophagy induction, and that PI3K (Phosphoinositide 3-kinase) regulates autophagy. [39-40] PI3K is a lipid kinase that phosphorylates the 3'-OH group of the inositol ring of phosphoinositides. Mammalian cells have three main classes of PI3K. Class I PI3K catalyzes the conversion of phosphatidylinositol (4,5)-bisphosphate [PtdIns(4,5)P_2] into phosphatidylinositol (3,4,5)-trisphosphate [PtdIns(3,4,5)P_3]. Class II and Class III PI3Ks use phosphatidylinositol as their *in vivo* substrate and, thus, produce PtdIns(3)P. The Class III PI3K has a single species (hVps34) in humans and relatively high catalytic activity in cells. [41-44] 3-MA (3-methyladenine) is a specific inhibitor of class III PI3K, preventing autophagy from occurring. Thus, PtdIns(3)P production is required for the induction of autophagy. [7, 45-47]

The PtdIns(3)P-binding protein Phafin2 plays a role in the initiation of autophagy [7, 36]. As illustrated in **Figure 3**, lysosomal accumulation of Phafin2, in complex with the serine/threonine kinase Akt (also known as protein kinase B, PKB), constitutes a critical step

in the induction of autophagy. There are three highly conserved Akt isoforms in mammalian genomes: Akt1 (PKBα), Akt2 (PKBβ), and Akt3 (PKBγ). These Akt family members are involved in many cellular functions, including cell growth, cell survival, vesicular trafficking, transcriptional regulation, and cytoskeletal organization. [37-38] Akt1 and Akt2, but not Akt3, interacted with Phafin2 in 293T cells by co-immunoprecipitation assays. The PI3K-Akt-mTOR (mechanistic target of rapamycin) pathway has an essential role in the regulation of autophagy. [37-38] After the induction of autophagy using rapamycin, Phafin2 is localized on lysosomes *via* interactions with PtdIns(3)P. Phafin2 recruits Akt to the lysosomal membranes in a PtdIns(3)P-dependent manner [7].

It is proposed that Akt plays a dual role in the regulation of autophagy. Akt has an N-terminal PH domain, a kinase domain in the middle, and a C-terminal regulatory domain. Phosphorylation is critical for Akt activity. The Akt PH domain has an inhibitory effect on the Akt-kinase domain, and Akt is in the inactive "PH-in" conformation [38]. The "PH-in" conformation is relieved after the Akt PH domain associates with PtdIns(3,4,5)P_3, resulting in a "PH-out" conformation. The Akt-kinase domain is available for phosphorylation by PDK1 (phosphoinositide-dependent protein kinase 1). PDK1 phosphorylates Akt at T308, leading to a partially activated Akt. Akt also requires S473 phosphorylation by mTORC2 (mechanistic target of rapamycin complex 2) to achieve its maximal activation [38]. In response to growth factor stimulation, class I PI3K is activated and increases the PtdIns(3,4,5)P_3 levels at the plasma membrane. The Akt PH domain associates with PtdIns(3,4,5)P_3, translocating Akt to the plasma membrane. An established model is that PtdIns(3,4,5)P_3 binding causes conformational changes of Akt and allosterically activates Akt. Activated Akt can phosphorylate downstream substrates, leading to the inhibition of autophagy [37]. However, after autophagy induction, Phafin2 translocates Akt to lysosomes, promoting autophagy. Phafin2 binds Akt in a non-phosphorylation dependent manner; both the phosphorylated and non-phosphorylated Akt bind Phafin2. [7] In the canonical Akt activation model, PtdIns(3,4,5)P_3 restricts Akt activity to the plasma membrane. It remains unknown whether Phafin2 binds phosphorylated or non-phosphorylated Akt for the induction of autophagy.

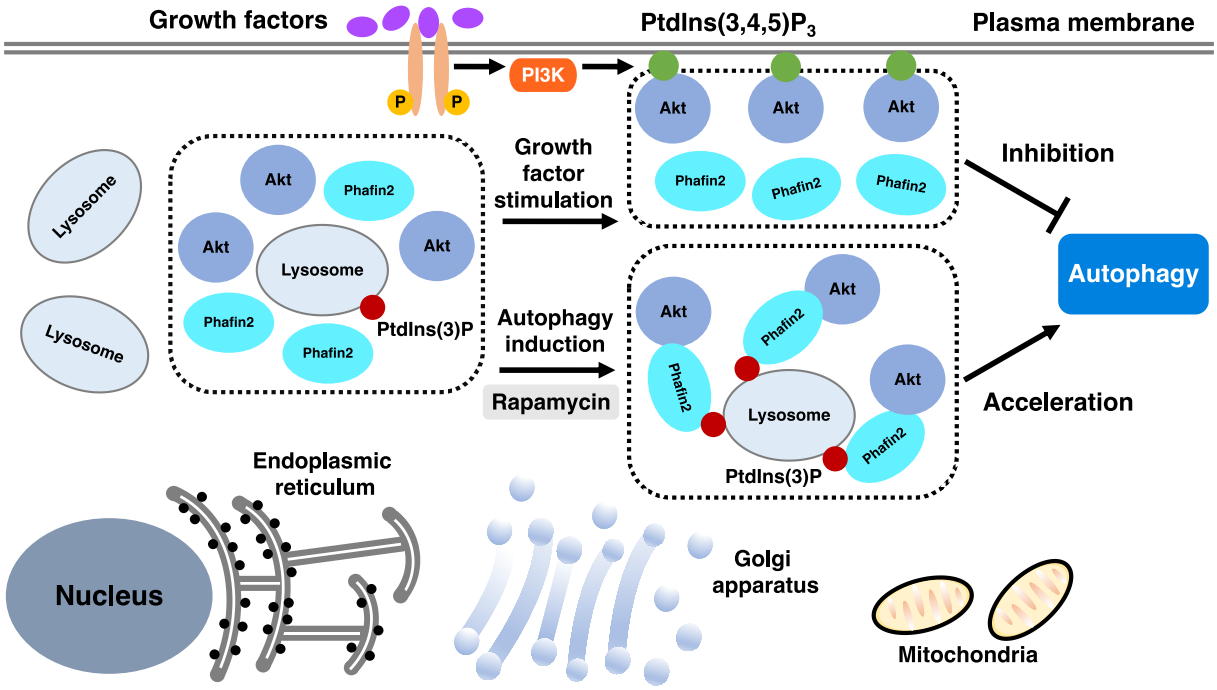

Figure 3. Spatial control of Akt determines the fate of autophagy.

In summary, Phafin2 has functions in endosomal cargo trafficking, apoptosis, macropinocytosis, and autophagy. Phafin2 is a PtdIns(3)P effector and acts as an adaptor protein in these signaling pathways, recruiting other binding partners to a specific organelle or membrane structures. There is some evidence showing that Phafin2 may be involved in human diseases. The *Phafin2* gene expression is upregulated in liver and breast cancer. [14, 48]

3. Phosphoinositides and their recognition domains

3.1 Seven phosphoinositides

Phosphoinositides (PI) are phosphorylated derivatives of phosphatidylinositol (PtdIns). The inositol headgroup of phosphatidylinositol can be phosphorylated at a single position or a combination of positions (3', 4', or 5'), producing seven different PIs: PtdIns(3)P, PtdIns(4)P, PtdIns(5)P, PtdIns(3,4)P_2, PtdIns(3,5)P_2, PtdIns(4,5)P_2, and PtdIns(3,4,5)P_3. [49-51] Although PIs represent a minor group of phospholipids (<10% of all phospholipids) and comprise approximately 1% of cellular lipids, they serve as key signaling molecules. PIs regulate multiple cellular functions, including membrane trafficking, signaling transduction, cell survival, and cytoskeletal dynamics. [52-54]

The amount and cellular distribution of each PI are spatially and temporally controlled by numerous kinases and phosphatases, which constitute a complicated regulatory network. PtdIns(4)P and PtdIns(4,5)P_2 are the largest pool of PIs [50]. They are constitutively present in cellular membranes, whereas PtdIns(3,4,5)P_3 is barely detectable in unstimulated cells [50]. Recent estimates showed that the amount of PtdIns(3,4,5)P_3 is about 2-5% of PtdIns(4,5)P_2 and the amount of PtdIns(3)P is about 20-30% of PtdIns(4)P. [50, 52] Different PI species show distinct cellular distributions, and some of them are viewed as hallmarks of various cellular membranes and compartments. PtdIns(4)P is enriched at the Golgi Apparatus membranes, whereas PtdIns(3)P is primarily found on early and late endosomes as well as lysosomes. [55-58]

3.2 Phosphoinositide recognition domains

Phosphoinositides serve as site-specific signals and docking sites on cellular membranes. Some cytosolic proteins are transiently recruited by these phospholipids to a specific membrane in a reversible and regulated manner. [59-65] Membrane recognition is mediated by PI binding domains, including ANTH (AP180 N-terminal homology) [66], BAR (Bin-Amphiphysin-Rvs) [67], C2 (conserved region-2 of protein kinase C) [68], ENTH (epsin N-terminal homology) [66], FYVE (Fab1, YOTB, Vac1, and EEA1), PH (Pleckstrin Homology), PROPPINs (β-propellers that bind PIs) [69], PTB (phosphotyrosine binding) [70], and PX (Phox homology) domains [71]. Different PI binding domains are diverse in specificity. Some of them specifically bind one type of PI, while others display broader specificity. For example, FYVE domains are specific for PtdIns(3)P, whereas PH domains often display broader specificities.

Although PI-binding domains display distinct structures and affinities, their lipid-binding mechanisms share many similarities. In most cases, binding is achieved by nonspecific electrostatic interactions involving the negatively charged PI headgroups and patches of positive charges within the target protein. Nearly all PI-binding domains have highly basic binding sites comprised of some positively charged residues. Furthermore, association of PI-binding proteins with PI-containing membranes involves multiple interactions. In addition to the electrostatic interactions, hydrophobic amino acid residues located in close proximity to the basic patch contribute to lipid ligation. Membrane anchoring is also augmented by

hydrophobic insertion, protonation of a histidine switch, and by coincidence detection. [58, 72-74]

3.2.1 PH domains

The PH domain was initially identified as a region of sequence homology duplicated in pleckstrin [50]. PH domains are small protein modules of 100-120 amino acids found in a wide range of proteins. [75] The amino acid sequence homology among different PH domains is only 7-30%, but they show similar three-dimensional structures. PH domain are characterized by the presence of seven β-strands forming two nearly orthogonal antiparallel β-sheets, which are capped at one end by a C-terminal α-helix. A positive binding pocket in the PH domain interacts with the negative head group of the phospholipids, and nonspecific electrostatic interactions are the major driving forces for binding. [76-80]

Most PH domains bind PIs, facilitating the recruitment of PH domain-containing proteins to specific cellular membranes, while some PH domains mediate protein-protein interactions. [81-82] It is estimated that about 15% of PH domains bind PIs with high affinity but dissociation constants range between 30 nM to 30 μM (Table 1). The specificity of PH domain varies widely. [83-85] For example, the PH domains of Pleckstrin and PLCδ_1 bind PtdIns(4,5)P_2, whereas the Btk and Grp1 PH domains have specificity for PtdIns(3,4,5)P_3 (Table 1). The PH domain of Akt/PKB binds both PtdIns(3,4)P_2 and PtdIns(3,4,5)P_3. Moreover, PH domains also bind PtdIns(3)P, PtdIns(4)P, PtdIns(5)P, and PtdIns(3,5)P_2 (Table 1).

Protein	Ligand	K_D (μM)	Method	References
Pleckstrin	PtdIns(4,5)P_2	30	NMR	[86]
PLC-δ_1	PtdIns(4,5)P_2	1.7	ITC	[87]
FAPP	PtdIns(4)P	41	NMR	[88]
CRET	PtdIns(4)P	3.2	SPR	[89]
PKB/AKT	PtdIns(3,4,5)P_3	0.4	TF	[90-91]
Btk	PtdIns(3,4,5)P_3	0.08	SPR	[92]
Grp1	PtdIns(3,4,5)P_3	0.03	SPR	[93]
CARMIL	PtdIns(5)P	12	LBA	[94]
Grp1	IP4	0.03	ITC	[95]
Kindlin-2	IP4	2.1	SPR	[96]
TAPP1	PtdIns(3,4)P_2	0.08	SPR	[92]
ORP5	PtdIns(3,5)P_2	26	ITC	[97]
Phafin2	PtdIns(3)P	11	LBA	[98]
AtPH1	PtdIns(3)P	N.D.	LPOA	[99]
TECPR1	PtdIns(3)P	N.D.	LPOA	[100]

Table 1. PI binding specificity and affinity of representative PH domains. The listed PH domains show different PI binding specificities and a range of binding affinities. Abbreviations: PLC-δ_1, phospholipase C-δ_1; FAPP, four-phosphate-adaptor protein; CRET, ceramide trafficking protein; PKB, Protein Kinase B; Btk, Bruton's tyrosine kinase; Grp1, General receptor for phosphoinositides isoform 1; CARMIL, CP Arp2/3 complex myosin-I linker; IP4, inositol 1,3,4,5-tetraphosphate; TAPP1, tandem-PH domain-containing protein-1; ORP5, a member of oxysterol-binding protein (OSBP)-related proteins; AtPH1, the

At2g29700 gene encoding a PH domain-containing protein; TECPR1, Tectonin β-propeller repeat-containing protein 1; N.D., not determined. NMR, Nuclear Magnetic Resonance; ITC, Isothermal Titration Calorimetry; SPR, Surface Plasmon Resonance; TF, Tryptophan Fluorescence; LBA, Liposome Binding Assay (also known as liposome co-sedimentation assay); LPOA, Lipid-Protein Overlay Assay.

The high affinity and specificity of some PH domains make them suitable probes for detecting a specific PI *in vivo*. Fusion proteins comprising green fluorescent protein (GFP) and PH domain have become useful and efficient tools to study the distribution of PIs in living cells. For example, the PH domain of PKB/AKT is a sensitive and selective biosensor for detecting PtdIns(3,4)P_2 and PtdIns(3,4,5)P_3. Cellular PtdIns(4,5)P_2 can be easily detected by the PH domain of PLC-δ_1. [101-102]

3.2.2. FYVE domains

The FYVE domain was named after the first letter of the four proteins (Fab1, YOTB, Vac1, and EEA1), in which it was first identified. FYVE domains are small (70-80 amino acids) cysteine-rich protein modules and highly conserved from yeast to human. FYVE domain-containing proteins are recruited to the PtdIns(3)P-enriched endocytic membranes through the specific interactions of their FYVE domains with PtdIns(3)P. [50, 103-106]

Three-dimensional structures of FYVE domains reveal a common protein fold. They display two double-stranded β-sheets, with each β-sheet formed by two antiparallel β-strands. Additionally, the structure contains a small C-terminal α-helix that carries one of the zinc-coordinating cysteines. There are three conserved PtdIns(3)P-binding motifs in FYVE domains: an N-terminal WxxD (in single-letter amino acid code; x, any amino acid) motif, a central (R/K)(R/K)HHCR motif, and a C-terminal RVC motif. [107-109] Certain FYVE domains bind PtdIns(3)P in a pH-dependent manner. An acidic pH (~6.0) favors PtdIns(3)P binding, whereas increasing the pH weakens PtdIns(3)P binding and membrane insertion. Two adjacent histidine residues in the (R/K)(R/K)HHCR signature motif modulate its pH dependency. [110-111]

The FYVE domain is a zinc-finger module; it contains eight cysteine residues (four CxxC motifs) that coordinate two Zn^{2+} ions. Tetrahedral coordination of the two Zn^{2+} ions by four CxxC motifs is critical to the structural stability and biological activity of the FYVE domains. Mutations in any of these zinc-coordinating residues are sufficient to cause structural loss and abolish PtdIns(3)P binding. Furthermore, some FYVE domains promote protein dimerization [103]. Structures of the *Drosophila* Hrs FYVE and the *S.cerevisiae* Vps 27p FYVE domains were determined by X-ray crystallography. The Hrs FYVE domain was crystallized in the presence of citrate (a substrate substitute), whereas the structure of the Vps 27p FYVE domain was solved in a ligand-free state. [104] These two FYVE domains showed a similar structure comprised of two double-stranded β-sheets and a C-terminal α-helix. According to the proposed models, two Hrs FYVE domains formed a homodimer, but the Vps 27p FYVE domain showed a monomeric structure. The crystal structure of the human EEA1 FYVE domain bound to inositol 1,3-bisphosphate also revealed that EEA1 FYVE domains form homodimers. [112-114]

PtdIns(3)P plays a pivotal role in endosome fusion, recycling, sorting, and conversion of early endosomes to late endosomes. FYVE domains show high specificity and affinity for PtdIns(3)P binding. The double FYVE finger (2×FYVE) is widely used to study the distribution and level of PtdIns(3)P in cells. [115-117]

4. Research aims

Previous studies showed that Phafin2 plays a role in endosomal trafficking [13, 14], macropinocytosis [18], apoptosis [6], and autophagy [7]. Phafin2 is a PtdIns(3)P effector in all these signaling pathways. Translocation of Phafin2 to a specific cellular membrane is mediated by its interactions of its PH and FYVE domains with PtdIns(3)P. This research project focuses on elucidating the structural features and PtdIns(3)P-binding properties of Phafin2. The overall goal was to understand why Phafin2 has two redundant PtdIns(3)P-binding domains and their possible functions. Various biophysical and biochemical methods were utilized to address specific questions and achieve research aims.

The structural features and PtdIns(3)P-binding properties of Phafin2 were unknown. The first research aim was to determine the structural organization and PtdIns(3)P-binding properties of Phafin2 given that it harbors two PtdIns(3)P-binding domains. The human Phafin2 cDNA was

cloned into a pGEX4T3 vector and expressed as a recombinant protein in *E.coli*. GST-tagged and untagged Phafin2 proteins were purified by affinity chromatography and size exclusion chromatography. Circular Dichroism (CD) spectropolarimetry and two-dimensional NMR (^{1}H-^{15}N HSQC, heteronuclear single quantum coherence) were used to collect structural information. Far-UV CD at 222 nm was employed to monitor the thermal stability of Phafin2 and estimate its melting temperature (T_M), the temperature at which half of the protein was unfolded. The hydrodynamic properties of Phafin2 were analyzed by size-exclusion chromatography and velocity sedimentation analytical ultracentrifugation (AUC). Surface Plasmon Resonance (SPR) was used to determine its PtdIns(3)P binding affinity. To identify which amino acid residues in Phafin2 were responsible for PtdIns(3)P binding, we performed structure modeling of Phafin2 based on its sequence homology and structural similarity with other proteins. The putative binding sites were utilized to design PtdIns(3)P-interaction defective mutants.

In chapter 2, we reported that Phafin2 was an elongated monomer. The T_M for Phafin2 was 48.4 °C. It preferentially bound PtdIns(3)P, and the binding affinity measured by SPR was 0.3 μM. Our structural analysis showed that Phafin2 was an α/β protein and displayed ~40% random coil in its secondary structural contents. PtdIns(3)P caused local conformational changes in Phafin2. Conserved PtdIns(3)P-binding pockets were predicted in the Phafin2 PH and FYVE domains.

To establish why Phafin2 bears two redundant PtdIns(3)P-binding domains, the second aim was to investigate PtdIns(3)P-binding properties of the Phafin2 FYVE domain and the Phafin2 PH domain. Different lipid-binding assays were utilized. Firstly, SPR experiments were used to measure the PtdIns(3)P binding affinity of Phafin2 PH domain and FYVE domain. Secondly, we prepared many PtdIns(3)P-interaction defective mutants: a single mutation in the Phafin2 PH domain (Phafin2 R53C), a double mutation in the Phafin2 FYVE domain (Phafin2 R172A/R173A), and a triple mutation in both domains (Phafin2 R53C/R172A/R173A). Liposome co-sedimentation assay and isothermal titration calorimetry (ITC) were used to study their PtdIns(3)P binding properties. Furthermore, we isolated the Phafin2 FYVE and PH domains, and their PtdIns(3)P-interaction defective mutants. The same set of lipid-protein binding assays was employed to study their PtdIns(3)P binding properties.

In chapter 3, we reported that, like the full-length wild-type Phafin2, Phafin2 FYVE bound the water-soluble and membrane-embedded PtdIns(3)P. However, the Phafin2 PH domain showed a different PtdIns(3)P binding property. It bound the membrane-embedded PtdIns(3)P, not the water-soluble PtdIns(3)P. An autoinhibition mechanism for PtdIns(3)P binding was found in Phafin2, by which a conserved C-terminal aspartic acid rich (polyD) motif in Phafin2 intramolecularly inhibited the Phafin2 PH domain binding to PtdIns(3)P. The PtdIns(3)P binding ability of the Phafin2 PH domain was recovered after removing the polyD motif in Phafin2.

The third aim was to determine whether the Phafin2 PH domain directly interacts with the polyD motif. A synthetic peptide was used to represent the Phafin2 polyD motif. Titration assays such as intrinsic tryptophan fluorescence and ITC were employed to study the interactions between the Phafin2 PH domain and the polyD peptide. To identify the PH domain residues that interact with the polyD peptide, the ^{15}N-labeled Phafin2 PH domain was titrated with the unlabeled polyD peptide, and ^{1}H-^{15}N HSQC spectra were collected for each peptide concentration.

Phafin2 plays a role in autophagy, endosome fusion, and tubulation of macropinosomes. All of these processes involve membrane remodeling. Therefore, we hypothesized that the Phafin2 protein causes membrane remodeling and, consequently, facilitates membrane fusion. To test this hypothesis, extruded liposomes were used to mimic cellular membranes. Phafin2 was incubated with PtdIns(3)P-free liposomes and PtdIns(3)P-containing liposomes. Transmission electron microscopy (TEM) was utilized to observe morphological changes of liposomes. To determine whether these morphological changes were PtdIns(3)P-dependent and which domain is responsible for membrane remodeling, PtdIns(3)P-interaction defective mutants of full-length Phafin2, Phafin2 FYVE and PH domains were subjected to the same approaches.

In chapter 4, we reported that the Phafin2 polyD motif specifically interacted with the Phafin2 PH domain. Phafin2 induced membrane tubulation in a PtdIns(3)P-dependent manner. Phafin2 PH domains triggered many short protrusions on the surface of PtdIns(3)P liposomes. In contrast, Phafin2 FYVE domains did not show tubulation activity.

The findings of this research project will help elucidate the structural basis for the interaction of Phafin2 with membrane PtdIns(3)P and understand why Phafin2 displays two PtdIns(3)P-

binding domains. More importantly, the resulting findings will reveal how the PtdIns(3)P binding activity is regulated. Future research will focus on how Phafin2 proteins utilize this regulatory mechanism to achieve their functions in different signaling pathways.

References

[1] Chen, W., N. Li, T. Chen, Y. Han, C. Li, Y. Wang, W. He, L. Zhang, T. Wan and X. Cao (2005). "The Lysosome-associated Apoptosis-inducing Protein Containing the Pleckstrin Homology (PH) and FYVE Domains (LAPF), Representative of a Novel Family of PH and FYVE Domain-containing Proteins, Induces Caspase-independent Apoptosis via the Lysosomal-Mitochondrial Pathway*." Journal of Biological Chemistry 280(49): 40985-40995.

[2] Fagerberg, L., B. M. Hallström, P. Oksvold, C. Kampf, D. Djureinovic, J. Odeberg, M. Habuka, S. Tahmasebpoor, A. Danielsson, K. Edlund, A. Asplund, E. Sjöstedt, E. Lundberg, C. A.-K. Szigyarto, M. Skogs, J. O. Takanen, H. Berling, H. Tegel, J. Mulder, P. Nilsson, J. M. Schwenk, C. Lindskog, F. Danielsson, A. Mardinoglu, Å. Sivertsson, K. von Feilitzen, M. Forsberg, M. Zwahlen, I. Olsson, S. Navani, M. Huss, J. Nielsen, F. Ponten and M. Uhlén (2014). "Analysis of the Human Tissue-specific Expression by Genome-wide Integration of Transcriptomics and Antibody-based Proteomics*." Molecular & Cellular Proteomics 13(2): 397-406.

[3] Li, N., Y. Zheng, W. Chen, C. Wang, X. Liu, W. He, H. Xu and X. Cao (2007). "Adaptor Protein LAPF Recruits Phosphorylated p53 to Lysosomes and Triggers Lysosomal Destabilization in Apoptosis." Cancer Research 67(23): 11176.

[4] Lin, W.-J., C.-Y. Yang, L.-L. Li, Y.-H. Yi, K.-W. Chen, Y.-C. Lin, C.-C. Liu and C.-H. Lin (2012). "Lysosomal targeting of phafin1 mediated by Rab7 induces autophagosome formation." Biochemical and Biophysical Research Communications 417(1): 35-42.

[5] Kim, A. and K. W. Cunningham (2015). "A LAPF/phafin1-like protein regulates TORC1 and lysosomal membrane permeabilization in response to endoplasmic reticulum membrane stress." Molecular Biology of the Cell 26(25): 4631-4645.

[6] Li, C., Q. Liu, N. Li, W. Chen, L. Wang, Y. Wang, Y. Yu and X. Cao (2008). "EAPF/Phafin-2, a novel endoplasmic reticulum-associated protein, facilitates TNF-α-triggered cellular apoptosis through endoplasmic reticulum-mitochondrial apoptotic pathway." Journal of Molecular Medicine 86(4): 471-484.

[7] Matsuda-Lennikov, M., F. Suizu, N. Hirata, M. Hashimoto, K. Kimura, T. Nagamine, Y. Fujioka, Y. Ohba, T. Iwanaga and M. Noguchi (2014). "Lysosomal Interaction of Akt with Phafin2: A Critical Step in the Induction of Autophagy." PLOS ONE 9(1): e79795.

[8] Green, D. R. (2019). "The Coming Decade of Cell Death Research: Five Riddles." Cell 177(5): 1094-1107.

[9] Elmore, S. (2007). "Apoptosis: A Review of Programmed Cell Death." Toxicologic Pathology 35(4): 495-516.

[10] Brankatschk, B., S. P. Wichert, S. D. Johnson, O. Schaad, M. J. Rossner and J. Gruenberg (2012). "Regulation of the EGF Transcriptional Response by Endocytic Sorting." Science Signaling 5(215): ra21.

[11] Raiborg, C. and H. Stenmark (2009). "The ESCRT machinery in endosomal sorting of ubiquitylated membrane proteins." Nature 458(7237): 445-452.

[12] Miaczynska, M., L. Pelkmans and M. Zerial (2004). "Not just a sink: endosomes in control of signal transduction." Current Opinion in Cell Biology 16(4): 400-406.

[13] Pedersen, N. M., C. Raiborg, A. Brech, E. Skarpen, I. Roxrud, H. W. Platta, K. Liestøl and H. Stenmark (2012). "The PtdIns3P-Binding Protein Phafin 2 Mediates Epidermal Growth Factor Receptor Degradation by Promoting Endosome Fusion." Traffic 13(11): 1547-1563.

[14] Lin, W.-J., C.-Y. Yang, Y.-C. Lin, M.-C. Tsai, C.-W. Yang, C.-Y. Tung, P.-Y. Ho, F.-J. Kao and C.-H. Lin (2010). "Phafin2 modulates the structure and function of endosomes by a Rab5-dependent mechanism." Biochemical and Biophysical Research Communications 391(1): 1043-1048.

[15] Commisso, C., S. M. Davidson, R. G. Soydaner-Azeloglu, S. J. Parker, J. J. Kamphorst, S. Hackett, E. Grabocka, M. Nofal, J. A. Drebin, C. B. Thompson, J. D. Rabinowitz, C. M. Metallo, M. G. Vander Heiden and D. Bar-Sagi (2013). "Macropinocytosis of protein is an amino acid supply route in Ras-transformed cells." Nature 497(7451): 633-637.

[16] Swanson, J. A. (2008). "Shaping cups into phagosomes and macropinosomes." Nature Reviews Molecular Cell Biology 9(8): 639-649.

[17] Mercer, J. and A. Helenius (2009). "Virus entry by macropinocytosis." Nature Cell Biology 11(5): 510-520.

[18] Schink, K. O., K. W. Tan, H. Spangenberg, D. Martorana, M. Sneeggen, C. Campsteijn, C. Raiborg and H. Stenmark (2017). "The PtdIns3P-binding protein Phafin2 escorts macropinosomes through the cortical actin cytoskeleton." bioRxiv: 180760.

[19] Tan, K. W., V. Nähse, C. Campsteijn, A. Brech, K. O. Schink and H. Stenmark (2020). "JIP4 is recruited by the phosphoinositide-binding protein Phafin2 to promote recycling tubules on macropinosomes." bioRxiv: 2020.2009.2029.319111.

[20] Kundu, M. and C. B. Thompson (2008). "Autophagy: Basic Principles and Relevance to Disease." Annual Review of Pathology: Mechanisms of Disease 3(1): 427-455.

[21] Levine, B. and G. Kroemer (2008). "Autophagy in the Pathogenesis of Disease." Cell 132(1): 27-42.

[22] Levine, B. and V. Deretic (2007). "Unveiling the roles of autophagy in innate and adaptive immunity." Nature Reviews Immunology 7(10): 767-777.

[23] Levine, B., N. Mizushima and H. W. Virgin (2011). "Autophagy in immunity and inflammation." Nature 469(7330): 323-335.

[24] Kawabata, T. and T. Yoshimori (2016). "Beyond starvation: An update on the autophagic machinery and its functions." Journal of Molecular and Cellular Cardiology 95: 2-10.

[25] Jang, D.-J. and J.-A. Lee (2016). "The roles of phosphoinositides in mammalian autophagy." Archives of Pharmacal Research 39(8): 1129-1136.

[26] Boya, P., F. Reggiori and P. Codogno (2013). "Emerging regulation and functions of autophagy." Nature Cell Biology 15(7): 713-720.

[27] Wilhelm, T. and H. Richly (2018). "Autophagy during ageing – from Dr Jekyll to Mr Hyde." The FEBS Journal 285(13): 2367-2376.

[28] Mizushima, N., B. Levine, A. M. Cuervo and D. J. Klionsky (2008). "Autophagy fights disease through cellular self-digestion." Nature 451(7182): 1069-1075.

[29] Shintani, T. and D. J. Klionsky (2004). "Autophagy in Health and Disease: A Double-Edged Sword." Science 306(5698): 990.

[30] Choi, A. M. K., S. W. Ryter and B. Levine (2013). "Autophagy in Human Health and Disease." New England Journal of Medicine 368(7): 651-662.

[31] Mowers, E. E., M. N. Sharifi and K. F. Macleod (2018). "Functions of autophagy in the tumor microenvironment and cancer metastasis." The FEBS Journal 285(10): 1751-1766.

[32] Noguchi, M., N. Hirata, T. Tanaka, F. Suizu, H. Nakajima and J. A. Chiorini (2020). "Autophagy as a modulator of cell death machinery." Cell Death & Disease 11(7): 517.

[33] Hara, T., K. Nakamura, M. Matsui, A. Yamamoto, Y. Nakahara, R. Suzuki-Migishima, M. Yokoyama, K. Mishima, I. Saito, H. Okano and N. Mizushima (2006). "Suppression of basal autophagy in neural cells causes neurodegenerative disease in mice." Nature 441(7095): 885-889.

[34] Nishino, I., J. Fu, K. Tanji, T. Yamada, S. Shimojo, T. Koori, M. Mora, J. E. Riggs, S. J. Oh, Y. Koga, C. M. Sue, A. Yamamoto, N. Murakami, S. Shanske, E. Byrne, E. Bonilla, I. Nonaka, S. DiMauro and M. Hirano (2000). "Primary LAMP-2 deficiency causes X-linked vacuolar cardiomyopathy and myopathy (Danon disease)." Nature 406(6798): 906-910.

[35] Lipinski, M. M., B. Zheng, T. Lu, Z. Yan, B. F. Py, A. Ng, R. J. Xavier, C. Li, B. A. Yankner, C. R. Scherzer and J. Yuan (2010). "Genome-wide analysis reveals mechanisms modulating autophagy in normal brain aging and in Alzheimer's disease." Proceedings of the National Academy of Sciences 107(32): 14164.

[36] Hirata, N., F. Suizu, M. Matsuda-Lennikov, T. Tanaka, T. Edamura, S. Ishigaki, T. Donia, P. Lithanatudom, C. Obuse, T. Iwanaga and M. Noguchi (2018). "Functional characterization of lysosomal interaction of Akt with VRK2." Oncogene 37(40): 5367-5386.

[37] Noguchi, M., N. Hirata and F. Suizu (2014). "The links between AKT and two intracellular proteolytic cascades: Ubiquitination and autophagy." Biochimica et Biophysica Acta (BBA) - Reviews on Cancer 1846(2): 342-352.

[38] Manning, B. D. and A. Toker (2017). "AKT/PKB Signaling: Navigating the Network." Cell 169(3): 381-405.

[39] Baskaran, S., Michael J. Ragusa, E. Boura and James H. Hurley (2012). "Two-Site Recognition of Phosphatidylinositol 3-Phosphate by PROPPINs in Autophagy." Molecular Cell 47(3): 339-348.

[40] Liang, R., J. Ren, Y. Zhang and W. Feng (2019). "Structural Conservation of the Two Phosphoinositide-Binding Sites in WIPI Proteins." Journal of Molecular Biology 431(7): 1494-1505.

[41] Lindmo, K. and H. Stenmark (2006). "Regulation of membrane traffic by phosphoinositide 3-kinases." Journal of Cell Science 119(4): 605.

[42] Vanhaesebroeck, B., L. Stephens and P. Hawkins (2012). "PI3K signalling: the path to discovery and understanding." Nature Reviews Molecular Cell Biology 13(3): 195-203.

[43] Schink, K. O., C. Raiborg and H. Stenmark (2013). "Phosphatidylinositol 3-phosphate, a lipid that regulates membrane dynamics, protein sorting and cell signalling." BioEssays 35(10): 900-912.

[44] O′Farrell, F., T. E. Rusten and H. Stenmark (2013). "Phosphoinositide 3-kinases as accelerators and brakes of autophagy." The FEBS Journal 280(24): 6322-6337.

[45] Seglen, P. O. and P. B. Gordon (1982). "3-Methyladenine: Specific inhibitor of autophagic/lysosomal protein degradation in isolated rat hepatocytes." Proceedings of the National Academy of Sciences 79(6): 1889.

[46] Vieira , O. V., R. J. Botelho, L. Rameh, S. M. Brachmann, T. Matsuo, H. W. Davidson, A. Schreiber, J. M. Backer, L. C. Cantley and S. Grinstein (2001). "Distinct roles of class I and class III phosphatidylinositol 3-kinases in phagosome formation and maturation." Journal of Cell Biology 155(1): 19-26.

[47] Raiborg, C., K. O. Schink and H. Stenmark (2013). "Class III phosphatidylinositol 3–kinase and its catalytic product PtdIns3P in regulation of endocytic membrane traffic." The FEBS Journal 280(12): 2730-2742.

[48] Weisz, A., W. Basile, C. Scafoglio, L. Altucci, F. Bresciani, A. Facchiano, P. Sismondi, L. Cicatiello and M. De Bortoli (2004). "Molecular identification of ERα-positive breast cancer cells by the expression profile of an intrinsic set of estrogen regulated genes." Journal of Cellular Physiology 200(3): 440-450.

[49] Choy, C. H., B.-K. Han and R. J. Botelho (2017). "Phosphoinositide Diversity, Distribution, and Effector Function: Stepping Out of the Box." BioEssays 39(12): 1700121.

[50] Balla, T. (2013). "Phosphoinositides: Tiny Lipids With Giant Impact on Cell Regulation." Physiological Reviews 93(3): 1019-1137.

[51] Wallroth, A. and V. Haucke (2018). "Phosphoinositide conversion in endocytosis and the endolysosomal system." Journal of Biological Chemistry 293(5): 1526-1535.

[52] Kutateladze, T. G. (2010). "Translation of the phosphoinositide code by PI effectors." Nature Chemical Biology 6(7): 507-513.

[53] Hammond, G. R. V. and T. Balla (2015). "Polyphosphoinositide binding domains: Key to inositol lipid biology." Biochimica et Biophysica Acta (BBA) - Molecular and Cell Biology of Lipids 1851(6): 746-758.

[54] Wang, H., W.-T. Lo and V. Haucke (2019). "Phosphoinositide switches in endocytosis and in the endolysosomal system." Current Opinion in Cell Biology 59: 50-57.

[55] Tsuji, T., S. Takatori and T. Fujimoto (2019). "Definition of phosphoinositide distribution in the nanoscale." Current Opinion in Cell Biology 57: 33-39.

[56] Picas, L., F. Gaits-Iacovoni and B. Goud (2016). "The emerging role of phosphoinositide clustering in intracellular trafficking and signal transduction." F1000Research 5: F1000 Faculty Rev-1422.

[57] Olivença, D. V., I. Uliyakina, L. L. Fonseca, M. D. Amaral, E. O. Voit and F. R. Pinto (2018). "A Mathematical Model of the Phosphoinositide Pathway." Scientific Reports 8(1): 3904.

[58] Kutateladze, T. G. (2012). Molecular Analysis of Protein–Phosphoinositide Interactions. Phosphoinositides and Disease. M. Falasca. Dordrecht, Springer Netherlands: 111-126.

[59] Simonsen, A., A. E. Wurmser, S. D. Emr and H. Stenmark (2001). "The role of phosphoinositides in membrane transport." Current Opinion in Cell Biology 13(4): 485-492.

[60] Di Paolo, G. and P. De Camilli (2006). "Phosphoinositides in cell regulation and membrane dynamics." Nature 443(7112): 651-657.

[61] Lemmon, M. A. (2008). "Membrane recognition by phospholipid-binding domains." Nature Reviews Molecular Cell Biology 9(2): 99-111.

[62] Downes, C. P., A. Gray and J. M. Lucocq (2005). "Probing phosphoinositide functions in signaling and membrane trafficking." Trends in Cell Biology 15(5): 259-268.

[63] Lystad, A. H. and A. Simonsen (2016). "Phosphoinositide-binding proteins in autophagy." FEBS Letters 590(15): 2454-2468.

[64] Schink, K. O., K.-W. Tan and H. Stenmark (2016). "Phosphoinositides in Control of Membrane Dynamics." Annual Review of Cell and Developmental Biology 32(1): 143-171.

[65] Krauß, M. and V. Haucke (2007). "Phosphoinositides: Regulators of membrane traffic and protein function." FEBS Letters 581(11): 2105-2111.

[66] Legendre-Guillemin, V., S. Wasiak, N. K. Hussain, A. Angers and P. S. McPherson (2004). "ENTH/ANTH proteins and clathrin-mediated membrane budding." Journal of Cell Science 117(1): 9.

[67] Gallop, J. L., C. C. Jao, H. M. Kent, P. J. G. Butler, P. R. Evans, R. Langen and H. T. McMahon (2006). "Mechanism of endophilin N-BAR domain-mediated membrane curvature." The EMBO Journal 25(12): 2898-2910.

[68] Raftopoulou, M., S. Etienne-Manneville, A. Self, S. Nicholls and A. Hall (2004). "Regulation of Cell Migration by the C2 Domain of the Tumor Suppressor PTEN." Science 303(5661): 1179.

[69] Gopaldass, N., B. Fauvet, H. Lashuel, A. Roux and A. Mayer (2017). "Membrane scission driven by the PROPPIN Atg18." The EMBO Journal 36(22): 3274-3291.

[70] Uhlik, M. T., B. Temple, S. Bencharit, A. J. Kimple, D. P. Siderovski and G. L. Johnson (2005). "Structural and Evolutionary Division of Phosphotyrosine Binding (PTB) Domains." Journal of Molecular Biology 345(1): 1-20.

[71] Chandra, M., Y. K. Y. Chin, C. Mas, J. R. Feathers, B. Paul, S. Datta, K.-E. Chen, X. Jia, Z. Yang, S. J. Norwood, B. Mohanty, A. Bugarcic, R. D. Teasdale, W. M. Henne, M. Mobli and B. M. Collins (2019). "Classification of the human phox homology (PX) domains based on their phosphoinositide binding specificities." Nature Communications 10(1): 1528.

[72] Yamamoto, E., J. Domański, F. B. Naughton, R. B. Best, A. C. Kalli, P. J. Stansfeld and M. S. P. Sansom (2020). "Multiple lipid binding sites determine the affinity of PH domains for phosphoinositide-containing membranes." Science Advances 6(8): eaay5736.

[73] Kutateladze, T. G., D. G. S. Capelluto, C. G. Ferguson, M. L. Cheever, A. G. Kutateladze, G. D. Prestwich and M. Overduin (2004). "Multivalent Mechanism of Membrane Insertion by the FYVE Domain*." Journal of Biological Chemistry 279(4): 3050-3057.

[74] Lo, W.-T., A. Vujičić Žagar, F. Gerth, M. Lehmann, D. Puchkov, O. Krylova, C. Freund, L. Scapozza, O. Vadas and V. Haucke (2017). "A Coincidence Detection Mechanism Controls PX-BAR Domain-Mediated Endocytic Membrane Remodeling via an Allosteric Structural Switch." Developmental Cell 43(4): 522-529.e524.

[75] Lemmon, M. A. (2007). "Pleckstrin homology (PH) domains and phosphoinositides." Biochemical Society Symposia 74: 81-93.

[76] Thomas, C. C., M. Deak, D. R. Alessi and D. M. F. van Aalten (2002). "High-Resolution Structure of the Pleckstrin Homology Domain of Protein Kinase B/Akt Bound to Phosphatidylinositol (3,4,5)-Trisphosphate." Current Biology 12(14): 1256-1262.

[77] Edlich, C., G. Stier, B. Simon, M. Sattler and C. Muhle-Goll (2005). "Structure and Phosphatidylinositol-(3,4)- Bisphosphate Binding of the C-Terminal PH Domain of Human Pleckstrin." Structure 13(2): 277-286.

[78]Auguin, D., P. Barthe, M.-T. Augé-Sénégas, M.-H. Stern, M. Noguchi and C. Roumestand (2004). "Solution Structure and Backbone Dynamics of the Pleckstrin Homology Domain of the Human Protein Kinase B (PKB/Akt). Interaction with Inositol Phosphates." Journal of Biomolecular NMR 28(2): 137-155.

[79] Lemmon, M. A. and K. M. Ferguson (2000). "Signal-dependent membrane targeting by pleckstrin homology (PH) domains." Biochemical Journal 350(1): 1-18.

[80] Pant, S. and E. Tajkhorshid (2020). "Microscopic Characterization of GRP1 PH Domain Interaction with Anionic Membranes." Journal of Computational Chemistry 41(6): 489-499.

[81] Yao, L., H. Suzuki, K. Ozawa, J. Deng, C. Lehel, H. Fukamachi, W. B. Anderson, Y. Kawakami and T. Kawakami (1997). "Interactions between Protein Kinase C and Pleckstrin Homology Domains: INHIBITION BY PHOSPHATIDYLINOSITOL 4,5-BISPHOSPHATE AND PHORBOL 12-MYRISTATE 13-ACETATE*." Journal of Biological Chemistry 272(20): 13033-13039.

[82] Agamasu, C., R. H. Ghanam and J. S. Saad (2015). "Structural and Biophysical Characterization of the Interactions between Calmodulin and the Pleckstrin Homology Domain of Akt*." Journal of Biological Chemistry 290(45): 27403-27413.

[83] Dowler, S., R. A. Currie, D. G. Campbell, M. Deak, G. Kular, C. P. Downes and D. R. Alessi (2000). "Identification of pleckstrin-homology-domain-containing proteins with novel phosphoinositide-binding specificities." Biochemical Journal 351(1): 19-31.

[84] Yu, J. W., J. M. Mendrola, A. Audhya, S. Singh, D. Keleti, D. B. DeWald, D. Murray, S. D. Emr and M. A. Lemmon (2004). "Genome-Wide Analysis of Membrane Targeting by S. cerevisiae Pleckstrin Homology Domains." Molecular Cell 13(5): 677-688.

[85] Jiang, Z., Z. Liang, B. Shen and G. Hu (2015). "Computational Analysis of the Binding Specificities of PH Domains." BioMed Research International 2015: 792904.

[86] Harlan, J. E., P. J. Hajduk, H. S. Yoon and S. W. Fesik (1994). "Pleckstrin homology domains bind to phosphatidylinositol-4,5-bisphosphate." Nature 371(6493): 168-170.

[87] Lemmon, M. A., K. M. Ferguson, R. Brien, P. B. Sigler and J. Schlessinger (1995). "Specific and high-affinity binding of inositol phosphates to an isolated pleckstrin homology domain." Proceedings of the National Academy of Sciences 92(23): 10472.

[88] Lenoir, M., Ü. Coskun, M. Grzybek, X. Cao, S. B. Buschhorn, J. James, K. Simons and M. Overduin (2010). "Structural basis of wedging the Golgi membrane by FAPP pleckstrin homology domains." EMBO reports 11(4): 279-284.

[89] Sugiki, T., K. Takeuchi, T. Yamaji, T. Takano, Y. Tokunaga, K. Kumagai, K. Hanada, H. Takahashi and I. Shimada (2012). "Structural Basis for the Golgi Association by the Pleckstrin Homology Domain of the Ceramide Trafficking Protein (CERT)*." Journal of Biological Chemistry 287(40): 33706-33718.

[90] Stephens, L., K. Anderson, D. Stokoe, H. Erdjument-Bromage, G. F. Painter, A. B. Holmes, P. R. J. Gaffney, C. B. Reese, F. McCormick, P. Tempst, J. Coadwell and P. T. Hawkins (1998). "Protein Kinase B Kinases That Mediate Phosphatidylinositol 3,4,5-Trisphosphate-Dependent Activation of Protein Kinase B." Science 279(5351): 710.

[91] Frech, M., M. Andjelkovic, E. Ingley, K. K. Reddy, J. R. Falck and B. A. Hemmings (1997). "High Affinity Binding of Inositol Phosphates and Phosphoinositides to the Pleckstrin Homology Domain of RAC/Protein Kinase B and Their Influence on Kinase Activity*." Journal of Biological Chemistry 272(13): 8474-8481.

[92] Manna, D., A. Albanese, W. S. Park and W. Cho (2007). "Mechanistic Basis of Differential Cellular Responses of Phosphatidylinositol 3,4-Bisphosphate- and Phosphatidylinositol 3,4,5-Trisphosphate-binding Pleckstrin Homology Domains*." Journal of Biological Chemistry 282(44): 32093-32105.

[93] He, J., R. M. Haney, M. Vora, V. V. Verkhusha, R. V. Stahelin and T. G. Kutateladze (2008). "Molecular mechanism of membrane targeting by the GRP1 PH domain*." Journal of Lipid Research 49(8): 1807-1815.

[94] Zwolak, A., C. Yang, E. A. Feeser, E. Michael Ostap, T. Svitkina and R. Dominguez (2013). "CARMIL leading edge localization depends on a non-canonical PH domain and dimerization." Nature Communications 4(1): 2523.

[95] Kavran, J. M., D. E. Klein, A. Lee, M. Falasca, S. J. Isakoff, E. Y. Skolnik and M. A. Lemmon (1998). "Specificity and Promiscuity in Phosphoinositide Binding by Pleckstrin Homology Domains*." Journal of Biological Chemistry 273(46): 30497-30508.

[96] Liu, J., K. Fukuda, Z. Xu, Y.-Q. Ma, J. Hirbawi, X. Mao, C. Wu, E. F. Plow and J. Qin (2011). "Structural Basis of Phosphoinositide Binding to Kindlin-2 Protein Pleckstrin Homology Domain in Regulating Integrin Activation*." Journal of Biological Chemistry 286(50): 43334-43342.

[97] Ghai, R., X. Du, H. Wang, J. Dong, C. Ferguson, A. J. Brown, R. G. Parton, J.-W. Wu and H. Yang (2017). "ORP5 and ORP8 bind phosphatidylinositol-4, 5-biphosphate (PtdIns(4,5)P2) and regulate its level at the plasma membrane." Nature Communications 8(1): 757.

[98] Tang, T.-X., C. V. Finkielstein and D. G. S. Capelluto (2020). "The C-terminal acidic motif of Phafin2 inhibits PH domain binding to phosphatidylinositol 3-phosphate." Biochimica et Biophysica Acta (BBA) - Biomembranes 1862(6): 183230.

[99] Agorio, A., J. Giraudat, M. W. Bianchi, J. Marion, C. Espagne, L. Castaings, F. Lelièvre, C. Curie, S. Thomine and S. Merlot (2017). "Phosphatidylinositol 3-phosphate–binding protein AtPH1 controls the localization of the metal transporter NRAMP1 in *Arabidopsis*." Proceedings of the National Academy of Sciences 114(16): E3354.

[100] Chen, D., W. Fan, Y. Lu, X. Ding, S. Chen and Q. Zhong (2012). "A Mammalian Autophagosome Maturation Mechanism Mediated by TECPR1 and the Atg12-Atg5 Conjugate." Molecular Cell 45(5): 629-641.

[101] Idevall-Hagren, O. and P. De Camilli (2015). "Detection and manipulation of phosphoinositides." Biochimica et Biophysica Acta (BBA) - Molecular and Cell Biology of Lipids 1851(6): 736-745.

[102] Gray, A., J. V AN Der Kaay and C. P. Downes (1999). "The pleckstrin homology domains of protein kinase B and GRP1 (general receptor for phosphoinositides-1) are sensitive and selective probes for the cellular detection of phosphatidylinositol 3,4-bisphosphate and/or phosphatidylinositol 3,4,5-trisphosphate in vivo." Biochemical Journal 344(3): 929-936.

[103] Kutateladze, T. G. (2006). "Phosphatidylinositol 3-phosphate recognition and membrane docking by the FYVE domain." Biochimica et Biophysica Acta (BBA) - Molecular and Cell Biology of Lipids 1761(8): 868-877.

[104] Gillooly, D. J., A. Simonsen and H. Stenmark (2001). "Cellular functions of phosphatidylinositol 3-phosphate and FYVE domain proteins." Biochemical Journal 355(2): 249-258.

[105] Stenmark, H., R. Aasland and P. C. Driscoll (2002). "The phosphatidylinositol 3-phosphate-binding FYVE finger." FEBS Letters 513(1): 77-84.

[106] Blatner, N. R., R. V. Stahelin, K. Diraviyam, P. T. Hawkins, W. Hong, D. Murray and W. Cho (2004). "The Molecular Basis of the Differential Subcellular Localization of FYVE Domains*." Journal of Biological Chemistry 279(51): 53818-53827.

[107] Stahelin, R. V., F. Long, K. Diraviyam, K. S. Bruzik, D. Murray and W. Cho (2002). "Phosphatidylinositol 3-Phosphate Induces the Membrane Penetration of the FYVE Domains of Vps27p and Hrs*." Journal of Biological Chemistry 277(29): 26379-26388.

[108] Hayakawa, A., S. J. Hayes, D. C. Lawe, E. Sudharshan, R. Tuft, K. Fogarty, D. Lambright and S. Corvera (2004). "Structural Basis for Endosomal Targeting by FYVE Domains*." Journal of Biological Chemistry 279(7): 5958-5966.

[109] Reinhart, E. F., N. A. Litt, S. Katzenell, M. Pellegrini, A. Yamamoto and M. J. Ragusa (2021). "A highly conserved glutamic acid in ALFY inhibits membrane binding to aid in aggregate clearance." Traffic 22(1-2): 23-37.

[110] Lee, S. A., R. Eyeson, M. L. Cheever, J. Geng, V. V. Verkhusha, C. Burd, M. Overduin and T. G. Kutateladze (2005). "Targeting of the FYVE domain to endosomal membranes is regulated by a histidine switch." Proceedings of the National Academy of Sciences of the United States of America 102(37): 13052.

[111] He, J., M. Vora, R. M. Haney, G. S. Filonov, C. A. Musselman, C. G. Burd, A. G. Kutateladze, V. V. Verkhusha, R. V. Stahelin and T. G. Kutateladze (2009). "Membrane insertion of the FYVE domain is modulated by pH." Proteins: Structure, Function, and Bioinformatics 76(4): 852-860.

[112] Dumas, J. J., E. Merithew, E. Sudharshan, D. Rajamani, S. Hayes, D. Lawe, S. Corvera and D. G. Lambright (2001). "Multivalent Endosome Targeting by Homodimeric EEA1." Molecular Cell 8(5): 947-958.

[113] Mao, Y., A. Nickitenko, X. Duan, T. E. Lloyd, M. N. Wu, H. Bellen and F. A. Quiocho (2000). "Crystal Structure of the VHS and FYVE Tandem Domains of Hrs, a Protein Involved in Membrane Trafficking and Signal Transduction." Cell 100(4): 447-456.

[114] Misra, S. and J. H. Hurley (1999). "Crystal Structure of a Phosphatidylinositol 3-Phosphate-Specific Membrane-Targeting Motif, the FYVE Domain of Vps27p." Cell 97(5): 657-666.

[115] Gillooly, D. J., I. C. Morrow, M. Lindsay, R. Gould, N. J. Bryant, J.-M. Gaullier, R. G. Parton and H. Stenmark (2000). "Localization of phosphatidylinositol 3-phosphate in yeast and mammalian cells." The EMBO Journal 19(17): 4577-4588.

[116] Liu, K., Y. Jian, X. Sun, C. Yang, Z. Gao, Z. Zhang, X. Liu, Y. Li, J. Xu, Y. Jing, S. Mitani, S. He and C. Yang (2016). "Negative regulation of phosphatidylinositol 3-phosphate levels in early-to-late endosome conversion." Journal of Cell Biology 212(2): 181-198.

[117] Nascimbeni, A. C., P. Codogno and E. Morel (2017). "Local detection of PtdIns3P at autophagosome biogenesis membrane platforms." Autophagy 13(9): 1602-1612.

Chapter 2 Structural, thermodynamic, and phosphatidylinositol 3-phosphate binding properties of Phafin2

Tuo-Xian Tang [a], Ami Jo [b], Jingren Deng [c], Jeffrey F. Ellena [d], Iulia M. Lazar [c], Richey M. Davis [b], and Daniel G. S. Capelluto [a,*]

[a] Protein Signaling Domains Laboratory, Department of Biological Sciences, Biocomplexity Institute, and Center for Soft Matter and Biological Physics, Virginia Tech, Blacksburg, VA 24061, United States; [b] Department of Chemical Engineering, Virginia Tech, Blacksburg, VA 24061, United States; [c] Department of Biological Sciences, Virginia Tech, Blacksburg, VA 24061, United States; [d] Biomolecular Magnetic Resonance Facility, University of Virginia, Charlottesville VA, 22904, United States.

Author contributions

Tuo-Xian Tang did protein purification, circular dichroism (CD), nuclear magnetic resonance (NMR), and surface plasmon resonance (SPR) experiments; Daniel G. S. Capelluto and Tuo-Xian Tang did formal analysis; Ami Jo and Richey M. Davis provided guidance on dynamic light scattering (DLS) experiments; Jingren Deng and Iulia M. Lazar did mass spectrometry experiments and data analysis; Daniel G. S. Capelluto supervised this research project, provided guidance on the experiments and wrote the manuscript. All authors contributed to the edition of the final manuscript.

As published in *Protein Science*:

Tang, T.-X., Jo, A., Deng, J., Ellena, J. F., Lazar, I. M., Davis, R. M., & Capelluto, D. G. S. (2017). Structural, thermodynamic, and phosphatidylinositol 3-phosphate binding properties of Phafin2. *Protein Science*, 26(4), 814-823.

DOI: https://doi.org/10.1002/pro.3128

Abstract

Phafin2 is a phosphatidylinositol 3-phosphate- (PtdIns(3)P) binding protein involved in the regulation of endosomal cargo trafficking and lysosomal induction of autophagy. Binding of Phafin2 to PtdIns(3)P is mediated by both its PH and FYVE domains. However, there are no studies on the structural basis, conformational stability, and lipid interactions of Phafin2 to better understand how this protein participates in signaling at the surface of endomembrane compartments. Here, we show that human Phafin2 is a moderately elongated monomer of ~28 kDa with an intensity-average hydrodynamic diameter of ~7 nm. Circular dichroism (CD) analysis indicates that Phafin2 exhibits an α/β structure and predicts ~40% random coil content in the protein. Heteronuclear NMR data indicates that a unique conformation of Phafin2 is present in solution and dispersion of resonances suggests that the protein exhibits random coiled regions, in agreement with the CD data. Phafin2 is stable, displaying a melting temperature of 48.4 °C. The folding-unfolding curves, obtained using urea- and guanidine hydrochloride-mediated denaturation, indicate that Phafin2 undergoes a two-state native-to-denatured transition. Analysis of these transitions shows that the free energy change for urea- and guanidine hydrochloride-induced Phafin2 denaturation in water is ~4 kcal mol^{-1}. PtdIns(3)P binding to Phafin2 occurs with high affinity, triggering minor conformational changes in the protein. Taken together, these studies represent a platform for establishing the structural basis of Phafin2 molecular interactions and the role of the two potentially redundant PtdIns(3)P-binding domains of the protein in endomembrane compartments.

Keywords: Phafin2, Phosphatidylinositol 3-phosphate, Conformation, Protein structure.

Abbreviations

AUC, analytical ultracentrifugation; CD, circular dichroism; DLS, dynamic light scattering; f/f_0, frictional ratio; GuHCl, guanidine hydrochloride; PtdIns(3)P, phosphatidylinositol 3-phosphate; *s*, sedimentation coefficient; $S_{20,w}$, sedimentation coefficient under standard conditions; SPR, surface plasmon resonance.

Introduction

Phafin2 (also known as EAPF or PLEKHF2) belongs to the Phafin family of proteins containing an N-terminal PH (Pleckstrin homology) and C-terminal FYVE (Fab1, YOTB, Vac1, and EEA1) domains (Fig. 1A) [1]. Both PH and FYVE domains of Phafin2 are phosphatidylinositol 3-phosphate-(PtdIns(3)P) binding modules [2]. PtdIns(3)P is a hallmark of endosomes as it mediates the recruitment of effector proteins to these compartments; thus, both PtdIns(3)P-interacting domains can target Phafin2 to PtdIns(3)P-enriched membranes. Phafin2 regulates the function and structure of endosomes through a Rab5-dependent process [3] although no direct interaction of Phafin2 and Rab5 occurs [4]. Several lines of evidence suggest that Phafin2, the Phafin family member protein Phafin1, and the *Drosophila* homologue Rush promote the enlargement of early endosomes [3-6] with their FYVE domains playing a dominant role [3]. Phafin2 interacts with the FYVE domain-containing protein EEA1, which regulates endosomal cargo trafficking and fusion events, but does not directly participate in cargo sorting [4]. A role for lysosomal Phafin2 in the induction of autophagy has also been recently reported. Phafin2-mediated autophagy requires the presence of PtdIns(3)P at the lysosomal surface and the serine/threonine kinase Akt [2]. Binding of Phafin2 to Akt requires both the PH and FYVE domains. The interaction of Phafin2 with PtdIns(3)P allows localization of the Phafin2-Akt complex to the lysosomal surface [2]. Phafin2 has previously been associated with caspase 12-dependent apoptosis through the endoplasmic reticulum (ER)-mitochondrial apoptotic pathway [7]. In this pathway, Phafin2 translocates to the ER after tumor necrosis factor-α (TNF-α)stimulation, inducing apoptosis in a PH- and FYVE domain-dependent manner [7]. The action of Phafin2 favors a more rapid increase of the cytosolic Ca^{2+} levels, which enhances TNF-α-mediated apoptosis and suppresses the unfolding protein response at the ER [7].

In this article, we report the first structural and thermodynamic characterization of Phafin2. We show that Phafin2 is a nonglobular monomer that contains α-helical and β-sheet elements. Temperature- and chemical-induced denaturation studies indicate that Phafin2 transitions from native to denatured states, without the presence of long-lived intermediate states. Binding of Phafin2 to PtdIns(3)P occurs with nanomolar affinity, which is accompanied by local conformational changes in the protein. PtdIns(3)P-binding sites in Phafin2 are predicted to be located at conserved regions found in related PH and FYVE domains.

Results and Discussion

Phafin2 is an elongated monomer

Optimal overexpression of glutathione S-transferase (GST)-tagged Phafin2 was obtained in the presence of Zn^{2+}, as the protein presents a C-terminal Zn^{2+} finger FYVE domain (Fig. 1A). Soluble GST-Phafin2 was immobilized on glutathione beads and the GST was removed by thrombin digestion. Recombinant Phafin2 remained soluble after removal of the GST tag. SDS-PAGE analysis showed a protein band with a molecular mass of ~28 kDa (Fig. 1B), close to the theoretical molecular mass of Phafin2 (27,941 Da). Removal of protein aggregates and other minor protein contaminants was carried out using an FPLC-driven Superdex 75 size-exclusion column (data not shown). MALDI-TOF was used to identify Phafin2, given the proximity of its molecular mass to GST's molecular mass. Tryptic products of Phafin2 accounted for ~77% amino acid sequence coverage of the protein, including its C-terminus (Tables 1 and S1). To address whether the Phafin2 N-terminus was also intact, the first 5 residues from the N-terminus were also sequenced, identifying Gly-Ser-Met-Val-Asp, with the first two corresponding to the amino acids translated from the vector. Size-exclusion chromatography was employed to study the hydrodynamic properties of Phafin2. Phafin2 consistently eluted as a single sharp peak with an estimated apparent molecular mass of ~42 kDa, a value far from its theoretical molecular mass (Fig. 2A-B), suggesting that the protein exhibits an elongated structure. Dynamic light scattering (DLS) analysis indicated that more than 99% of the mass of Phafin2 was in a peak with an intensity-average value of ~ 7 nm at 25ºC (Fig. 2C). This data confirms that Phafin2 exhibits only one conformational state. Sedimentation velocity analytical ultracentrifugation (AUC) analysis showed that Phafin2 was monodispersed with an estimated molecular mass of 27,115 Da (Fig. 3), in close agreement with the predicted value for a monomeric state. Phafin2 displayed a sedimentation coefficient under standard conditions ($S^0_{20,w}$) of 2.42 S and a frictional ratio (f/f_o) of 1.35 (Fig. 3C). The f/f_o ratio represents the frictional coefficient of an unknown molecule to that of an ideal spherical molecule of the same density and volume, which consequently, features the anisotropy of a molecule [8]. The f/f_o value of Phafin2, which is over 1, indicates that the protein is asymmetrical with a moderately elongated structure [9].

Structural features of Phafin2

Far-UV circular dichroism (CD) spectroscopy was carried out to study the secondary structural content of Phafin2. The spectrum of Phafin2 exhibited two minima at 208 and 226 nm (Fig.

4A), with the latter being more pronounced, suggesting that it is an α/β protein. By using the CDSSTR algorithm, the secondary structural content of Phafin2 was estimated to be 23% α-helix, 21% β-strand, 15% β-turn, and 41% random coil (NRMSD= 0.018). The ratio of mean residue ellipticity (MRE) values at 222 and 208 nm can be used to characterize α-helices in proteins. A ratio of ~1.0 predicts that α-helices exhibit extensive interhelical contact in helical bundles and coiled coil regions, whereas a ratio of ~0.8 predicts limited interhelical contacts [10]. The MRE values at 208 and 222 nm were -7,882.22 and -8,376.92 deg.cm^2.dmol^{-1}, respectively, giving a ratio of 1.06. Thus, far-UV CD analysis suggests that there are extensive interhelical contacts in Phafin2. Addition of the water-soluble phosphoinositide ligand, dibutanoyl PtdIns(3)P, did not induce secondary structural changes in the protein (Fig. 4A). The near-UV CD spectrum provides valuable information about the tertiary structure of a protein [11]. Phafin2 exhibits a spectrum dominated by the contributions of two positive bands from Trp residues, one negative band at 275 nm for Tyr and vibronic bands at 258 and 270 nm, which are often attributed to a region associated with Phe residues (Fig. 4B) (Phafin2 has three Trp, five Tyr, and nine Phe residues). Addition of water-soluble dibutanoyl PtdIns(3)P led to minor changes in the region comprising the aromatic regions, with the exception of the positive band at 294 nm, a peak likely associated with Trp residues. Local conformational changes around one or more Trp residues in Phafin2 were also observed when the protein was titrated with water-soluble dibutanoyl PtdIns(3)P. Addition of PtdIns(3)P decreased the intrinsic tryptophan fluorescence of the protein at 339 nm (Fig. 4C), suggesting that binding of the phosphoinositide changes the polarity of the environment near one or more Phafin2 Trp residues.

Thermostability of Phafin2

Far-UV CD at 222 nm was employed to monitor Phafin2's thermal stability and to estimate its melting temperature (T_M), that is, the temperature at which half of the protein is unfolded. Phafin2 denatured with a single transition over the range of 20 to 90 °C (Fig. 5). The T_M for Phafin2 is 48.4 ± 0.6 °C. Significant precipitation was observed at the end of the denaturation curve, indicating that the transition was irreversible.

NMR studies of Phafin2

The structural properties of Phafin2 were further investigated by solution NMR spectroscopy. Fig. 6 shows that the ^{1}H, ^{15}N TROSY-HSQC spectrum of Phafin2 yielded a single set of resonances, indicating that the protein was highly homogenous at 30 °C. Also, ~235 HN cross-peaks were identified, which is very close to the expected number (238). The presence of

crowded resonances in the center of the ^{1}H, ^{15}N TROSY-HSQC spectrum of Phafin2 is consistent with the presence of random coil regions in the protein as deduced from far-UV CD analysis. NMR spectra of Phafin2 at higher temperatures than 30 °C were also recorded, yielding loss of resonances, and aggregation and precipitation of the protein (data not shown).

Denaturant-induced unfolding of Phafin2

To study protein folding, the standard Gibbs free energy in water (ΔG^{0}_{H2O}) is the most relevant parameter for the quantification of protein stability. Furthermore, the linear extrapolation method is often used for determining ΔG^{0}_{H2O} by the use of chemical denaturants, such as guanidine hydrochloride (GuHCl) and urea [12]. To monitor denaturant-induced structural changes of Phafin2, we employed intrinsic tryptophan fluorescence and far-UV CD studies. Phafin2 emits a fluorescent emission maximum at 339 nm, but it shifts to 356 nm in the presence of 8 M urea or 6 M GuHCl (Fig. 7A). By representing the reduction of fluorescence intensity at 339 nm, we found that the unfolding curve of Phafin2 is sigmoidal (Fig. 7B). Thermodynamic analysis showed that the ΔG^{0}_{H2O} was 4.07 and 3.80 kcal mol^{-1} for urea and GuHCl, respectively (Table 2 and Suppl. Fig. 1). Data analysis also indicated that Phafin2 was susceptible to unfolding, showing C_m ($\Delta G^{0}_{H2O}/m$) values of 3.42 and 1.30 M for urea and GuHCl, respectively (Table 2 and Suppl. Fig. 1). These parameters were also calculated by monitoring structural changes in Phafin2 at 222 nm using CD spectroscopy. The ΔG^{0}_{H2O} and C_m values of Phafin2 for urea-induced unfolding were 4 kcal mol^{-1} and 3.45 M, respectively, whereas GuHCl-induced unfolding showed ΔG^{0}_{H2O} and C_m values of 3.75 kcal mol^{-1} and 1.51 M, respectively (Table 2 and Suppl. Fig. 1). Therefore, the Phafin2 thermodynamic parameters obtained by two independent methodologies were similar. By comparing the urea-induced unfolding traces obtained by intrinsic tryptophan fluorescence and CD, the Phafin2 structure remained unchanged up to ~2 M of urea concentration and reached a maximum denaturation at ~4.5 M of the denaturant. In the case of GuHCl-mediated denaturation, the Phafin2 structure was stable at ~0.5 M of GuHCl concentration, but achieved full denaturation at ~3 M of the denaturant using both methodologies. Unfolding of small globular proteins occurs through a process that conforms to the two-state mechanism [12]; however elongated proteins, such as the Notch ankyrin domain [13], spectrin [14], and the bacterial surface protein SasG [15], among others, exhibit chemical denaturation sigmoidal plots. In this scenario, the population level of intermediate states is insignificant [16]. The denaturation curves of Phafin2 indicate that the protein follows a two-state mechanism without the presence of intermediate states. The presence of a single steep transition in these curves suggests that the Phafin2 PH and FYVE

domains are thermodynamically coupled, possibly due to inter-domain interactions, as observed in other multi-domain containing proteins [17-19].

Analysis of Phafin2 association to PtdIns(3)P

To obtain a more quantitative measurement of PtdIns(3)P binding to Phafin2, we performed surface plasmon resonance (SPR) binding analysis using liposomes immobilized on an L1 sensor chip. Measurements were carried out relative to a sensor chip surface containing 100% phosphatidylcholine. Phafin2 bound to PtdIns(3)P liposomes with a fast association rate, but the steady state was transient and response dropped slightly at the end of the injection (Fig. 8A). The interaction best fit the two-state conformational change model, in agreement with the local conformational changes induced by the phosphoinositide (Fig. 4B-C), with an estimated dissociation constant (K_D) of 285 ± 80 nM (χ^2=3.5 RU^2). This value is in agreement with the phosphoinositide affinity values calculated for other PH and FYVE domain-containing proteins [20]. PH domains strongly bind to poly-phosphoinositides and are mediated, in most cases, by the basic $KX_n(K/R)XR$ motif [21], which is represented by the sequence 49-KPKAR-53 sequence in the Phafin2 PH domain. Binding of the PH domain to mono-phosphate phosphoinositides, such as the case for the Phafin2 PH domain [2] is rare; a well-documented example is the GLUE domain of Vps36, which shows a split PH-domain fold that specifically binds PtdIns(3)P in a mode that differs from other phosphoinositide-binding domains [22]. On the other hand, FYVE domains bind specifically to PtdIns(3)P with reports showing binding affinities for the lipid ranging from nanomolar to micromolar concentrations [23]. Lipid and membrane insertion of the FYVE domain is mediated by three consensus sequences, WxxD, RR/KHHCR, and RVC motifs [20], all of which are present in the Phafin2 FYVE domain. A model of the structure of human Phafin2 (Fig. 8B) was obtained from its protein sequence and homology modeling using Phyre2 [24] with >90% accuracy using the 5 closest templates (PDB accession codes 3KY9, 1JOC, 3BJI, 2YQM, 2VRW). The elongated predicted structure shows the two putative PtdIns(3)P-dependent membrane-binding sites located at predominantly flexible regions (Fig. 8B-D). In addition to PtdIns(3)P, it is possible that the FYVE and PH domains associate to other lipid ligands through acidic electrostatic interactions [25], which may be required for Phafin2 targeting to endomembrane compartments.

Conclusions

In conclusion, we demonstrate that Phafin2 is an α/β moderately elongated and stable monomer. Unfolding traces that were measured using urea and GuHCl indicate that Phafin2 denatures in a two-state transition model. The lack of an intermediate state suggests that the PH and FYVE domains cooperate during the unfolding process. Phafin2 interacts with PtdIns(3)P with nanomolar affinity, inducing local conformational changes in its tertiary structure. The PtdIns(3)P binding sites are predicted to be located in flexible regions in the protein. The quality of the purified and stable Phafin2 at room temperature makes the protein appropriate for solution NMR structural studies, which can contribute to a better understanding of its molecular interactions in PtdIns(3)P-enriched endomembrane compartments.

Material and Methods

Protein expression and purification

The Phafin2 cDNA was isolated from a human liver cDNA library (Clontech) by PCR and cloned into a pGEX4T3 vector (GE Healthcare). Protein was expressed in *Escherichia coli* (Rosetta; Stratagene). Bacterial cells were grown in Luria-Bertani media at 37 °C until cells reached an optical density of ~0.8. Induction of the GST fusion Phafin2 resulted from the addition of 1 mM isopropyl β-D-1-thiogalactopyranoside and 1 μM $ZnCl_2$ followed by 4-h incubation at 25 °C. Phafin2 was purified using the glutathione bead-based procedure as previously described [26]. Proteins were further purified using an FPLC-driven Superdex 75 column (GE Healthcare) previously equilibrated with 50 mM Tris-HCl (pH 8) and 0.5 M NaCl. Fractions containing the purified protein were pooled and concentrated in the indicated buffers for biochemical or biophysical analysis. Protein concentration was calculated using the UV-light absorbance method at 280 nm.

Mass spectrometry and N-terminal sequencing analyses

Phafin2 (50 mM Tris-HCl, pH~8) was reduced with 1,4-dithiothreitol (5 mM) in the presence of urea (8 M), and digested with trypsin at a substrate-enzyme ratio of 50:1 w/w (37 °C, overnight). After cleanup with a C18 cartridge, a solution of Phafin2 (0.5 μM, 8 μL) was injected in a micro HPLC system (HPLC 1100, Agilent Technologies) and delivered for MS analysis at ~180 nL/min with a 4 h long gradient of 10 % to 100 % solvent B (where solvent A was H_2O:CH_3CN:TFA, 98/2/0.01 v/v; and, solvent B was H_2O:CH_3CN:TFA, 10/90/0.01 v/v). The HPLC system was adapted in-house to operate in the nano flow mode. MS analysis

was performed with a linear trap quadruple MS system (Thermo Electron, San Jose, CA) with the ESI voltage set at +2.0 kV. Tandem MS data were acquired using data dependent analysis on the top 5 most intense peaks using parameters described in [27]. The database search was performed with Proteome Discoverer 1.4 (Thermo Electron) against an *E. coli* database appended with the sequence of Phafin2. The *E. coli* database was used to enable the identification of possible contaminants from the expression system of Phafin2. Post-translational modifications were not allowed in the search, the allowed missed cleavage sites was set to 2, and the false discovery rate was set at <3 % [28]. Using these experimental conditions, Phafin2 (Q9H8W4) could be identified by up to 29 unique peptides accounting for a sequence coverage over 70%. Intact Phafin2 was also subjected to N-terminal sequencing at the Tufts University Core Facility (Boston, MA).

Sedimentation velocity analytical ultracentrifugation

Sedimentation velocity AUC was carried out at the Center for Analytical Ultracentrifugation of Macromolecular Assemblies at the University of Texas Health Science Center, San Antonio using a Beckman Optima XL-I analytical ultracentrifuge with absorbance and interference optical detection systems (Beckman Coulter). Sedimentation velocities were analyzed using the UltraScan3 software suite as described [[29], http: //www.ultrascan.uthscsa.edu]. Phafin2 (10 μM was prepared in a buffer containing 8 mM Tris-HCl (pH 7.3) and 50 mM NaCl. Absorbance data was obtained at a wavelength of 230 nm at 20 °C, and at a rotor speed of 50,000 rpm using standard double-channel centerpieces. Data were first subjected to 2D spectrum analysis with simultaneous removal of time-invariant noise [30] followed by a parametrically constrained spectrum analysis - Monte Carlo analysis [31].

Dynamic light scattering

DLS experiments were performed at 25 °C using a Malvern Zetasizer Nano-ZS instrument. DLS studies were with Phafin2 (0.8 mg/ml) in 5 mM sodium citrate (pH 7.3) and 50 mM KF. Each run was recorded for 120 s and three accumulated runs were averaged with protein samples previously equilibrated for 2 min.

Circular dichroism spectroscopy

Far-UV CD spectra were obtained using Phafin2 (20 μM) in 5 mM sodium citrate (pH 7.3) and 50 mM KF on a Jasco J-815 spectropolarimeter. Spectra were collected in a 1-mm path length

quartz cell at 25 °C. Three accumulated scans of the protein from 250 to 190 nm were recorded using a bandwidth of 1-nm and a response time of 1 s at a scan speed of 20 nm/min. Secondary structure content of Phafin2 was estimated using the CDSSTR algorithm available at Dichroweb (http://dichroweb.cryst.bbk.ac.uk/html/process.shtml). Three accumulated near-UV CD spectra of Phafin2 (40 μM) were collected using a 1-mm path length at 20 nm/min between 350 and 250 nm with a response time of 1 s and a data pitch of 0.5 nm. All CD spectra were corrected for buffer background. Far-UV CD signal changes at 222 nm were monitored as a function of increasing temperature from 20 to 90 °C, with steps of 1 °C and with an equilibration time of 30 sec at each temperature before recording a reading. For the urea- and GuHCl-induced unfolding experiments, Phafin2 was incubated for 1 h at room temperature with the indicated concentrations of the denaturant before the spectra were recorded.

Tryptophan fluorescence

Intrinsic tryptophan fluorescence emission spectra of Phafin2 (0.25 μM), in 5 mM sodium citrate (pH 7.3) and 50 mM KF, were recorded after excitation of the protein at 295 nm on a Jasco J-815 spectropolarimeter. Emission spectra were collected between 300-400 nm using a 10-mm quartz cuvette at room temperature. Phafin2 was titrated with increasing concentrations of PtdIns(3)P (0.25-8.0 μM). For the urea- and GuHCl-induced unfolding experiments, Phafin2 was incubated for 1 h at room temperature with the indicated concentrations of the denaturant before the spectra were recorded.

NMR spectroscopy

NMR experiments of ^{1}H, ^{15}N Phafin2 (200 μM) in 20 mM d_{11}Tris-HCl (pH 7.3), 100 mM NaCl, 2 mM d_{18} DTT, 1 mM NaN_3, 10% D_2O were performed on a Bruker AVANCE III 800 MHz NMR spectrometer equipped with a cryoprobe (University of Virginia). Two dimensional [^{15}N,^{1}H]-transverse relaxation optimized spectroscopy (TROSY)-heteronuclear single quantum coherence (HSQC) was performed for the protein sample. Data were processed and analyzed using Topspin 3.2 and NMRpipe [32].

Analysis of denaturant unfolding transitions

The transition curves acquired after representing each spectral property (*i.e.*, fluorescence changes of Phafin2 from F_{339} to F_{356}, CD spectral changes of Phafin2 at 222 nm) against denaturant concentration were analyzed to calculate the Gibbs free energy of unfolding

(ΔG^0_{H2O}) in the absence of denaturant. To calculate ΔG^0_{H2O} for each spectral analysis, a model in which monomeric native Phafin2 (f_N) was converted to a denatured (f_D) form without the presence of highly populated intermediates was first considered. This state, known as the equilibrium two-state is represented as:

$$K_{eq} = f_D / f_N \quad (1)$$

The estimation of K_{eq} was used to calculate the dependence of the standard Gibbs energy of denaturation for each denaturant concentration (ΔG) using the relation:

$$\Delta G = -RT \ln K_{eq} = -RT \ln (f_D / 1 - f_D) \quad (2)$$

where R is the universal gas constant (1.986 cal mol^{-1} K^{-1}) and T is the temperature on the Kelvin scale. The ΔG value varies linearly with denaturant concentration following the equation:

$$\Delta G\,(x) = \Delta G^0_{H2O} + m[x] \quad (3)$$

where [x] is the molar concentration of the denaturant and m is the slope of the plot. Thus, linear plots of ΔG *versus* denaturant concentration were obtained. Data was fitted to the nonlinear least-squares method using Microsoft Excel (Microsoft Corporation, Redmond WA) for the calculation of the ΔG^0_{H2O} and m for each experimental condition [12]. Using these parameters, the C_m, the denaturant concentration at the midpoint of the unfolding transition when ΔG is 0, was estimated. Similarly, the T_M of Phafin2 was calculated by following the denaturation of the protein by its CD ellipticity at 222 nm and by determining the temperature at which ΔG is 0 using equation 2.

SPR analysis

Liposomes were prepared as previously described [33]. Briefly, lipids including 1-palmitoyl-2-oleoyl-*sn*-glycero-3-phosphatidylcholine (DOPC; control), or DOPC and dipalmitoyl PtdIns(3)P (1.5%) were dissolved in chloroform/methanol/water (65:35:0.8). The lipid mixture was first dried under N_2 and further under vacuum to remove residual chloroform. Phospholipids were resuspended in 20 mM HEPES (pH 7.0) and 100 mM NaCl to a final concentration of 4 mM, sonicated, and extruded for 100-nm liposome size at 65 °C. SPR

analysis was performed on a BIAcore X100 instrument with a liposome-coated L1 sensor chip at room temperature. Typical liposome loading was ~5,000 RU/channel. Kinetic SPR measurements were performed with the flow rate set at 30 μl/min. Apparent K_D values were estimated using the BIAevaluation software, version 2.0 (GE Healthcare). Experiments determining K_D values for PtdIns(3)P were carried out by collecting four independent experiments.

Acknowledgments

We thank Dr. Janet Webster for critical reading and comments on the manuscript.

References

1. Chen W, Li N, Chen T, Han Y, Li C, Wang Y, He W, Zhang L, Wan T, Cao X (2005) The Lysosome-associated apoptosis-inducing protein containing the pleckstrin homology (PH) and FYVE domains (LAPF), representative of a novel family of PH and FYVE domain-containing proteins, induces caspase-independent apoptosis via the lysosomal-mitochondrial pathway. J Biol Chem 280:40985-40995.

2. Matsuda-Lennikov M, Suizu F, Hirata N, Hashimoto M, Kimura K, Nagamine T, Fujioka Y, Ohba Y, Iwanaga T, Noguchi M (2014) Lysosomal interaction of Akt with Phafin2: A critical step in the induction of autophagy. PloS ONE 9(1):e79795.

3. Lin WJ, Yang CY, Lin YC, Tsai MC, Yang CW, Tung CY, Ho PY, Kao FJ, Lin CH (2010) Phafin2 modulates the structure and function of endosomes by a Rab5-dependent mechanism. Biochem Biophys Res Comm 391:1043-1048.

4. Pedersen NM, Raiborg C, Brech A, Skarpen E, Roxrud I, Platta HW, Liestol K, Stenmark H (2012) The PtdIns3P-binding protein Phafin2 mediates epidermal growth factor receptor degradation by promoting endosome fusion. Traffic 13:1547-1563.

5. Lin WJ, Yang CY, Li LL, Yi YH, Chen KW, Lin YC, Liu CC, Lin CH (2012) Lysosomal targeting of phafin1 mediated by Rab7 induces autophagosome formation. Biochem Biophys Res Comm 417:35-42.

6. Gailite I, Egger-Adam D, Wodarz A (2012) The phosphoinositide-associated protein rush hour regulates endosomal trafficking in drosophila. Mol Biol Cell 23:433-447.

7. Li C, Liu Q, Li N, Chen W, Wang L, Wang Y, Yu Y, Cao X (2008) Eapf/phafin-2, a novel endoplasmic reticulum-associated protein, facilitates TNF-alpha-triggered cellular apoptosis through endoplasmic reticulum-mitochondrial apoptotic pathway. J Mol Med 86:471-484.

8. Demeler B (2010) Methods for the design and analysis of sedimentation velocity and sedimentation equilibrium experiments with proteins. In: John EC, Ben MD, David, WS, Paul, TW, Ed. Curr Prot Protein Sci. John Wiley & Sons, New York, pp1-24.

9. Erickson HP (2009) Size and shape of protein molecules at the nanometer level determined by sedimentation, gel filtration, and electron microscopy. Biol Proced Online 11:32-51.

10. Lau SY, Taneja AK, Hodges RS (1984) Synthesis of a model protein of defined secondary and quaternary structure. Effect of chain length on the stabilization and formation of two-stranded alpha-helical coiled-coils. J Biol Chem 259:13253-13261.

11. Kelly SM, Jess TJ, Price NC (2005) How to study proteins by circular dichroism. Biochim Biophys Acta 1751:119-139.

12. Shaw KL, Scholtz JM, Pace CN, Grimsley GR (2009) Determining the conformational stability of a protein using urea denaturation curves. Methods Mol Biol 490:41-55.

13. Mello CC, Barrick D (2004) An experimentally determined protein folding energy landscape. Proc Natl Acad Sci U S A 101:14102-14107.

14. Patra M, Mukhopadhyay C, Chakrabarti A (2015) Probing conformational stability and dynamics of erythroid and nonerythroid spectrin: Effects of urea and guanidine hydrochloride. PloS ONE 10(1):e0116991.

15. Gruszka DT, Whelan F, Farrance OE, Fung HK, Paci E, Jeffries CM, Svergun DI, Baldock C, Baumann CG, Brockwell DJ, Jennifer RP, Jane C (2015) Cooperative folding of intrinsically disordered domains drives assembly of a strong elongated protein. Nat Commun 6:7271.

16. Freire E, Murphy KP (1991) Molecular basis of co-operativity in protein folding. J Mol Biol 222:687-698.

17. Zweifel ME, Leahy DJ, Barrick D (2005) Structure and notch receptor binding of the tandem wwe domain of deltex. Structure 13:1599-1611.

18. Courtemanche N, Barrick D (2008) Folding thermodynamics and kinetics of the leucine-rich repeat domain of the virulence factor internalin b. Protein Sci 17:43-53.

19. Haupt C, Weininger U, Kovermann M, Balbach J (2011) Local and coupled thermodynamic stability of the two-domain and bifunctional enzyme slyd from *Escherichia coli*. Biochemistry 50(34):7321-7329.

20. Kutateladze TG (2010) Translation of the phosphoinositide code by PI effectors. Nat Chem Biol 6:507-513.

21. Moravcevic K, Oxley CL, Lemmon MA (2012) Conditional peripheral membrane proteins: Facing up to limited specificity. Structure 20:15-27.

22. Teo H, Gill DJ, Sun J, Perisic O, Veprintsev DB, Vallis Y, Emr SD, Williams RL (2006) ESCRT-I core and ESCRT-II glue domain structures reveal role for glue in linking to ESCRT-I and membranes. Cell 125:99-111.

23. Kutateladze TG (2006) Phosphatidylinositol 3-phosphate recognition and membrane docking by the FYVE domain. Biochim Biophys Acta 1761:868-877.

24. Kelley LA, Mezulis S, Yates CM, Wass MN, Sternberg MJ (2015) The phyre2 web portal for protein modeling, prediction and analysis. Nat Prot 10:845-858.

25. Kutateladze TG, Capelluto DG, Ferguson CG, Cheever ML, Kutateladze AG, Prestwich GD, Overduin M (2004) Multivalent mechanism of membrane insertion by the FYVE domain. J Biol Chem 279:3050-3057.

26. Capelluto DG, Kutateladze TG, Habas R, Finkielstein CV, He X, Overduin M (2002) The dix domain targets dishevelled to actin stress fibres and vesicular membranes. Nature 419:726-729.

27. Lee W, Lazar IM (2014) Endogenous protein "barcode" for data validation and normalization in quantitative ms analysis. Anal Chem 86:6379-6386.

28. Deng J, Lazar IM (2016) Proteolytic digestion and TiO2 phosphopeptide enrichment microreactor for fast ms identification of proteins. J Am Soc Mass Spectrom 27:686-698.

29. Cao W, Demeler B (2005) Modeling analytical ultracentrifugation experiments with an adaptive space-time finite element solution of the lamm equation. Biophys J 89:1589-1602.

30. Brookes E, Cao W, Demeler B (2010) A two-dimensional spectrum analysis for sedimentation velocity experiments of mixtures with heterogeneity in molecular weight and shape. Eur Biophys J 39:405-414.

31. Gorbet G, Devlin T, Hernandez Uribe BI, Demeler AK, Lindsey ZL, Ganji S, Breton S, Weise-Cross L, Lafer EM, Brookes EH, Demeler B (2014) A parametrically constrained optimization method for fitting sedimentation velocity experiments. Biophys J 106:1741-1750.

32. Delaglio F, Grzesiek S, Vuister GW, Zhu G, Pfeifer J, Bax A (1995) Nmrpipe-a multidimensional spectral processing system based on unix pipes. J Biomol NMR 6:277-293.

33. Xiao S, Brannon MK, Zhao X, Fread KI, Ellena JF, Bushweller JH, Finkielstein CV, Armstrong GS, Capelluto DG (2015) Tom1 modulates binding of tollip to phosphatidylinositol 3-phosphate via a coupled folding and binding mechanism. Structure 23:1910-1920.

Tables:

Table 1. Identification of human Phafin2. MS/MS results obtained on peptides generated by trypsin proteolysis of Phafin2.

Peptide	Phafin2	Sequence
1	14-34	RISIVENCFGAAGQPLTIPGR
2	15-44	ISIVENCFGAAGQPLTIPGRVLIGEGVLTK
3	35-47	VLIGEGVLTKLCR
4	74-97	YNKQHIIPLENVTIDSIKDEGDLR
5	98-107	NGWLIKTPTK
6	108-119	SFAVYAATATEK
7	120-128	SEWMNHINK
8	137-163	SGKTPSNEHAAVWVPDSEATVCMRCQK
9	140-165	TPSNEHAAVWVPDSEATVCMRCQKAK
10	177-191	KCGFVVCGPCSEKR
11	191-202	RFLLPSQSSKPVR
12	192-223	FLLPSQSSKPVRICDFCYDLLSAGDMATCQPAR
13	224-249	SDSYSQSLKSPLNDMSDDDDDDDSSD

Table 2. Thermodynamic parameters obtained from urea- and GuHCl-induced denaturation of Phafin2.

Condition	Probe	ΔG^0_{H2O} (kcal mol^{-1})	*m*, kcal mol^{-1} M^{-1}	C_m, M
Urea	Fluorescence	4.07	1.19	3.42
	CD	4.00	1.16	3.45
GuHCl	Fluorescence	3.80	2.93	1.30
	CD	3.75	2.48	1.51

Figure legends:

Figure 1. Purification of human Phafin2. (A) Modular organization of Phafin2. (B) SDS-PAGE showing IPTG-induced overexpression and purification of GST-Phafin2.

Figure 2. Phafin2 is an elongated monomer. (A) Analytical size-exclusion chromatography showing that Phafin2 eluted between ovalbumin and chymotrypsinogen A. The standards were: BSA (67 kDa), ovalbumin (44 kDa), chymotrypsinogen (25 kDa), myoglobin (17 kDa), and cytochrome C (12.4 kDa). (B) SDS-PAGE showing the purity and size of Phafin2 from the chromatographic peak displayed in (A). (C) DLS plot of Phafin2 at 25 °C.

Figure 3. Sedimentation velocity AUC analysis of Phafin2. (A) Representative interference scans of Phafin2 tracked during AUC. (B) Representative residuals obtained from the data fitting analysis described in Methods. (C) Representative molecular mass distribution of Phafin2 in relationship with its frictional ratio and partial concentration of the protein.

Figure 4. Phafin2 is an α/β protein that undergoes local conformational changes upon PtdIns(3)P binding. (A) Far-UV CD spectra of Phafin2 in the absence and presence of 2-fold PtdIns(3)P. (B) Near-UV CD spectra of Phafin2 in the absence and presence of 2-fold PtdIns(3)P. (C) Intrinsic tryptophan fluorescence of Phafin2 titrated with PtdIns(3)P.

Figure 5. Thermostability of Phafin2. Thermal denaturation plot of Phafin2 monitored by CD spectroscopy. Data represents an average of three independent experiments.

Figure 6. NMR studies of Phafin2. TROSY-HSQC spectrum of ^{1}H, ^{15}N-labeled Phafin2 collected at 30 °C.

Figure 7. Urea- and GuHCl-mediated denaturation of Phafin2 followed by tryptophan fluorescence and CD spectroscopy. (A) Fluorescence emission spectra of Phafin2 in the absence (solid line) and presence of 6 M urea (dashed line) or 8 M GuHCl (dotted line). (B) Changes in the fluorescence intensity of Phafin2 at 339 nm induced by increasing urea (filled circles) or GuHCl (empty circles) concentrations. (C) Changes in the CD ellipticity of Phafin2 at 222 nm induced by increasing urea (filled circles) or GuHCl (empty circles) concentrations.

Figure 8. Analysis of Phafin2 binding to PtdIns(3)P. (A) Raw SPR sensorgram for the association of Phafin2 to PtdIns(3)P liposomes, in which the lipid was incorporated in liposomes containing dioleoyl phosphatidylcholine and immobilized onto an L1 sensorchip flow cell. The other flow cell contained dioleoyl phosphatidylcholine liposomes employed as a control. Binding kinetics were recorded at room temperature. The concentrations of Phafin2 flown on the sensor chip are color-coded. a.u., arbitrary units. Data is a representation of four independent experiments. (B) Structure of human Phafin2 modeled using Phyre2. The potential PtdIns(3)P-dependent membrane-binding sites in the PH domain (left, in olive) and in the FYVE domain (right, in pink) are boxed. (D-E) A close-up view of the putative PtdIns(3)P-binding sites in the PH (C) and FYVE (D) domains. The regions displayed correspond to the 49-KPKAR-53 motif in the PH domain and the 149-WVPD-152, 171-RRHHCR-176, and 202-RVC-204 motifs in the FYVE domain.

Figure 1.

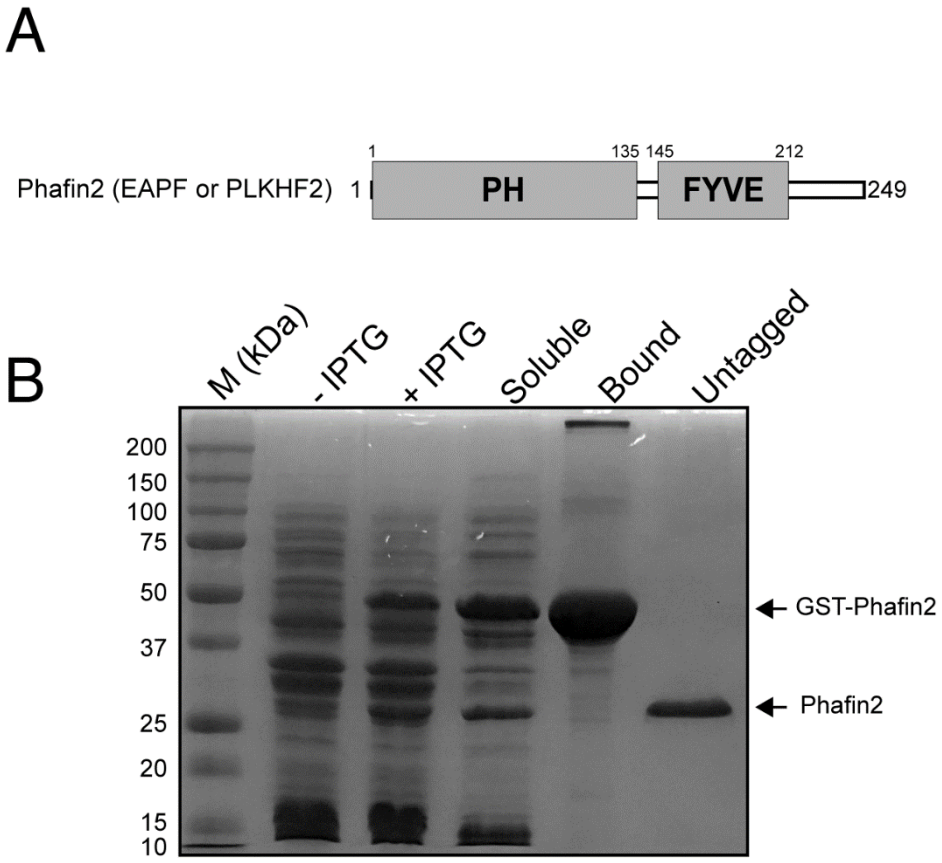
A
Phafin2 (EAPF or PLKHF2)
1
135 145
212
249
PH
FYVE
B
M (kDa)
- IPTG
+ IPTG
Soluble
Bound
Untagged
200
150
100
75
50
37
25
20
15
10
GST-Phafin2
Phafin2

Figure 2.

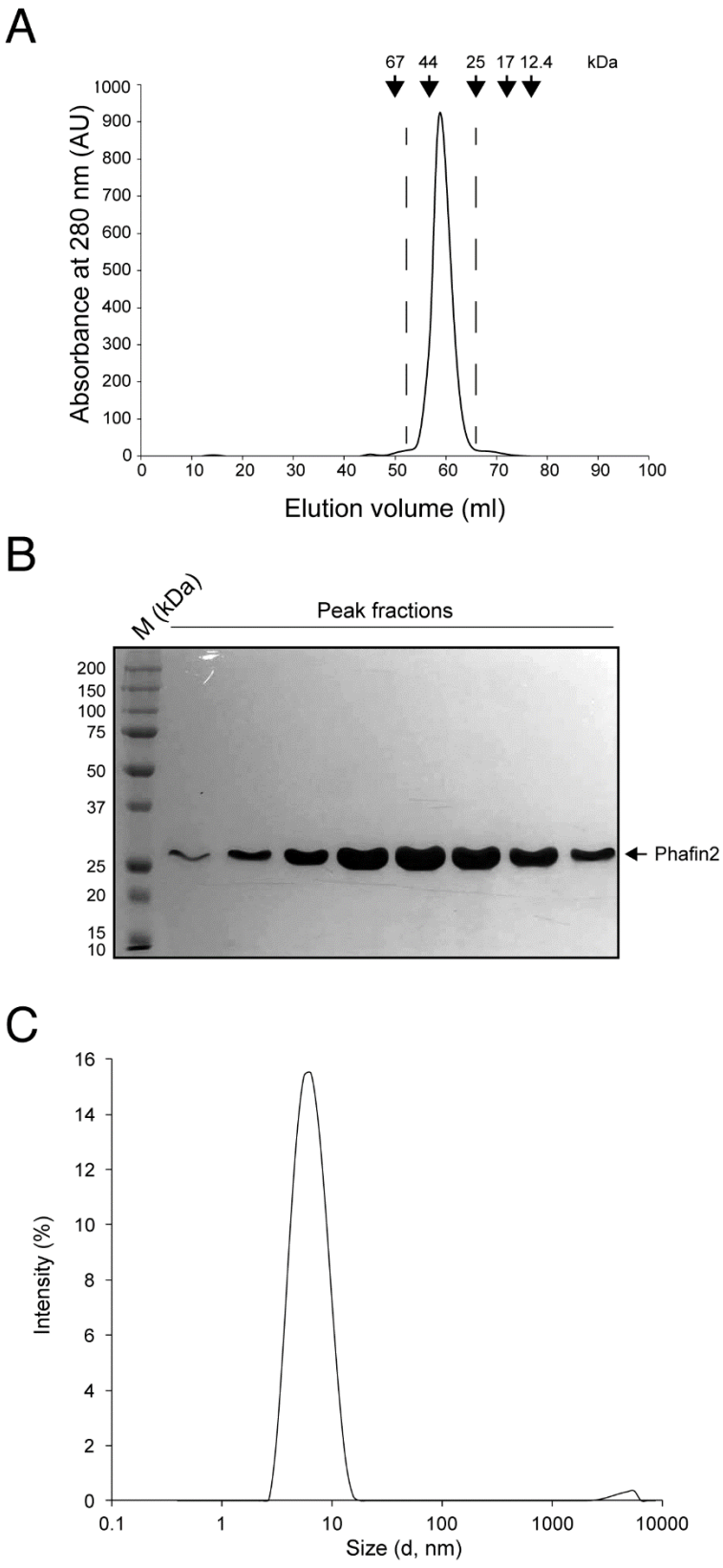
A
67 44 25 17 12.4 kDa
Absorbance at 280 nm (AU)
Elution volume (ml)
B
M (kDa)
Peak fractions
200
150
100
75
50
37
25
20
15
10
Phafin2
C
Intensity (%)
Size (d, nm)

Figure 3.

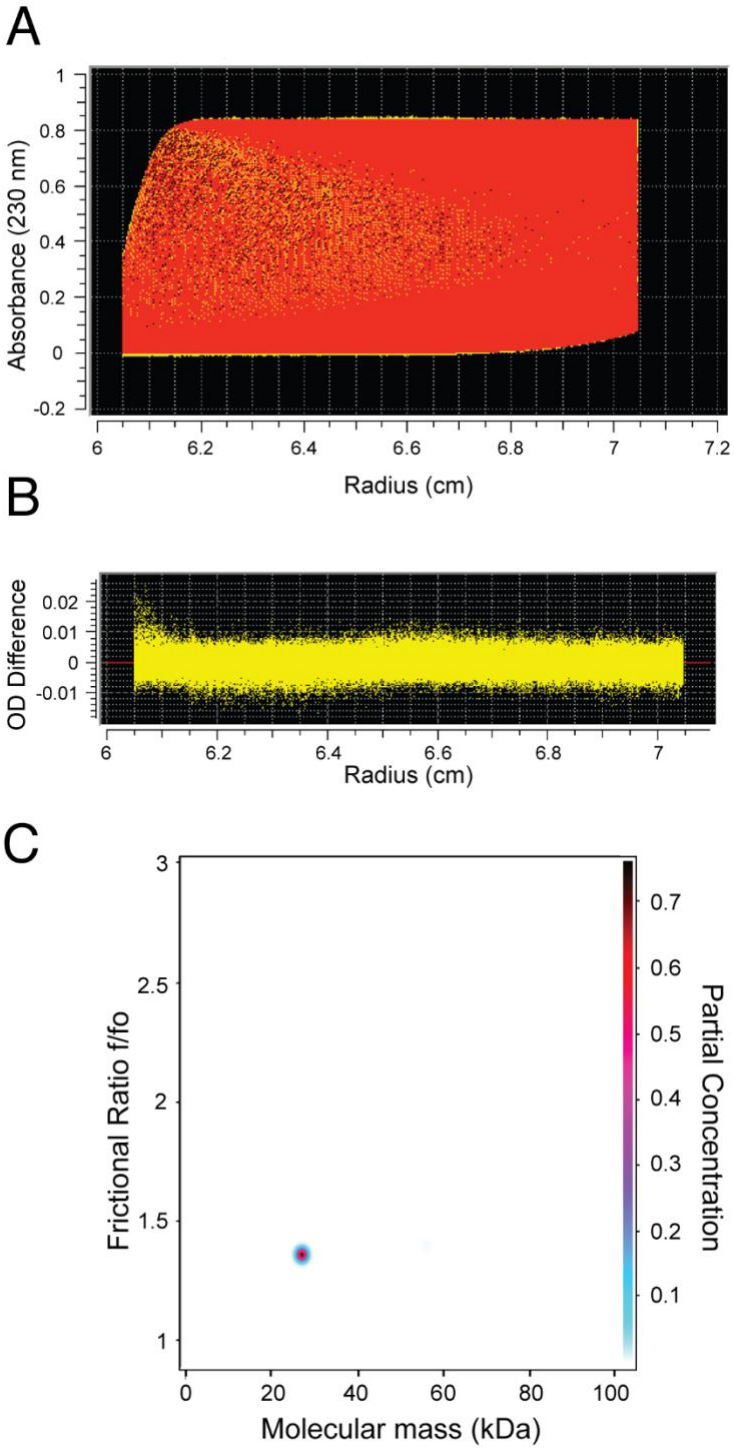
A
Absorbance (230 nm)
1
0.8
0.6
0.4
0.2
0
-0.2
6
6.2
6.4
6.6
6.8
7
7.2
Radius (cm)
B
OD Difference
0.02
0.01
0
-0.01
6
6.2
6.4
6.6
6.8
7
Radius (cm)
C
Frictional Ratio f/fo
3
2.5
2
1.5
1
0
20
40
60
80
100
Molecular mass (kDa)
Partial Concentration
0.7
0.6
0.5
0.4
0.3
0.2
0.1

Figure 4.

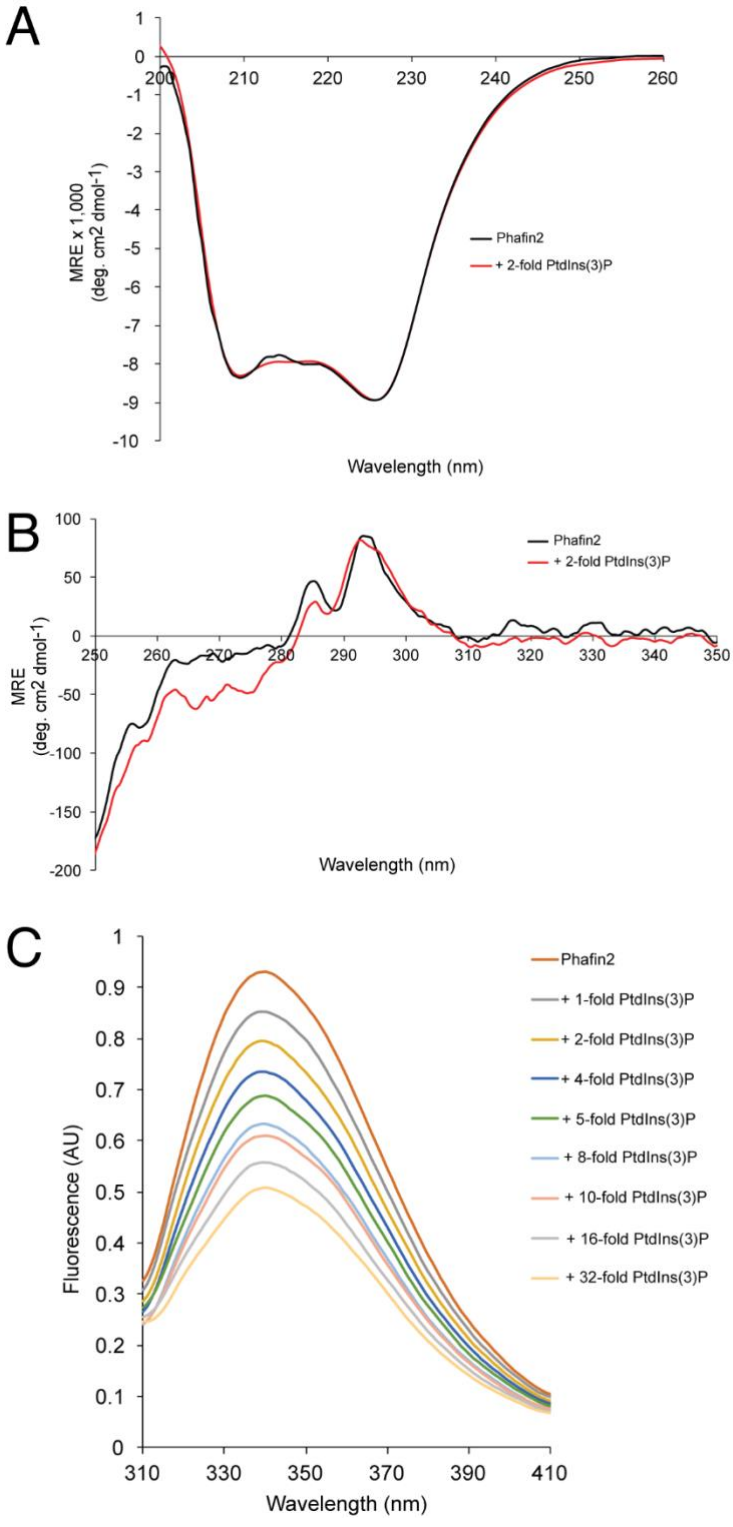
A
MRE x 1,000
(deg. cm2 dmol-1)
Wavelength (nm)
Phafin2
+ 2-fold PtdIns(3)P
B
MRE
(deg. cm2 dmol-1)
Wavelength (nm)
Phafin2
+ 2-fold PtdIns(3)P
C
Fluorescence (AU)
Wavelength (nm)
Phafin2
+ 1-fold PtdIns(3)P
+ 2-fold PtdIns(3)P
+ 4-fold PtdIns(3)P
+ 5-fold PtdIns(3)P
+ 8-fold PtdIns(3)P
+ 10-fold PtdIns(3)P
+ 16-fold PtdIns(3)P
+ 32-fold PtdIns(3)P

Figure 5.

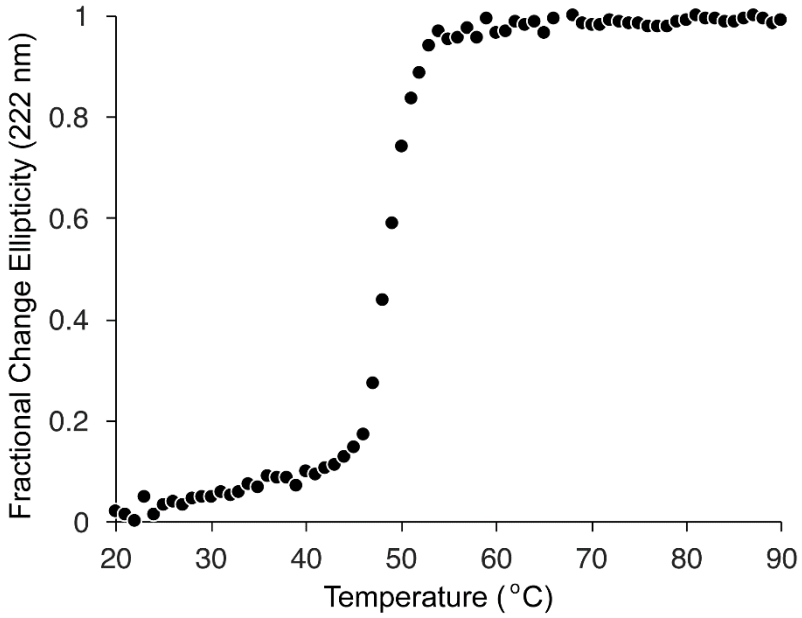
Fractional Change Ellipticity (222 nm)
1
0.8
0.6
0.4
0.2
0
20
30
40
50
60
70
80
90
Temperature (°C)

Figure 6.

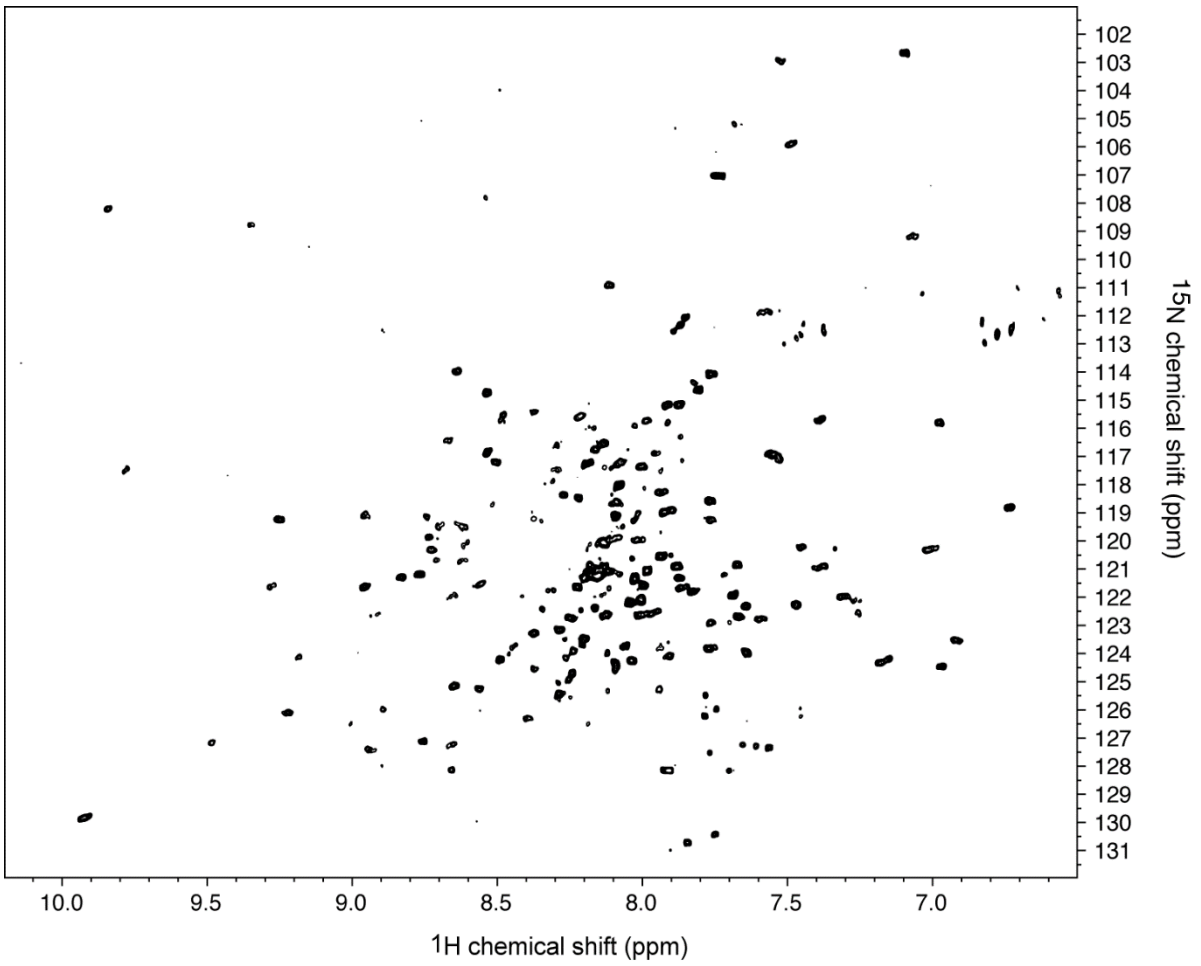
102
103
104
105
106
107
108
109
110
111
112
113
114
115
116
117
118
119
120
121
122
123
124
125
126
127
128
129
130
131
15N chemical shift (ppm)
10.0
9.5
9.0
8.5
8.0
7.5
7.0
1H chemical shift (ppm)

Figure 7.

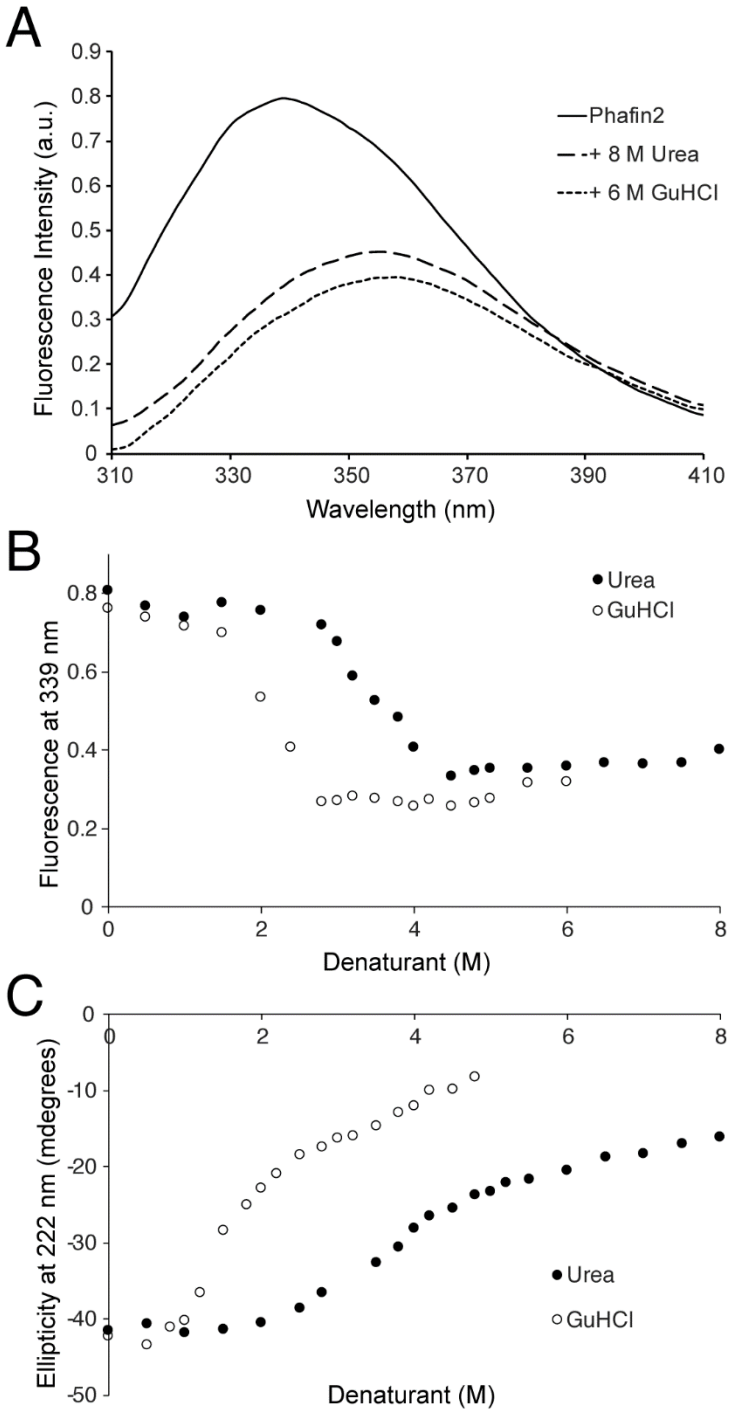
A
Fluorescence Intensity (a.u.)
Wavelength (nm)
Phafin2
+ 8 M Urea
+ 6 M GuHCl
B
Fluorescence at 339 nm
Denaturant (M)
Urea
GuHCl
C
Ellipticity at 222 nm (mdegrees)
Denaturant (M)
Urea
GuHCl

Figure 8.

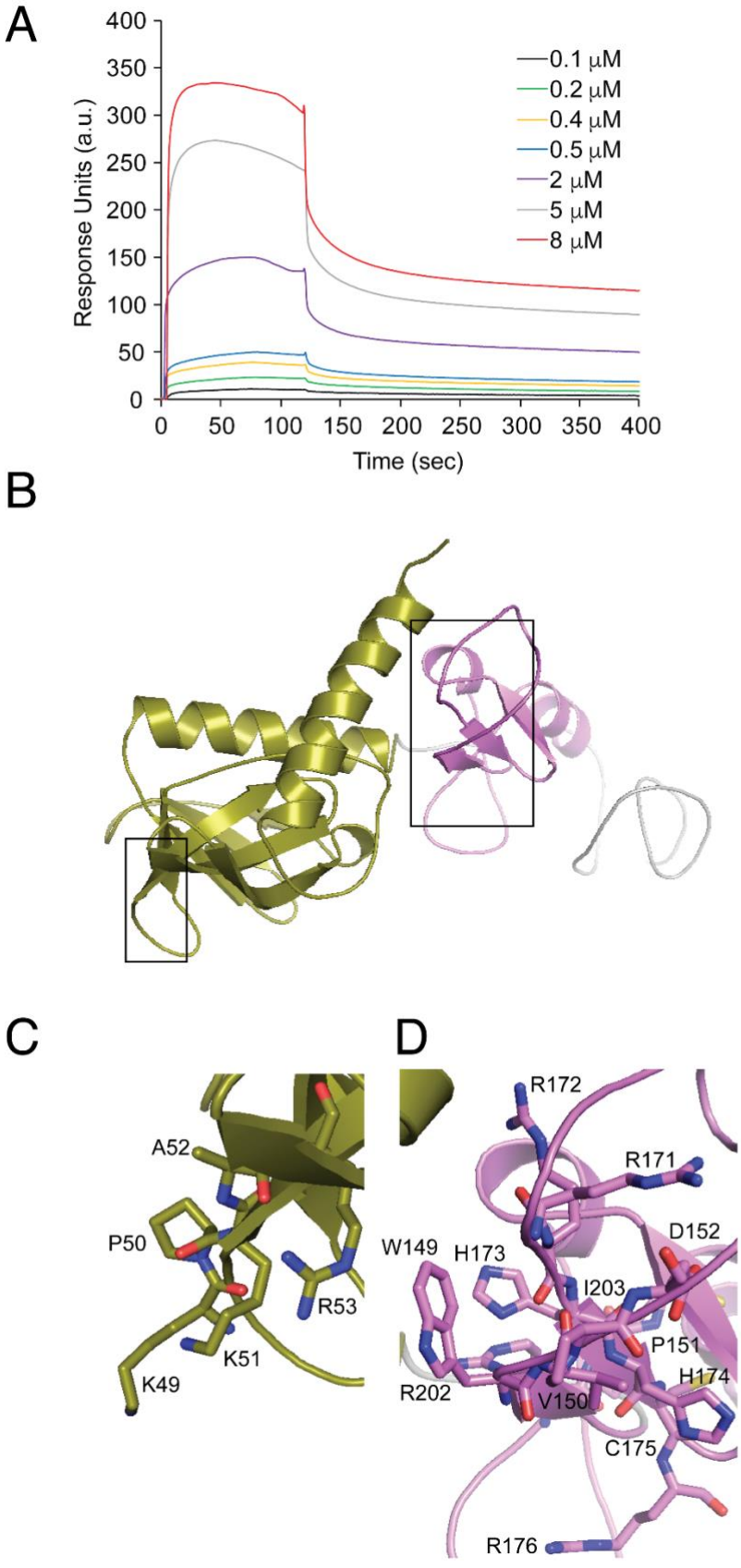
A
Response Units (a.u.)
Time (sec)
0.1 μM
0.2 μM
0.4 μM
0.5 μM
2 μM
5 μM
8 μM
B
C
A52
P50
R53
K51
K49
D
R172
R171
D152
W149
H173
I203
P151
H174
R202
V150
C175
R176

Supplementary Information

Structural, thermodynamic, and phosphatidylinositol 3-phosphate binding properties of Phafin2

Tuo-Xian Tang, Ami Jo, Jingren Deng, Jeffrey F. Ellena,
Iulia M. Lazar, Richey M. Davis, and Daniel G. S. Capelluto *

Table S1. Identification of human Phafin2. MS/MS results obtained on additional 16 peptides generated by trypsin proteolysis of Phafin2.

Peptide	Phafin2	Sequence
1	15-34	ISIVENCFGAAGQPLTIPGR
2	35-44	VLIGEGVLTK
3	74-91	YNKQHIIPLENVTIDSIK
4	77-91	QHIIPLENVTIDSIK
5	77-97	QHIIPLENVTIDSIKDEGDLR
6	77-103	QHIIPLENVTIDSIKDEGDLRNGWLIK
7	104-119	TPTKSFAVYAATATEK
8	107-128	SFAVYAATATEKSEWMNHINK
9	137-160	SGKTPSNEHAAVWVPDSEATVCMR
10	140-160	TPSNEHAAVWVPDSEATVCMR
11	140-163	TPSNEHAAVWVPDSEATVCMRCQK
12	177-190	KCGFVVCGPCSEK
13	178-190	CGFVVCGPCSEK
14	192-202	FLLPSQSSKPVR
15	203-223	ICDFCYDLLSAGDMATCQPAR
16	233-249	SPLNDMSDDDDDDDSSD

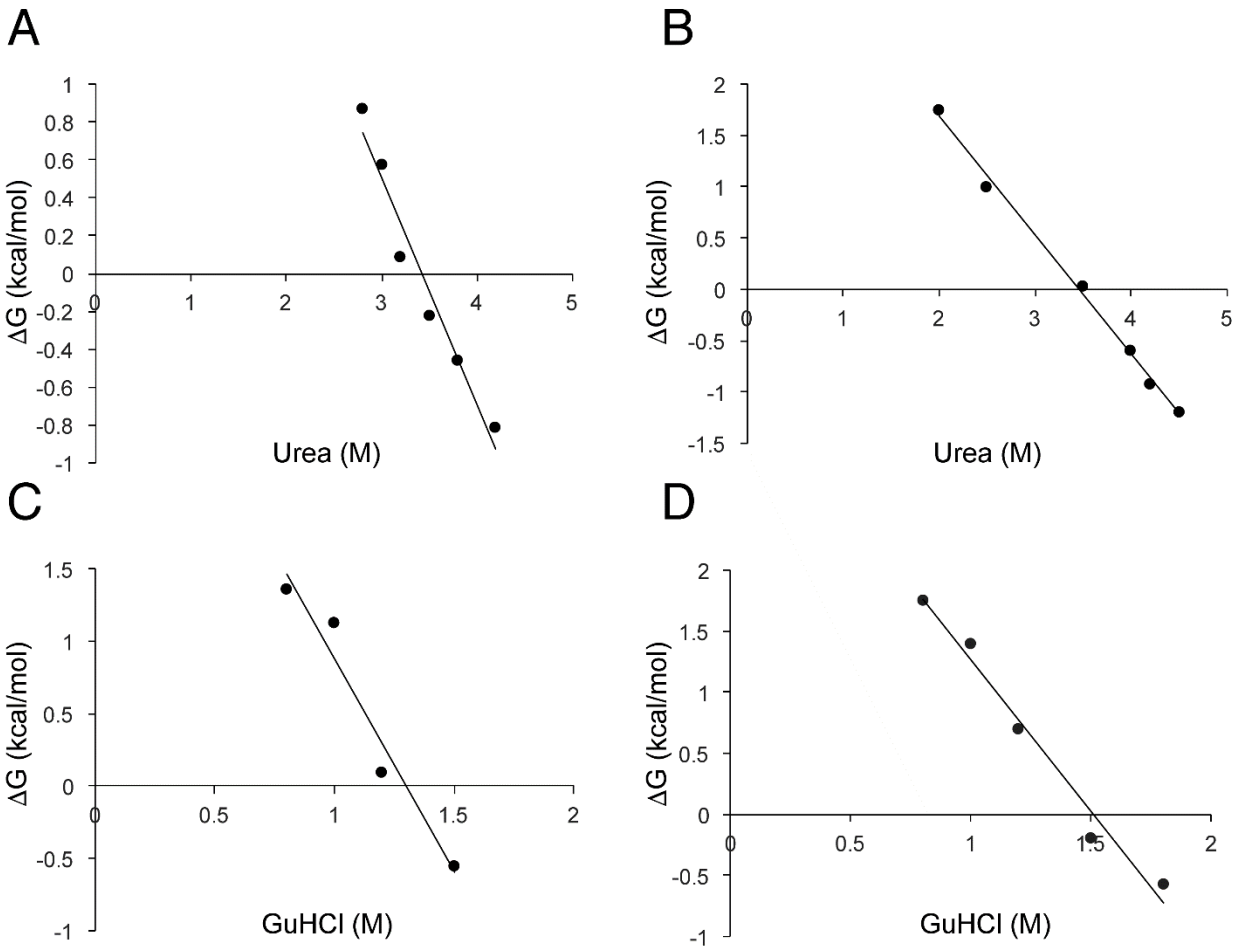

Supplementary Figure 1. Gibbs free energy change (ΔG) in the transition region plotted as a function of the denaturant concentration. (A-B) Urea denaturation plots of Phafin2 monitored by intrinsic tryptophan fluorescence (A) and far-UV circular dichroism (B). (C-D) Guanidine hydrochloride denaturation plots of Phafin2 monitored by intrinsic tryptophan fluorescence (C) and far-UV circular dichroism (D). The ΔG^0_{H2O} was estimated from the intercept on the Y axis using the linear extrapolation method.

Chapter 3 The C-terminal acidic motif of Phafin2 inhibits PH domain binding to phosphatidylinositol 3-phosphate

Tuo-Xian Tang [a], Carla V. Finkielstein [b], and Daniel G. S. Capelluto [a,*]

[a] Protein Signaling Domains Laboratory, Department of Biological Sciences, Fralin Life Sciences Institute, and Center for Soft Matter and Biological Physics, Virginia Tech, Blacksburg, VA 24061, United States

[b] Integrated Cellular Responses Laboratory, Department of Biological Sciences, Fralin Life Sciences Institute, 1015 Life Science Circle, Virginia Tech, Blacksburg, VA 24061, United States

Author Contributions

Tuo-Xian Tang: Conceptualization; Methodology; Formal analysis; **Carla V. Finkielstein:** Conceptualization; Writing; **Daniel G. S. Capelluto**: Conceptualization; Methodology; Investigation; Formal analysis; Resources; Supervision; Writing; Project administration.

As published in *Biochimica et Biophysica Acta (BBA) - Biomembranes*:

Tang, T.-X., Finkielstein, C. V., & Capelluto, D. G. S. (2020). The C-terminal acidic motif of Phafin2 inhibits PH domain binding to phosphatidylinositol 3-phosphate. *Biochimica et Biophysica Acta (BBA) - Biomembranes*, 1862(6), 183230.

DOI: https://doi.org/10.1016/j.bbamem.2020.183230

Abstract

Changes in membrane curvature are required to control the function of subcellular compartments; malfunctions of such processes are associated with a wide range of human diseases. Membrane remodeling often depends upon the presence of phosphoinositides, which recruit protein effectors for a variety of cellular functions. Phafin2 is a phosphatidylinositol 3-phosphate (PtdIns3P)-binding effector involved in endosomal and lysosomal membrane-associated signaling. Both the Phafin2 PH and the FYVE domains bind PtdIns3P, although their redundant function in the protein is unclear. Through a combination of lipid-binding assays, we found that, unlike the FYVE domain, recognition of the PH domain to PtdIns3P requires a lipid bilayer. Using site-directed mutagenesis and truncation constructs, we discovered that the Phafin2 FYVE domain is constitutive for PtdIns3P binding, whereas PH domain binding to PtdIns3P is autoinhibited by a conserved C-terminal acidic motif. These findings suggest that binding of the Phafin2 PH domain to PtdIns3P in membrane compartments occurs through a highly regulated mechanism. Potential mechanisms are discussed throughout this report.

Keywords: Phafin2; FYVE domain; PH domain; phosphatidylinositol 3-phosphate; surface plasmon resonance; isothermal titration calorimetry.

1. Introduction

Membrane remodeling is an essential process that controls flux through subcellular compartments. Malfunctions have been linked to a number of human diseases including cancer, immune disorders, and muscular and neuronal diseases [1]. Membrane remodeling for cellular events, such as for tethering, fusion, fission, or bending, is often driven by phosphoinositides [2]. These lipids, despite having very low-abundance, recruit phosphoinositide-binding protein effectors when they cluster together, triggering a wide variety of membrane-associated processes. An example of this is observed in cellular autophagy (self-eating), in which phosphoinositides are the master regulators. Due to their inverted cone shape, phosphoinositides facilitate membrane bending in autophagic organelles [3]. Furthermore, recruitment of protein effectors to the plasma membrane or to lysosomal membranes inhibit or activate autophagy, respectively, depending upon what phosphoinositide is produced [4].

The pro-autophagic protein effector Phafin2 is an elongated monomer [5] that contains an N-terminal PH (Pleckstrin Homology) domain followed by a central FYVE (Fab1, YOTB, Vac1, and EEA1) domain. Both domains are proposed to bind phosphatidylinositol 3-phosphate (PtdIns3P) [6], a major phosphoinositide found at endosomal and lysosomal membrane surfaces [7]. Phafin2 induces autophagy when coupled with lysosomal PtdIns3P and the serine/threonine kinase v-AKT murine thymoma viral oncogene homolog (AKT) [6]. The Phafin2/AKT/PtdIns3P complex is required for bacterial digestion and lipopolysaccharide-induced autophagy in macrophages [6]. Genetic polymorphism of Phafin2 has been associated with high levels of interferon-α in patients with systemic lupus erythematosus [8], providing a link between the reported deficiencies in autophagy and this inflammatory disease [9].

In a PtdIns3P-dependent process, Phafin2 binding to endosomal membranes is required to control Rab5 activity by an uncharacterized mechanism [10] and to promote endosomal enlargement, a process that has also been observed to be mediated by other Phafin family proteins, including Phafin1 and Rush [10-13]. Indeed, Phafin2 associates to the early endosome antigen 1 (EEA1), an endosomal protein that controls protein trafficking and membrane fusion events *via* its FYVE domain [11]. More recently, Phafin2 has been shown to escort macropinosomes in a PtdIns3P-dependent process and by association to the actin crosslinking protein Filamin A [14].

The PH domains are ~100-amino acid globular modules found in proteins involved in cell signaling and as components of the cytoskeleton [15]. Despite displaying low sequence conservation, most of their structures are characterized by the presence of seven β-strands, which form two perpendicular anti-parallel β-sheets, and a short α-helix at the C-terminus [16]. Most PH domains are lipid-binding modules that exhibit a wide range of specificities for membrane phosphoinositides [16]; however, some are also reported to mediate protein-protein interactions [17]. The PH domains are classified into four distinct classes based on their preferences for phosphoinositide binding [18]. Whereas the most common phosphoinositide ligands for PH domains are the polyphosphorylated phosphoinositides, few PH domains are reported to directly bind PtdIns3P. Some that do are those found in the vacuolar protein-sorting associated protein 36 (Vps36) [19] and *Toxoplasma gondii* PH-containing protein-1 (TgPH1) [20]. The FYVE domains, on the other hand, are small zinc-binding modules that, in most cases, specifically bind to PtdIns3P and serve as a bridge for numerous cytosolic proteins to be recruited at PtdIns3P-containing membrane compartments, including endosomes, phagosomes, lysosomes, and multivesicular bodies. The exception is the FYVE-like domain of caspase 8/10-associated RING protein 2 (CARP2), which is unable to bind PtdIns3P or insert into lipid bilayers due to structural differences and a lack of critical PtdIns3P-binding residues found in canonical FYVE domains [21]. Other FYVE domains, such as those found in the Fgd proteins, have been suggested to display broader specificity for phosphoinositides [22]. Structurally, FYVE domains exhibit a common fold comprising two double-stranded antiparallel β-sheets and two α-helices [23]. As demonstrated for the EEA1, hepatocyte growth factor-regulated tyrosine kinase substrate (Hrs), RUN and FYVE domain containing 1 (RUFY1), and WD repeat and FYVE domain-containing protein 1 (WDFY1) containing-FYVE domain proteins, binding to PtdIns3P is driven by two proximal histidine residues and occurs in a pH-dependent manner [24]. Curiously, binding of the Phafin2 FYVE domain to PtdIns3P appears to be pH-independent [25]. Most FYVE domain-containing proteins control endosomal fusion events as well as endosomal protein trafficking [26]. In addition to PtdIns3P, few PH and FYVE-containing proteins were reported to display a hydrophobic insertion loop that serves as a supplementary point of contact for nonspecific electrostatic interactions with membrane acidic lipids [27, 28].

As Phafin2 presents a PH domain followed by a FYVE domain, both of which are reported to bind PtdIns3P, we investigated whether each domain displays unique features that distinguish one from the other and, thus, should avoid redundancy in lipid binding. Using a combination of lipid binding assays, we demonstrated that in Phafin2, the FYVE domain binds constitutively to PtdIns3P, whereas binding of the PH domain to the phosphoinositide is downregulated by a conserved C-terminal acidic motif. Furthermore, we show that the Phafin2 PH domain binds PtdIns3P only when the phosphoinositide is embedded in a lipid bilayer. Possible scenarios of PH domain activation for PtdIns3P binding are discussed in this report.

2. Material and methods

2.1. Materials

Dibutanoyl and dipalmitoyl PtdIns3P were purchased from Echelon Biosciences, whereas dioleoyl phosphatidylcholine (PtdCho) and dioleoyl phosphatidylserine (PtdSer) were obtained from Avanti Lipids.

2.2. Cloning and mutagenesis of Phafin2

Human Phafin2 cDNA was amplified from a human liver cDNA library (Clontech) by PCR and ligated into a pGEX4T3 vector (GE Healthcare). The PH (residues 1-135) and FYVE (residues 145-212) domains were subcloned into pGEX6P1 and pGEX4T3 vectors (GE Healthcare), respectively, between BamH1 and EcoRI restriction enzyme sites. Deletion of the polyD region at the C-terminus of Phafin2 consisted of the removal of residues 240-249. All these constructs were used as templates for producing the reported mutants by employing site-directed mutagenesis.

2.3. Expression and purification of recombinant proteins

Proteins were expressed in *Escherichia coli* (Rosetta; Stratagene). Protein overexpression and purification were performed as previously reported [5].

2.4 Protein-lipid overlay assay

Membrane strips were prepared by immobilizing 1 μl of the indicated amount of PtdIns3P dissolved in chloroform/methanol/water (65:35:8) onto Hybond-C extra membranes (GE Healthcare) and dried for 1 h at room temperature. To avoid nonspecific protein binding, membrane strips were blocked with 3% (w/v) fatty acid-free BSA (Sigma) in 20 mM Tris-HCl

(pH 8.0), 150 mM NaCl, and 0.1 % Tween-20 for 1 h at room temperature. Blocked membranes were incubated with GST fusion proteins (1 μg/mL) in the same buffer overnight at 4°C. After four washes with the same buffer without fatty acid-free BSA, bound proteins were first probed with rabbit anti-GST antibodies (Proteintech) followed by incubation with donkey anti-rabbit-horseradish peroxidase antibodies (GE Healthcare). Visualization of protein binding to PtdIns3P was possible by the use of the Supersignal West Pico chemiluminescent reagent (Pierce).

2.5. Liposome sedimentation assay

PtdCho liposomes, with or without either 10% PtdIns3P or 20% PtdSer, were prepared by hydration of a lipid film with a buffer containing 20 mM HEPES, pH 7.3, 100 mM NaCl, followed by extrusion using 100-nm membranes (Avanti Polar Lipids). Two hundred microliters of liposomes (~2 mg/ml lipid) were mixed with 200 μl of untagged protein (20 μM) and incubated for 1 h at room temperature. Protein bound to liposomes was sedimented by ultracentrifugation at 45,000 rpm (rotor TYPE 50.4 Ti; Beckman Coulter) for 1 h at 20 °C. Pellet and supernatant protein fractions were analyzed by SDS-PAGE. Semi-quantifications of protein binding to PtdIns3P- and PtdSer-containing liposomes were carried out by incubating the indicated untagged protein (20 μM) with liposomes containing the indicated concentrations of either PtdIns3P or PtdSer. Curve fitting was performed using GraphPad Prism. Binding data best fit the one-site binding (PH and FYVE domains with PtdIns3P) or specific binding with Hill slope (Phafin2 with PtdIns3P and PH domain with PtdSer) to estimate their corresponding apparent dissociation constant (K_D).

2.6. Surface plasmon resonance

Collection of surface plasmon resonance (SPR) data was performed on a BIAcore X100 instrument with a 100-nm-liposome-coated L1 sensorchip at room temperature. Phospholipids, including PtdCho (control), or PtdCho and PtdIns3P (1.5%), were solubilized in chloroform/methanol/water (65:35:0.8). The mixture was then dried under N_2 followed by vacuum to remove traces of chloroform. Lipid mixture was then resuspended in 20 mM HEPES (pH 7.0) and 100 mM NaCl to reach a final concentration of 4 mM, sonicated, and extruded for 100-nm liposome size at 65 °C. L1 sensorchips (GE Healthcare) with 20 mM HEPES (pH 7.0) and 100 mM NaCl as a running buffer were employed in all experiments. L1 sensorchip pretreatment was carried out using 40 mM octyl β-D-glucopyranoside. Then, at a 30 μl/min

flow rate, PtdCho liposomes were immobilized onto one of the L1 sensorchip channels whereas a second channel was loaded with PtdIns3P-containing liposomes. Typical liposome loading was ~5,000 response units/sensorchip channel. The BIAevaluation software, version 2.0 (GE Healthcare), was used to estimate the apparent K_D values.

2.7. Isothermal titration calorimetry

Isothermal titration calorimetry (ITC) measurements were carried out in 20 mM HEPES, pH 7.3, 100 mM NaCl. Water soluble dibutanoyl PtdIns3P at a concentration of 120 μM was titrated into 300 μl of 12-14 μM of untagged protein in a series of twelve injections of 3 μl each using a MicroCal PEAQ (Malvern) equilibrated at 25 °C. To test Phafin2 FYVE-PH domain interaction, 330 μM of untagged Phafin2 FYVE domain was titrated into 58 μM of untagged Phafin2 PH domain. All experiments were performed at least in triplicate. Data were analyzed using MicroCal PEAQ-ITC analysis software.

2.8. Circular dichroism spectropolarimetry

Far-UV circular dichroism (CD) spectra for all proteins were recorded using a Jasco J-815 spectropolarimeter with a temperature-controlled cell holder connected to a Peltier unit. Untagged Phafin2 proteins (20 μM each) were prepared in 5 mM sodium citrate (pH 7.3) and 50 mM KF. Five accumulated CD protein spectra were acquired at 25 °C with a scan speed of 50 nm/min and a response time of 1 s in a 1-mm path length quartz cell using a bandwidth of 1-nm. The estimated secondary structure content of the proteins were calculated using the CDSSTR algorithm available at the DICHROWEB server [29]. Final CD protein spectra were corrected for buffer background. Near-UV region measurements were recorded in a 1-mm cell containing 80 μM untagged proteins in 5 mM sodium citrate (pH 7.3) and 50 mM KF. Final CD protein spectra were corrected for buffer background.

3. Results and discussion

3.1. Mutations in the FYVE domain are sufficient to impair Phafin2 binding to PtdIns3P

Using the lipid-protein overlay assay, Phafin2 preferentially bound to PtdIns3P as observed with the PtdIns3P-binding Vamp7p PX domain (**Supplementary Fig. S1A**). This was consistent with an earlier report [6]. Also, combined mutations within the PH (R53C) and FYVE (R171/R172A) domains (**Fig. 1A**), which were previously reported in Phafin2 [6],

abolished PtdIns3P binding (**Supplementary Fig. S1B**) without altering the structure of the protein (**Supplementary Fig. S1C-D)**. We then investigated Phafin2 interactions with PtdIns3P using mimics of lipid bilayers such as by the use of 100-nm liposomes. PtdIns3P-dependent binding capacity was significantly reduced when Phafin2 was mutated in both domains (**Fig. 1B**). Using SPR detection, we estimated that Phafin2 bound PtdIns3P-liposomes with an apparent K_D of ~0.4 μM (**Supplementary Fig. S2A**), which was consistent with previous measurements [5]. As expected, Phafin2 R53C/R171A/R172A was unable to bind PtdIns3P-containing liposomes using SPR (**Supplementary Fig. S2B**). Next, we evaluated whether Phafin2 can bind water soluble dibutanoyl PtdIns3P using ITC. The critical micellar concentration for dioctanoyl PtdIns3P is 700±200 μM [30]. Because the final concentration of dibutanoyl PtdIns3P in the ITC sample cell ranges between 1.2-15 μM during titration, the lipid is expected to be primarily in a monodispersed form. Binding of water soluble PtdIns3P to Phafin2 was exothermic with the resulting isotherm best fitting a one binding site model (**Fig. 1C**) with a K_D of 3.21 μM and a ΔG of -7.51 kcal mol^{-1} (**Table 1**). Despite both the PH and FYVE domains being considered to be PtdIns3P-binding domains, unexpectedly, Phafin2 isotherms did not fit a two-binding site model (data not shown). Soluble PtdIns3P was also titrated into Phafin2 using tryptophan fluorescence and data best fit a one-site binding model with a resultant K_D of 1.9±0.4 μM (**Supplementary Fig. S2C**), which is very close to that estimated using ITC. The Phafin2 R53C/R171A/R172A mutant was impaired for binding to water-soluble PtdIns3P (**Supplementary Fig. S2D**), in agreement with the results obtained using PtdIns3P-containing liposomes (**Fig. 1B** and **Supplementary Fig. S2B**).

As ITC data suggested the presence of a single PtdIns3P-binding site in Phafin2, we next investigated whether both the PH and FYVE domains bind PtdIns3P in Phafin2 using the liposome sedimentation assay. Surprisingly, a mutation in the PH domain (Phafin2 R53C) did not alter Phafin2 binding to PtdIns3P-embedded liposomes, whereas mutations in the FYVE domain (Phafin2 R171A/R172A) were sufficient to significantly diminish lipid binding, mimicking the combined mutations in the PH and FYVE domains (**Fig. 1B**). Similar results were obtained using ITC, in which Phafin2 R53C bound soluble PtdIns3P with an affinity close to that observed for the wild type protein (**Fig. 1D; Table 1**). Also, mutations in the FYVE domain impaired Phafin2 binding to the soluble phosphoinositide (**Fig. 1E**). Overall, our results show that mutations in the FYVE domain are necessary and sufficient to completely abolish Phafin2 binding to PtdIns3P independent of the presence of a lipid bilayer.

3.2. The isolated PH and FYVE domains display unique properties for PtdIns3P binding

Previous reports suggest that the Phafin2 PH domain preferentially binds PtdIns3P [6, 14]. However, we were unable to detect the contribution of the PH domain in PtdIns3P binding in Phafin2. Our results then prompted us to isolate both the PH and FYVE domains of Phafin2 and analyze their functionality. To confirm that the boundaries of each domain were properly chosen, we collected CD spectra to characterize their structural features. At the far-UV region, the isolated PH domain showed two minima at 208 and 226 nm, indicating the presence of an α/β structure (**Fig. 2A**) with an estimated 20% α-helical and 27% β-sheet content. Although most PH domains are characterized by enriched β-stranded structures, few noncanonical PH domains exhibit α/β structures [31, 32] as observed for the Phafin2 PH domain. The near UV CD spectrum of the Phafin2 PH domain displayed a major peak at ~293 nm (**Fig. 2B**), likely representing a signal from the two tryptophan residues in the protein [33]. The far-UV CD spectrum of the isolated Phafin2 FYVE domain depicted a wide negative band, suggesting the presence of α and β structural elements (**Fig. 2C**). Despite the Phafin2 FYVE domain having one tyrosine, one tryptophan, and four phenylalanine residues, the protein displayed poor CD signals in the near-UV region (**Fig. 2D**). Proteins that exhibit poorly resolved CD spectra in this region are considered to present highly mobile side chains, although the chemical environment and the direct interaction between aromatic residues also contribute to this behavior [34].

Both Phafin2 PH and FYVE domains efficiently bound PtdIns3P embedded in liposomes (**Fig. 3A**). Mutation of R53 to cysteine significantly reduced binding of the PH domain to PtdIns3P, whereas mutations of R171 and R172 to alanine in the isolated FYVE domain blocked phosphoinositide binding (**Fig. 3A**). These results are in line with the proposed $KX_n(K/R)XR$ site for phosphoinositide binding in PH domains [35] represented by the sequence 49-KPKAR-53 in the Phafin2 PH domain. Likewise, R171 and R172 map within one of the consensus sites for PtdIns3P binding of FYVE domains, RR/KHHCR [26]. To determine and compare the affinities of the isolated PH domain with the FYVE domain and full-length Phafin2 for PtdIns3P binding, proteins were titrated with increasing concentrations of PtdIns3P-containing liposomes using the liposome sedimentation assay. This method is semi-quantitative, as it cannot detect transient interactions and consequently underestimates the binding affinity [36]. Interestingly, the Phafin2 PH domain bound PtdIns3P liposomes in a saturable fashion with an

apparent K_D of 11 μM (r^2=0.883), about two-fold stronger than that for the isolated Phafin2 FYVE domain (23 μM; r^2=0.951) (**Fig. 3B-C**) and full-length Phafin2 (20 μM; r^2=0.977) (**Supplementary Fig. 3A** and **Supplementary Fig. 4**). Phafin2 is primarily localized to endosomes, intracellular organelles that contain the highest levels of PtdSer [37]. In contrast to the FYVE domain, PH domains exhibit a broad preference for phospholipids [35]. Using the liposome sedimentation assay, we found that the Phafin2 PH domain bound PtdSer-containing liposomes with an apparent K_D of 31 μM (r^2=0.982) (**Supplementary Fig. 3B** and **Supplementary Fig. 4**), about 3-fold weaker than that estimated for PtdIns3P. Interestingly, Phafin2 very weakly bound PtdSer, and this was likely through the remaining binding activity of the PH domain as the FYVE domain did not bind PtdSer (**Supplementary Fig. 3C and D** and **Supplementary Fig. 4**). Altogether, these results indicate that the Phafin2 PH domain has a preference for binding to PtdIns3P over PtdSer. Also, our data suggest that the PH domain might interact with other membrane acidic lipids, such as PtdSer.

To obtain a more accurate quantification of the interactions, we performed SPR titrations of the proteins with immobilized PtdIns3P-embedded liposomes. The SPR kinetic analysis indicated that Phafin2 PH interacted with immobilized PtdIns3P liposomes but data could not be fitted due to the unusual shape of the sensorgrams (**Fig. 3D**). The Phafin2 FYVE domain, on the other hand, exhibited sharp association and dissociation curves with an apparent K_D for PtdIns3P of ~0.7 μM (**Fig. 3E**), a value close to that estimated for the full-length protein using the same methodology. This affinity value of Phafin2 FYVE for PtdIns3P is within the range of those estimated for other FYVE domains to the lipid [38].

We also investigated the PtdIns3P binding properties of both Phafin2 PH and FYVE domains for water soluble PtdIns3P using ITC. Phafin2 PH was unable to bind to PtdIns3P (**Fig. 3F**), in agreement with the observed lack of PtdIns3P binding of Phafin2 R171A/R172A using the same methodology (**Fig. 1E**). These results also indicate that the Phafin2 PH domain only binds to the phosphoinositide if it is embedded in a lipid bilayer. In this regard, the class II phosphoinositide 3-kinase C2α PX domain also binds PtdIns(4,5)P_2 only when the phosphoinositide is present in liposomes [39]. On the other hand, the Phafin2 FYVE domain bound PtdIns3P in an exothermically-driven process (**Fig. 3G**) with an apparent K_D of 2.74 μM, very close to that measured for the full-length protein (**Table 1**). Overall, our results

indicate that both PH and FYVE are PtdIns3P-binding domains and that the PH domain only recognizes the phosphoinositide when it is inserted into a lipid bilayer.

3.3. The acidic C-terminal motif of Phafin2 precludes PH domain binding to PtdIns3P

Our results indicate that mutations in the FYVE domain abolish binding of Phafin2 to PtdIns3P but the isolated PH domain is capable of interacting with a liposome-embedded lipid as strong as the isolated FYVE domain. We, therefore, thought that an internal region within Phafin2 might specifically block binding of its PH domain to PtdIns3P. Intramolecular interactions of the PH domain likely occur as Phafin2 is monomeric [5]. The internal region is not the FYVE domain as it does not directly interact with the PH domain (**Supplementary Fig. S5**). Analysis of the sequence alignment of the Phafin family of proteins identified a conserved C-terminal region containing a stretch of seven to eight aspartic acid residues (referred to as the polyD region; residues 240-249) (**Fig. 1A and 4A**). Deletion of this region (Phafin2 ΔpolyD) did not alter Phafin2 binding to PtdIns3P-containing liposomes (**Fig. 4B**). Mutation at R53 within the PH domain (Phafin2 R53C ΔpolyD) did not alter PtdIns3P binding (**Fig. 4B**), indicating that the FYVE domain is sufficient for Phafin2's lipid binding. Mutations of R171A/R172A (Phafin2 R171A/R172A ΔpolyD) mirrored the strength of binding to the phosphoinositide observed for the isolated PH domain (**Fig. 3A and 4B**), suggesting that the PH domain becomes functional in the absence of the C-terminal acidic motif. Consequently, combined mutations in the PH and FYVE domains of Phafin2 ΔpolyD (Phafin2 R53C/R171A/R172A ΔpolyD) significantly reduced PtdIns3P binding (**Fig. 4B**), as the R53C mutation in the isolated PH domain does not completely abolish lipid binding (**Fig. 3A**). Given that the Phafin2 PH domain showed higher apparent affinity for the lipid than the FYVE domain (**Fig. 3B-C**), our data explains why the PH domain, but not the FYVE domain, is autoregulated by the acidic C-terminal region.

Phosphorylation of Phafin2 has been reported at S16 (within the PH domain) [40] and at S239, S247, and S248 within the polyD region [41]. The apparent electrostatic interaction between the PtdIns3P-binding basic residues of the Phafin2 PH domain and the C-terminal polyD motif suggest that phosphorylation may disrupt this interaction. Alternatively, binding of Phafin2 to other protein partners, such as AKT1 [6], may release the PH domain of Phafin2 from the polyD region.

Given that the PH domain is specifically autoregulated in Phafin2, we anticipate that the FYVE and PH domains exhibit distinct activities in the protein despite both binding PtdIns3P. Indeed, a Phafin2 construct lacking the PH domain is still able to associate to and promote the enlargement of endosomes, whereas the absence of the FYVE domain impairs this activity [10]. This observation can also be extended to Phafin1 [12].

3.4. The FYVE domain in Phafin2 remains dominant for binding to soluble PtdIns3P independent of the presence of the C-terminal acidic motif

We next evaluated the role of the C-terminal polyD region for Phafin2 recognition to soluble PtdIns3P. ITC analysis for the interaction of Phafin2 ΔpolyD was indistinguishable from the wild-type protein (**Fig. 1C and 5A**), suggesting that the poly aspartic acid residues do not influence the strength of binding of Phafin2 for soluble PtdIns3P (**Table 1**). Also, these results show that the FYVE domain does not cooperate with the PH domain for binding to soluble PtdIns3P. The presence of an inactive FYVE domain in Phafin2 ΔpolyD was sufficient to abolish binding to soluble PtdIns3P (**Fig. 5B-C**). Overall, these data indicate that the FYVE domain of Phafin2 is constitutive for PtdIns3P, independent of the presence of the C-terminal polyD region.

4. Conclusions

In this report, we demonstrate that the Phafin2 PH and FYVE domains are regulated and constitutive, respectively, for binding to PtdIns3P. The Phafin2 FYVE domain indistinctly binds PtdIns3P when soluble or when embedded in liposomes, but binding is ~10-fold stronger when the phosphoinositide is embedded in a lipid bilayer. On the other hand, the Phafin2 PH domain only recognizes PtdIns3P when it is embedded in lipid bilayers.

Downregulation of Phafin2 PH domain binding to PtdIns3P is mediated by the C-terminal acidic motif of the protein, which is conserved within the Phafin family of proteins. As both the PH and FYVE domains bind PtdIns3P, the major question is why the PH domain is autoinhibited for PtdIns3P binding. In this scenario, the protein would still be able to bind to PtdIns3P-embedded membranes because of the presence of a constitutive FYVE domain. It is tempting to speculate that the PH domain of Phafin2 exhibits unique membrane binding properties, which are absent in its FYVE domain. For example, we show that the PH domain,

but not the FYVE domain, bind PtdSer. In addition, the PH domain of Phafin2 can share properties found in both FAPP2 and the Arfgap with Coil coil, Ankyrin Repeat, and PH domain protein 1 (ACAP1), which are capable of inducing membrane curvature in a PH domain- and phosphoinositide-dependent manner [42, 43].

Mechanisms that might promote release of the PH domain from the C-terminal acidic motif include potential phosphorylation sites, predicted by the PhosphoSitePlus database [44], which have been mapped in both the PH domain and the C-terminal acidic motif of Phafin2. For example, binding of the PH domain of the ceramide transfer protein to PtdIns4P is inhibited by hyperphosphorylation at an adjacent serine-repeat motif of the protein [45]. Alternatively, the interaction of Phafin2 with other proteins might promote a conformational change to expose its PH domain for PtdIns3P recognition. The protein Tectonin β-propeller repeat containing 1 (TECPR1) participates in autophagy by promoting autophagosome-lysosome fusion [46]. Binding of its PH domain to PtdIns3P is required for TECPR1 recruitment to autolysosomes, in a mechanism that depends on the initial binding of TECPR1 with the Atg12-Atg5 conjugate. In the absence of Atg12-Atg5, the PH domain of TECPR1 is intramolecularly inhibited by the AIR domain, suggesting that Atg12-Atg5-mediated conformational changes in TECPR1 are required for PtdIns3P binding [46]. Future studies to address how the PH domain is released from the autoinhibitory C-terminal acidic motif and what specific functions are conferred to Phafin2 are warranted to better understand why this protein exhibits two apparently redundant PtdIns3P-binding domains.

Acknowledgments

We thank Dr. Janet Webster for critical reading of the manuscript. This project was supported by the Virginia Academy of Sciences and the National Institutes for Health (**R01GM129525**) (D.G.S.C.) and the National Science Foundation (MCB-1517298) (C.V.F).

References

[1] S. Suetsugu, S. Kurisu, T. Takenawa, Dynamic shaping of cellular membranes by phospholipids and membrane-deforming proteins, Physiol Rev 94(4) (2014) 1219-48.

[2] K.O. Schink, K.W. Tan, H. Stenmark, Phosphoinositides in Control of Membrane Dynamics, Annu Rev Cell Dev Biol 32 (2016) 143-171.

[3] C.F. Bento, M. Renna, G. Ghislat, C. Puri, A. Ashkenazi, M. Vicinanza, F.M. Menzies, D.C. Rubinsztein, Mammalian Autophagy: How Does It Work?, Annu Rev Biochem 85 (2016) 685-713.

[4] M. Noguchi, N. Hirata, F. Suizu, The links between AKT and two intracellular proteolytic cascades: ubiquitination and autophagy, Biochim Biophys Acta 1846(2) (2014) 342-52.

[5] T.X. Tang, A. Jo, J. Deng, J.F. Ellena, I.M. Lazar, R.M. Davis, D.G. Capelluto, Structural, thermodynamic, and phosphatidylinositol 3-phosphate binding properties of Phafin2, Protein Sci 26(4) (2017) 814-823.

[6] M. Matsuda-Lennikov, F. Suizu, N. Hirata, M. Hashimoto, K. Kimura, T. Nagamine, Y. Fujioka, Y. Ohba, T. Iwanaga, M. Noguchi, Lysosomal interaction of Akt with Phafin2: a critical step in the induction of autophagy, PLoS ONE 9(1) (2014) e79795.

[7] H. Wang, W.T. Lo, V. Haucke, Phosphoinositide switches in endocytosis and in the endolysosomal system, Curr Opin Cell Biol 59 (2019) 50-57.

[8] S.N. Kariuki, Y. Ghodke-Puranik, J.M. Dorschner, B.S. Chrabot, J.A. Kelly, B.P. Tsao, R.P. Kimberly, M.E. Alarcon-Riquelme, C.O. Jacob, L.A. Criswell, K.L. Sivils, C.D. Langefeld, J.B. Harley, A.D. Skol, T.B. Niewold, Genetic analysis of the pathogenic molecular sub-phenotype interferon-alpha identifies multiple novel loci involved in systemic lupus erythematosus, Genes Immun 16(1) (2015) 15-23.

[9] A.M. Choi, S.W. Ryter, B. Levine, Autophagy in human health and disease, N Engl J Med 368(7) (2013) 651-62.

[10] W.J. Lin, C.Y. Yang, Y.C. Lin, M.C. Tsai, C.W. Yang, C.Y. Tung, P.Y. Ho, F.J. Kao, C.H. Lin, Phafin2 modulates the structure and function of endosomes by a Rab5-dependent mechanism, Biochem Biophys Res Commun 391(1) (2010) 1043-8.

[11] N.M. Pedersen, C. Raiborg, A. Brech, E. Skarpen, I. Roxrud, H.W. Platta, K. Liestol, H. Stenmark, The PtdIns3P-binding protein Phafin 2 mediates epidermal growth factor receptor degradation by promoting endosome fusion, Traffic 13(11) (2012) 1547-63.

[12] W.J. Lin, C.Y. Yang, L.L. Li, Y.H. Yi, K.W. Chen, Y.C. Lin, C.C. Liu, C.H. Lin, Lysosomal targeting of phafin1 mediated by Rab7 induces autophagosome formation, Biochem Biophys Res Commun 417(1) (2012) 35-42.

[13] I. Gailite, D. Egger-Adam, A. Wodarz, The phosphoinositide-associated protein Rush hour regulates endosomal trafficking in Drosophila, Mol Biol Cell 23(3) (2012) 433-47.

[14] K. Schink, Tan, K., Spangenberg, H., Martorana, D., Sneeggen, M., Campsteijn, S., Raiborg, C., and Stenmark, H., The PtdIns3P-binding protein Phafin2 escorts macropinosomes through the cortical actin cytoskeleton, bioxRxiv unpublished results (2017).

[15] M.A. Lemmon, K.M. Ferguson, Signal-dependent membrane targeting by pleckstrin homology (PH) domains, Biochem J 350 Pt 1 (2000) 1-18.

[16] J. Feng, L. He, Y. Li, F. Xiao, G. Hu, Modeling of PH Domains and Phosphoinositides Interactions and Beyond, Adv Exp Med Biol (2018).

[17] K. Scheffzek, S. Welti, Pleckstrin homology (PH) like domains - versatile modules in protein-protein interaction platforms, FEBS Lett 586(17) (2012) 2662-73.

[18] Z. Jiang, Z. Liang, B. Shen, G. Hu, Computational Analysis of the Binding Specificities of PH Domains, Biomed Res Int 2015 (2015) 792904.

[19] H. Teo, D.J. Gill, J. Sun, O. Perisic, D.B. Veprintsev, Y. Vallis, S.D. Emr, R.L. Williams, ESCRT-I core and ESCRT-II GLUE domain structures reveal role for GLUE in linking to ESCRT-I and membranes, Cell 125(1) (2006) 99-111.

[20] K. Chintaluri, B.D. Goulden, C. Celmenza, G. Saffi, E. Miraglia, G.R.V. Hammond, R.J. Botelho, The PH domain from the Toxoplasma gondii PH-containing protein-1 (TgPH1) serves as an ectopic reporter of phosphatidylinositol 3-phosphate in mammalian cells, PloS one 13(6) (2018).

[21] M.D. Tibbetts, E.N. Shiozaki, L. Gu, E.R. McDonald, 3rd, W.S. El-Deiry, Y. Shi, Crystal structure of a FYVE-type zinc finger domain from the caspase regulator CARP2, Structure 12(12) (2004) 2257-63.

[22] G. Eitzen, C.C. Smithers, A.G. Murray, M. Overduin, Structure and function of the Fgd family of divergent FYVE domain proteins (1), Biochem Cell Biol 97(3) (2019) 257-264.

[23] T.G. Kutateladze, Phosphatidylinositol 3-phosphate recognition and membrane docking by the FYVE domain, Biochimica et biophysica acta 1761(8) (2006) 868-77.

[24] J. He, M. Vora, R.M. Haney, G.S. Filonov, C.A. Musselman, C.G. Burd, A.G. Kutateladze, V.V. Verkhusha, R.V. Stahelin, T.G. Kutateladze, Membrane insertion of the FYVE domain is modulated by pH, Proteins 76(4) (2009) 852-60.

[25] T.X. Tang, W. Xiong, C.V. Finkielstein, D.G.S. Capelluto, Identification of lipid binding modulators using the protein-lipid overlay assay, Methods Mol Biol 1647 (2017) 197-206.

[26] T.G. Kutateladze, Translation of the phosphoinositide code by PI effectors, Nat Chem Biol 6(7) (2010) 507-13.

[27] J. He, R.M. Haney, M. Vora, V.V. Verkhusha, R.V. Stahelin, T.G. Kutateladze, Molecular mechanism of membrane targeting by the GRP1 PH domain, J Lipid Res 49(8) (2008) 1807-15.

[28] T.G. Kutateladze, D.G. Capelluto, C.G. Ferguson, M.L. Cheever, A.G. Kutateladze, G.D. Prestwich, M. Overduin, Multivalent mechanism of membrane insertion by the FYVE domain, J Biol Chem 279(4) (2004) 3050-7.

[29] L. Whitmore, B.A. Wallace, DICHROWEB, an online server for protein secondary structure analyses from circular dichroism spectroscopic data, Nucleic Acids Res 32(Web Server issue) (2004) W668-73.

[30] Y.K. Wang, W. Chen, D. Blair, M. Pu, Y. Xu, S.J. Miller, A.G. Redfield, T.C. Chiles, M.F. Roberts, Insights into the structural specificity of the cytotoxicity of 3-deoxyphosphatidylinositols, J Am Chem Soc 130(24) (2008) 7746-55.

[31] S. Gorai, S. Paul, G. Sankaran, R. Borah, M.K. Santra, D. Manna, Inhibition of phosphatidylinositol-3,4,5-trisphosphate binding to the AKT pleckstrin homology domain by 4-amino-1,2,5-oxadiazole derivatives, Medchemcomm 6(10) (2015) 1798-1808.

[32] M. Ludolphs, D. Schneeberger, T. Soykan, J. Schafer, T. Papadopoulos, N. Brose, H. Schindelin, C. Steinem, Specificity of collybistin-phosphoinositide interactions: Impact of the individual protein domains, J Biol Chem 291(1) (2016) 244-254.

[33] S.M. Kelly, T.J. Jess, N.C. Price, How to study proteins by circular dichroism, Biochim Biophys Acta 1751(2) (2005) 119-39.

[34] S.M. Kelly, N.C. Price, The use of circular dichroism in the investigation of protein structure and function, Curr Protein Pept Sci 1(4) (2000) 349-84.

[35] K. Moravcevic, C.L. Oxley, M.A. Lemmon, Conditional peripheral membrane proteins: facing up to limited specificity, Structure 20(1) (2012) 15-27.

[36] T. Wollert, Reconstituting multivesicular body biogenesis with purified components, Methods Cell Biol 108 (2012) 73-92.

[37] Y. Uchida, J. Hasegawa, D. Chinnapen, T. Inoue, S. Okazaki, R. Kato, S. Wakatsuki, R. Misaki, M. Koike, Y. Uchiyama, S. Iemura, T. Natsume, R. Kuwahara, T. Nakagawa, K. Nishikawa, K. Mukai, E. Miyoshi, N. Taniguchi, D. Sheff, W.I. Lencer, T. Taguchi, H. Arai, Intracellular phosphatidylserine is essential for retrograde membrane traffic through endosomes, Proceedings of the National Academy of Sciences of the United States of America 108(38) (2011) 15846-51.

[38] R.C. Wills, B.D. Goulden, G.R.V. Hammond, Genetically encoded lipid biosensors, Mol Biol Cell 29(13) (2018) 1526-1532.

[39] K.E. Chen, V.A. Tillu, M. Chandra, B.M. Collins, Molecular Basis for Membrane Recruitment by the PX and C2 Domains of Class II Phosphoinositide 3-Kinase-C2alpha, Structure 26(12) (2018) 1612-1625 e4.

[40] H. Zhou, S. Di Palma, C. Preisinger, M. Peng, A.N. Polat, A.J. Heck, S. Mohammed, Toward a comprehensive characterization of a human cancer cell phosphoproteome, J Proteome Res 12(1) (2013) 260-71.

[41] J.V. Olsen, M. Vermeulen, A. Santamaria, C. Kumar, M.L. Miller, L.J. Jensen, F. Gnad, J. Cox, T.S. Jensen, E.A. Nigg, S. Brunak, M. Mann, Quantitative phosphoproteomics reveals widespread full phosphorylation site occupancy during mitosis, Sci Signal 3(104) (2010) ra3.

[42] X. Cao, U. Coskun, M. Rossle, S.B. Buschhorn, M. Grzybek, T.R. Dafforn, M. Lenoir, M. Overduin, K. Simons, Golgi protein FAPP2 tubulates membranes, Proc Natl Acad Sci U S A 106(50) (2009) 21121-5.

[43] X. Pang, J. Fan, Y. Zhang, K. Zhang, B. Gao, J. Ma, J. Li, Y. Deng, Q. Zhou, E.H. Egelman, V.W. Hsu, F. Sun, A PH domain in ACAP1 possesses key features of the BAR domain in promoting membrane curvature, Dev Cell 31(1) (2014) 73-86.

[44] P.V. Hornbeck, B. Zhang, B. Murray, J.M. Kornhauser, V. Latham, E. Skrzypek, PhosphoSitePlus, 2014: mutations, PTMs and recalibrations, Nucleic Acids Res 43(Database issue) (2015) D512-20.

[45] T. Sugiki, D. Egawa, K. Kumagai, C. Kojima, T. Fujiwara, K. Takeuchi, I. Shimada, K. Hanada, H. Takahashi, Phosphoinositide binding by the PH domain in ceramide transfer protein (CERT) is inhibited by hyperphosphorylation of an adjacent serine-repeat motif, J Biol Chem 293(28) (2018) 11206-11217.

[46] D. Chen, W. Fan, Y. Lu, X. Ding, S. Chen, Q. Zhong, A mammalian autophagosome maturation mechanism mediated by TECPR1 and the Atg12-Atg5 conjugate, Mol Cell 45(5) (2012) 629-41.

Table 1. Thermodynamic parameters of binding of the indicated Phafin2 constructs to water soluble PtdIns3P. Values represent the mean of at least three independent experiments. Errors are shown as standard deviation values.

Phafin2 construct	K_D (μM)	ΔH (kcal. mol^{-1})	T ΔS (kcal. mol^{-1})	ΔG (kcal. mol^{-1})	N
Wild-type	3.21±1.06	-13.40±2.35	-5.90±2.55	-7.51±0.19	0.93±0.17
R53C/R171A/R172A	No binding	-	-	-	
R53C	3.34±0.73	-8.83±2.39	-1.35±2.48	-7.45±0.13	0.86±0.09
R171A/R172A	No binding	-	-	-	
PH	No binding	-	-	-	
FYVE	2.74±0.12	-22.20±1.41	-14.60±1.41	-7.59±0.03	0.94±0.04
ΔpolyD	2.61±0.67	-18.6±5.66	-10.96±5.66	-7.59±0.21	0.98±0.09
R171A/R172A ΔpolyD	No binding	-	-	-	
R53C/R171A/R172A ΔpolyD	No binding	-	-	-	

Figure Legends

Figure 1. The FYVE domain in Phafin2 is indispensable for PtdIns3P binding. (A) Modular organization of Phafin2. R53 (within the PH domain) and R171 and R172 (within the FYVE domain) are critical residues for PtdIns3P binding. (B) Liposome sedimentation assay of the indicated proteins with PtdIns3P-containing (top) and -free (bottom) liposomes. Quantification of the intensity of the protein bands was obtained by densitometry using Image J. Data represent the mean of three independent experiments; * $P < 0.001$, n.s., not significant; both as per one-way ANOVA analysis. (C-E) ITC analysis for the binding of the indicated proteins to water soluble PtdIns3P. The left panels depict the heat change produced upon successive injections of dibutanoyl PtdIns3P to the indicated proteins. The right panels display the integrated binding isotherms as a function of PtdIns3P/protein ratio. When applicable, binding isotherms were fitted to the subtracted data using the one-site binding model. Each ITC titration is representative of at least three independent experiments.

Figure 2. Structural analysis of the Phafin2 PH and FYVE domains. (A-B) Far- (A) and near-UV (B) CD spectra of the Phafin2 PH domain. (C-D) Far- (C) and near-UV CD (D) spectra of the Phafin2 FYVE domain.

Figure 3. Both isolated PH and FYVE domains exhibit distinct properties for PtdIns3P binding. (A) Left, liposome sedimentation assays of the indicated proteins with PtdIns3P-containing (top) and -free (bottom) liposomes. The panel is a representative of at least three independent experiments. Right, quantification of the intensity of the protein bands was obtained by densitometry using Image J. Data represent the mean ± SD of three experiments; * $P < 0.001$ as per one-way ANOVA; n.s., not significant. (B-C) Estimation of the apparent K_D using the liposome sedimentation assay. Relative bound Phafin2 PH (B) and FYVE domains (C) are plotted against effective PtdIns3P concentration. Error bars represent the standard deviation from three independent experiments. (D-E) SPR analysis for the binding of Phafin2 PH (D) and Phafin2 FYVE (E) domains for binding to immobilized PtdIns3P-containing liposomes. Each plot is representative of two independent experiments. (F-G) ITC analysis for the binding of Phafin2 PH (F) and FYVE (G) domains for binding to water soluble PtdIns3P. When applicable, binding isotherms were fitted to the subtracted data using the one-site binding model. Each titration is representative of three independent experiments.

Figure 4. The C-terminal acidic motif of Phafin2 downregulates PH domain binding to PtdIns3P. (A) Alignment of Phafin sequences corresponding to their C-terminal region. Sequences were aligned with Clustal Omega. Aspartic acid residues are shaded in salmon color. (B) Liposome sedimentation assays of the indicated proteins with PtdIns3P-containing (top) and -free (bottom) liposomes. The panel is a representative of three independent experiments. Quantification of the intensity of the protein bands was obtained by densitometry using Image J. Data represent the mean ± SD of three experiments; * $P < 0.005$ as per one-way ANOVA; n.s., not significant.

Figure 5. Removal of the C-terminal acidic motif in Phafin2 does not alter binding to soluble PtdIns3P. ITC analysis for the interaction of Phafin2 ΔpolyD (A), Phafin2 R171A/R172A ΔpolyD (B), and Phafin2 R53C/R171A/R172A ΔpolyD (C) with water soluble PtdIns3P. When applicable, binding isotherms were fitted to the subtracted data using the one-site binding model. Each titration is representative of at least three independent experiments.

Figure 1

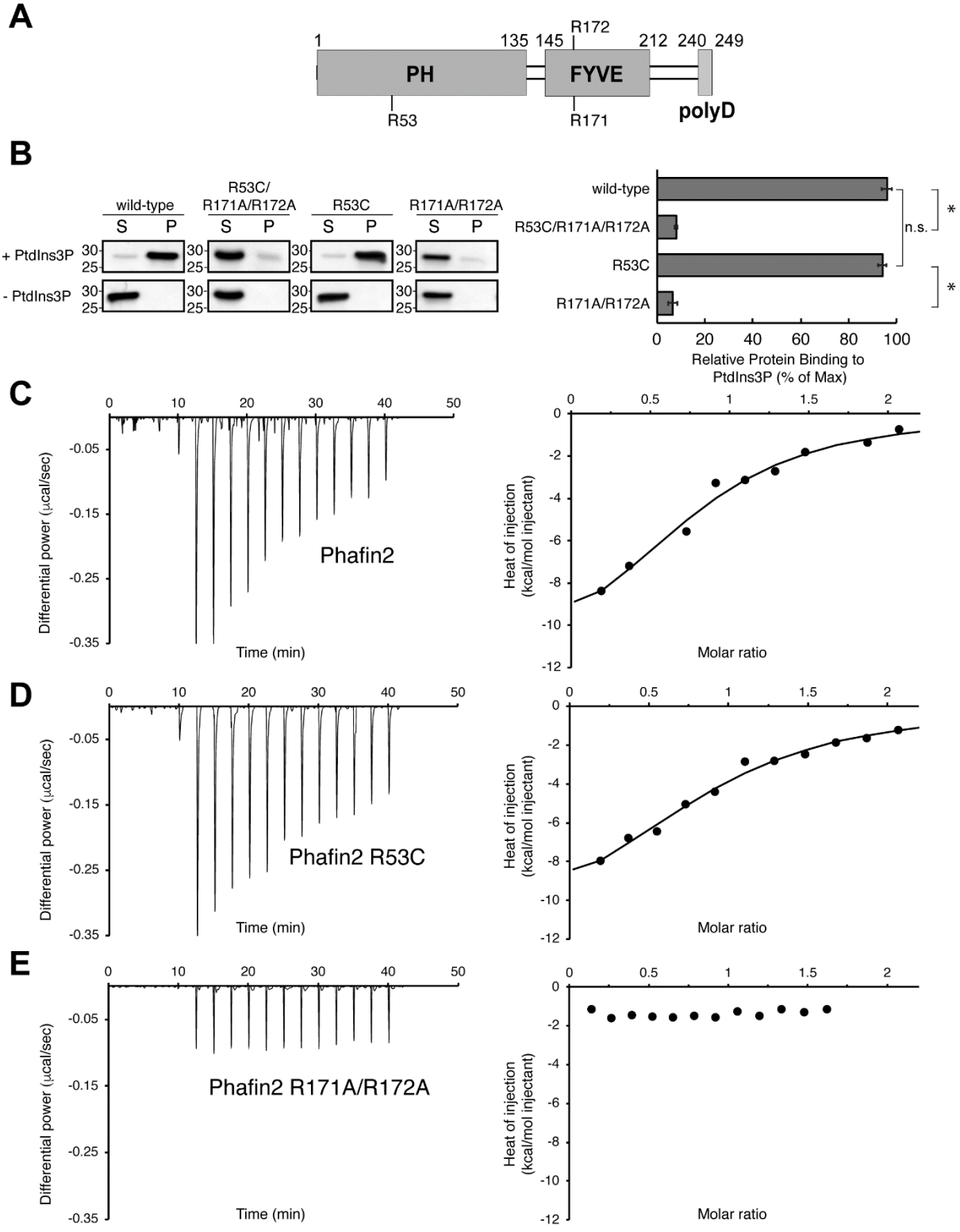
A
1
135 145
R172
212 240 249
PH
FYVE
polyD
R53
R171
B
wild-type
R53C/
R171A/R172A
R53C
R171A/R172A
S P
+ PtdIns3P
- PtdIns3P
30
25
wild-type
R53C/R171A/R172A
R53C
R171A/R172A
n.s.
*
*
0 20 40 60 80 100
Relative Protein Binding to
PtdIns3P (% of Max)
C
D
E
Differential power (µcal/sec)
Time (min)
Phafin2
Phafin2 R53C
Phafin2 R171A/R172A
Heat of injection
(kcal/mol injectant)
Molar ratio

Figure 2

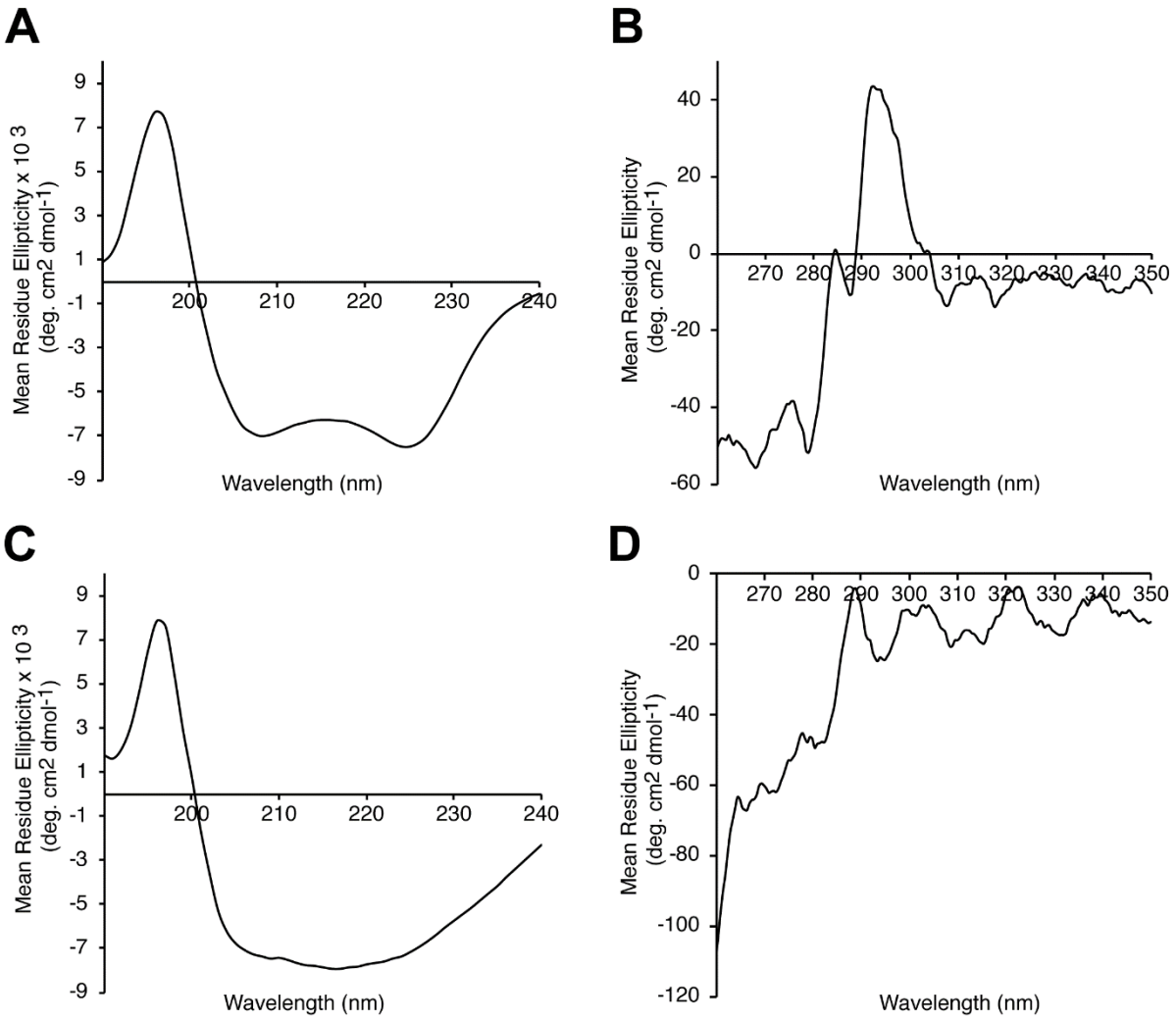
A
B
C
D
Mean Residue Ellipticity x 10 3
(deg. cm2 dmol-1)
Mean Residue Ellipticity
(deg. cm2 dmol-1)
Wavelength (nm)
9
7
5
3
1
-1
-3
-5
-7
-9
200
210
220
230
240
40
20
0
-20
-40
-60
270
280
290
300
310
320
330
340
350
-80
-100
-120

Figure 3

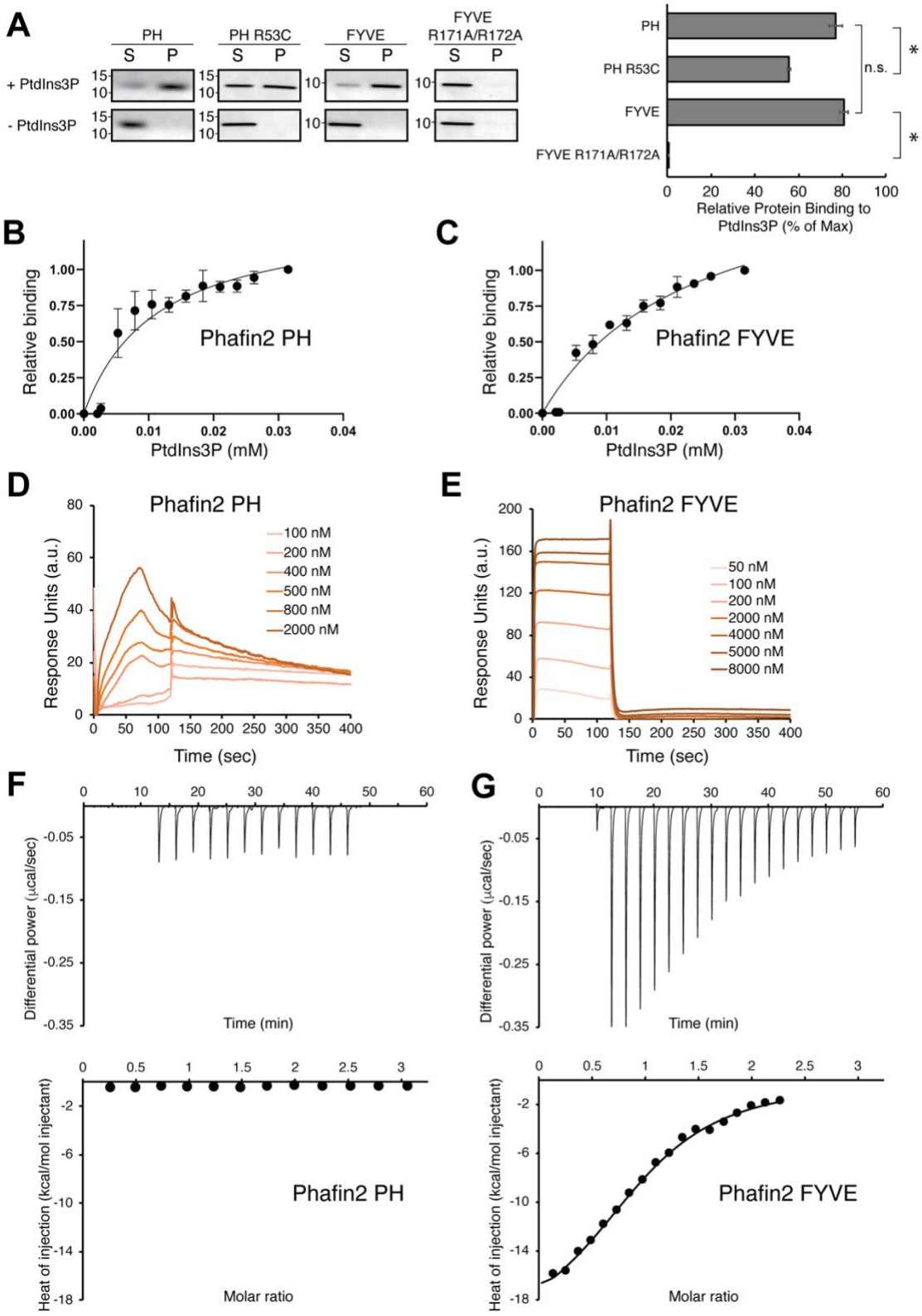
A
PH
PH R53C
FYVE
FYVE R171A/R172A
S P
+ PtdIns3P
- PtdIns3P
15
10
PH
PH R53C
FYVE
FYVE R171A/R172A
n.s.
*
*
0 20 40 60 80 100
Relative Protein Binding to PtdIns3P (% of Max)
B
Relative binding
Phafin2 PH
PtdIns3P (mM)
C
Relative binding
Phafin2 FYVE
PtdIns3P (mM)
D
Phafin2 PH
Response Units (a.u.)
100 nM
200 nM
400 nM
500 nM
800 nM
2000 nM
Time (sec)
E
Phafin2 FYVE
Response Units (a.u.)
50 nM
100 nM
200 nM
2000 nM
4000 nM
5000 nM
8000 nM
Time (sec)
F
Differential power (µcal/sec)
Time (min)
Heat of injection (kcal/mol injectant)
Phafin2 PH
Molar ratio
G
Differential power (µcal/sec)
Time (min)
Heat of injection (kcal/mol injectant)
Phafin2 FYVE
Molar ratio

Figure 4

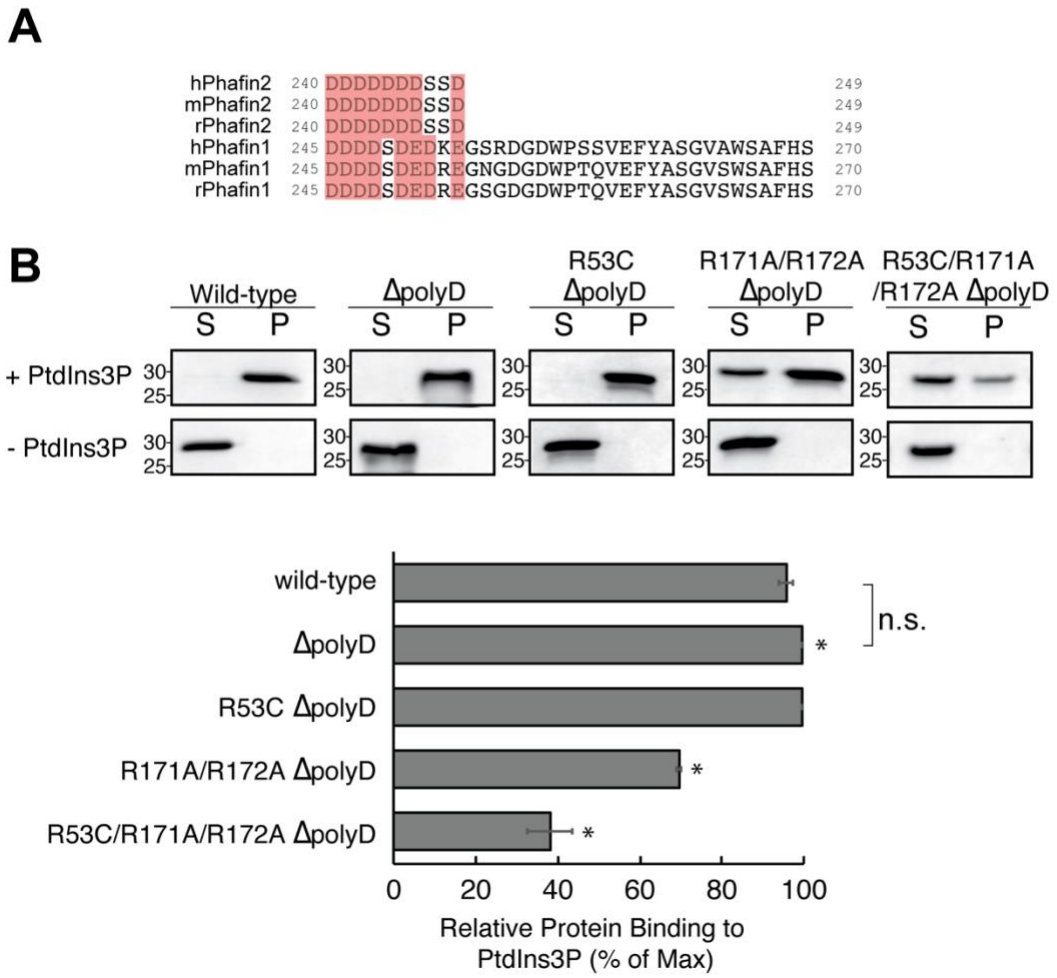
A
hPhafin2 240 DDDDDDDSSD 249
mPhafin2 240 DDDDDDDSSD 249
rPhafin2 240 DDDDDDDSSD 249
hPhafin1 245 DDDDSDEDKEGSRDGDWPSSVEFYASGVAWSAFHS 270
mPhafin1 245 DDDDSDEDREGNGDGDWPTQVEFYASGVSWSAFHS 270
rPhafin1 245 DDDDSDEDREGSGDGDWPTQVEFYASGVSWSAFHS 270
B
Wild-type
ΔpolyD
R53C ΔpolyD
R171A/R172A ΔpolyD
R53C/R171A /R172A ΔpolyD
S P
+ PtdIns3P
- PtdIns3P
30
25
wild-type
ΔpolyD
R53C ΔpolyD
R171A/R172A ΔpolyD
R53C/R171A/R172A ΔpolyD
n.s.
*
0 20 40 60 80 100
Relative Protein Binding to PtdIns3P (% of Max)

Figure 5

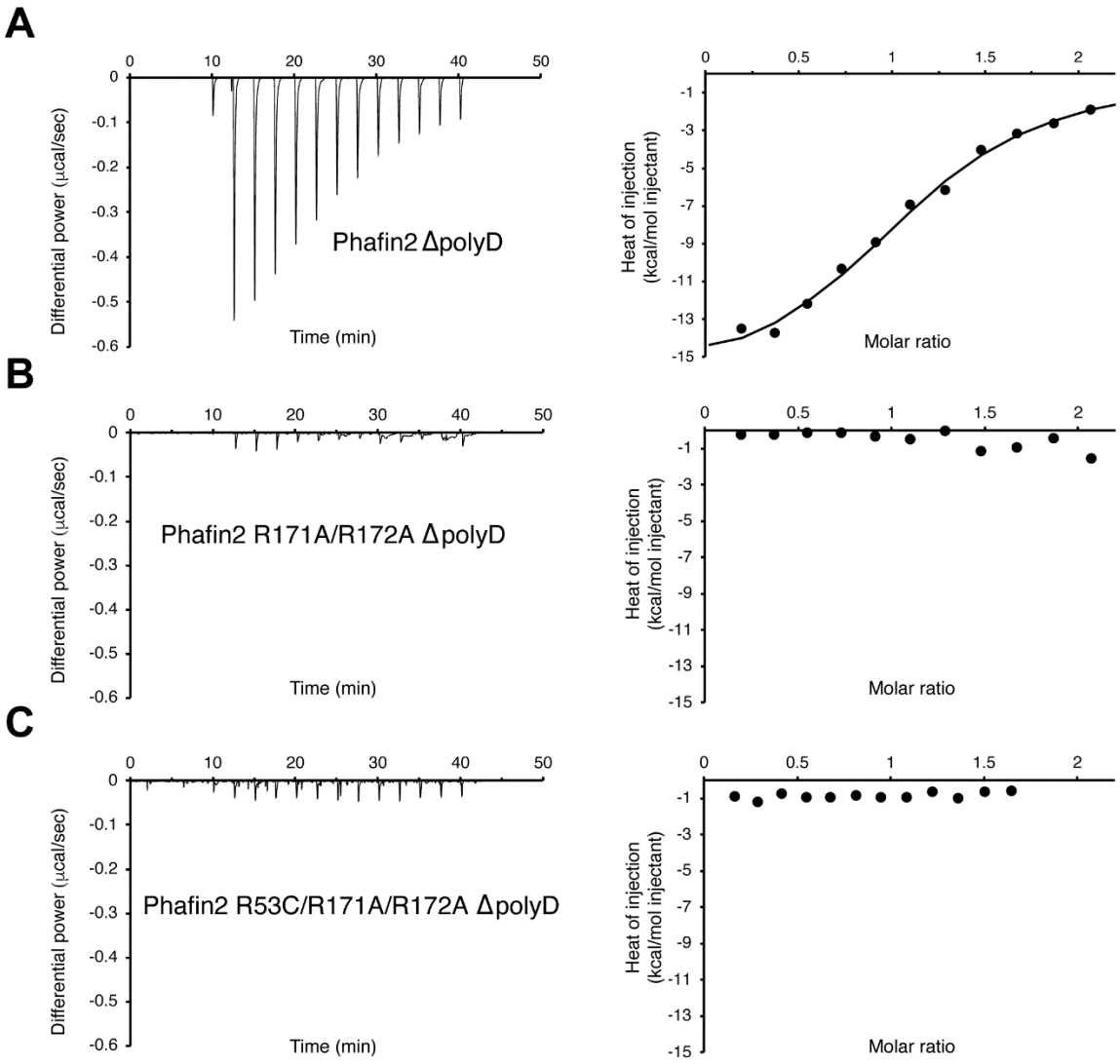
A
Differential power (µcal/sec)
Time (min)
Phafin2 ΔpolyD
Heat of injection (kcal/mol injectant)
Molar ratio
B
Phafin2 R171A/R172A ΔpolyD
C
Phafin2 R53C/R171A/R172A ΔpolyD

Supplementary information

The C-terminal acidic motif of Phafin2 inhibits PH domain binding to phosphatidylinositol 3-phosphate

Tuo-Xian Tang [a], Carla V. Finkielstein [b], and Daniel G. S. Capelluto [a,*]

[a] Protein Signaling Domains Laboratory, Department of Biological Sciences, Fralin Life Sciences Institute, and Center for Soft Matter and Biological Physics, Virginia Tech, Blacksburg, VA 24061, United States

[b] Integrated Cellular Responses Laboratory, Department of Biological Sciences, Fralin Life Sciences Institute, 1015 Life Science Circle, Virginia Tech, Blacksburg, VA 24061, United States

Supplementary Material and Methods

Intrinsic tryptophan fluorescence

Tryptophan fluorescence traces were collected using a Jasco J-815 spectropolarimeter. The excitation fluorescence was at 295 nm. The emission fluorescence spectra of Phafin2 (250 nM) were recorded in a buffer containing 5 mM sodium citrate and 50 mM KF (pH 7.3). Protein emission spectra, in the absence and presence of water-soluble PtdIns3P, were recorded between 310-410 nm using a 10-mm quartz cuvette at 25 °C. Data were analyzed using GraphPad Prism, version 8.

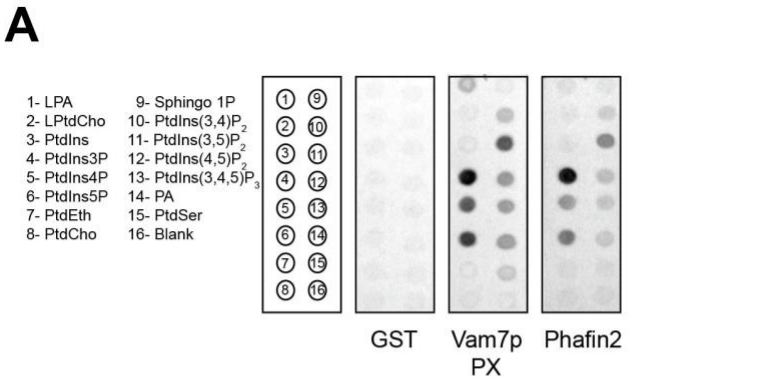
A
1- LPA
2- LPtdCho
3- PtdIns
4- PtdIns3P
5- PtdIns4P
6- PtdIns5P
7- PtdEth
8- PtdCho
9- Sphingo 1P
10- PtdIns(3,4)P2
11- PtdIns(3,5)P2
12- PtdIns(4,5)P2
13- PtdIns(3,4,5)P3
14- PA
15- PtdSer
16- Blank
GST
Vam7p PX
Phafin2

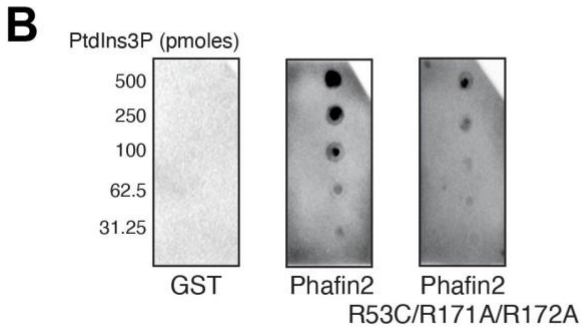
B
PtdIns3P (pmoles)
500
250
100
62.5
31.25
GST
Phafin2
Phafin2 R53C/R171A/R172A

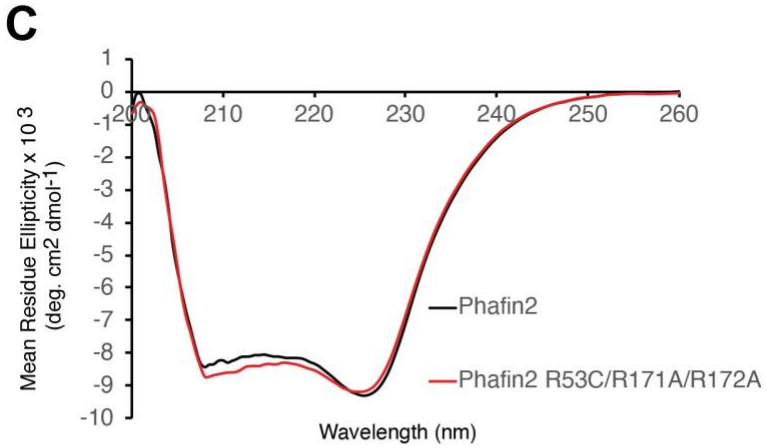
C
Mean Residue Ellipticity x 10 3 (deg. cm2 dmol-1)
Wavelength (nm)
Phafin2
Phafin2 R53C/R171A/R172A

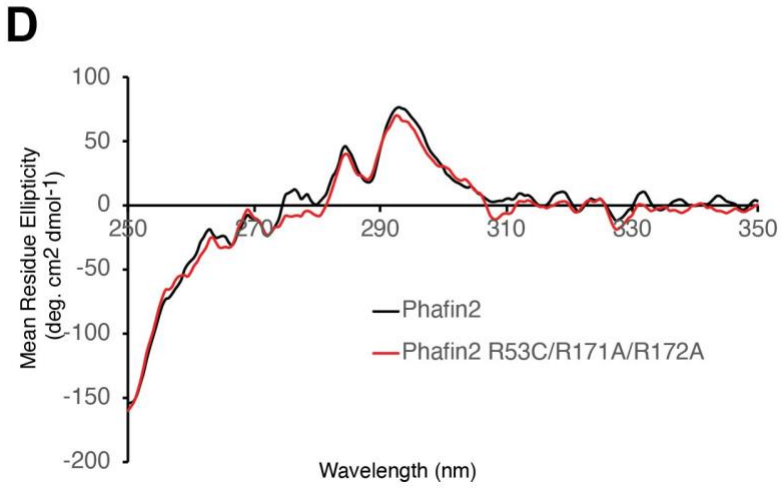
D
Mean Residue Ellipticity (deg. cm2 dmol-1)
Wavelength (nm)
Phafin2
Phafin2 R53C/R171A/R172A

Supplementary Figure S1. Role of key amino acids of Phafin2 for the interaction with PtdIns3P. (A) Lipid-protein overlay assay comparing the ability of Phafin2 and Vam7p PX domain to bind to phospholipids. (B) Lipid-protein overlay assay comparing the ability of Phafin2 and the Phafin2 R53C/R171A/R172A mutant to bind to PtdIns3P. GST was employed as a negative control. (C) Overlay of far-UV circular dichroism spectra for Phafin2 (black) and Phafin2 R53C/R171A/R172A (red). (D) Overlay of near-UV circular dichroism spectra for Phafin2 (black) and Phafin2 R53C/R171A/R172A (red).

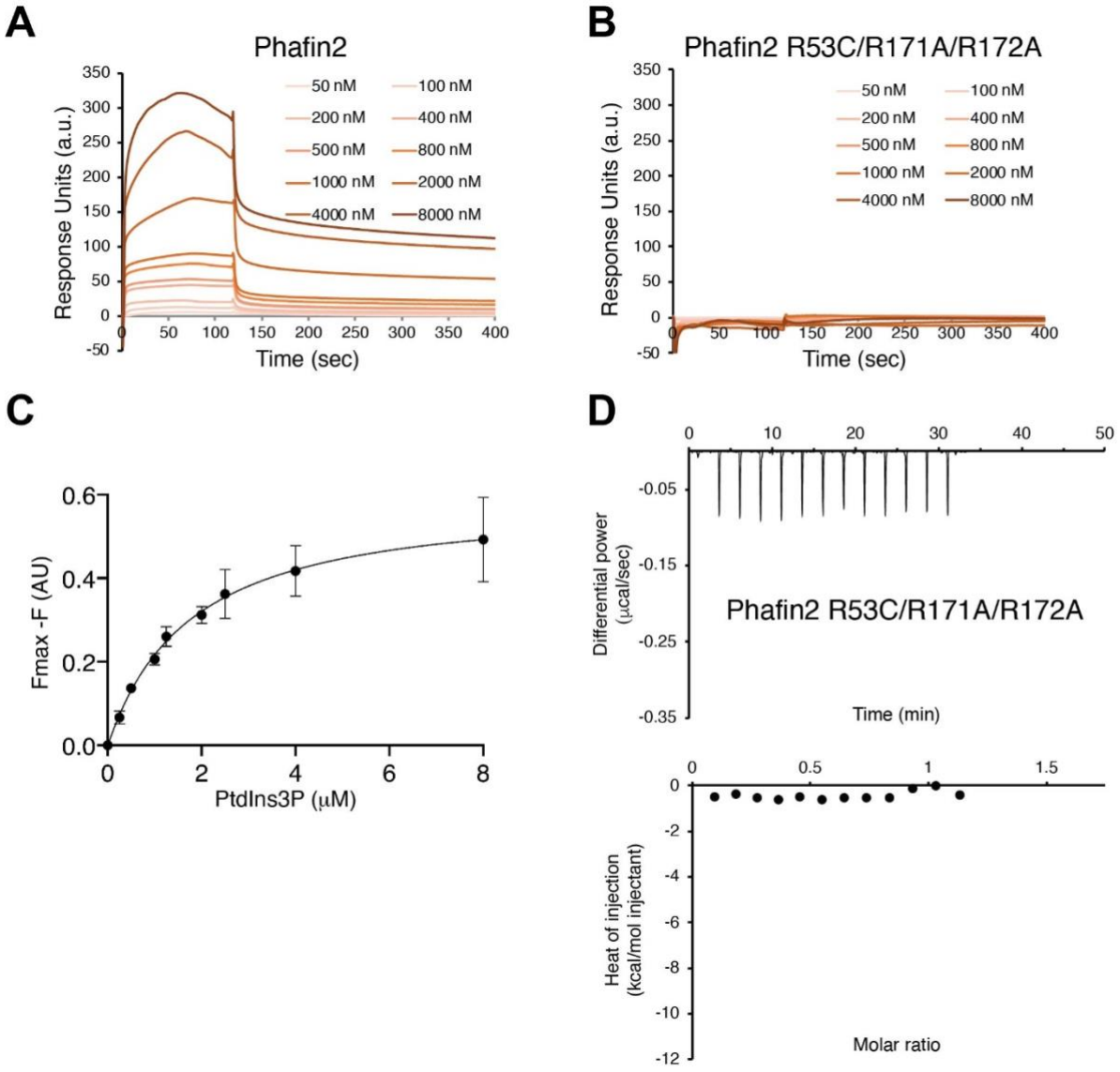

Supplementary Figure S2. Binding of Phafin2 to PtdIns3P in a lipid bilayer- and water-soluble forms. (A-B) SPR analysis for the binding of Phafin2 (A) and Phafin2 R53C/R171A/R172A (B) to immobilized PtdIns3P-containing liposomes. Each plot is representative of two independent experiments. (C) Plot representing fluorescence quenching of Phafin2 in the presence of increasing concentrations of PtdIns3P. (D) ITC analysis for the interaction of Phafin2 R53C/R171A/R172A with water-soluble PtdIns3P.

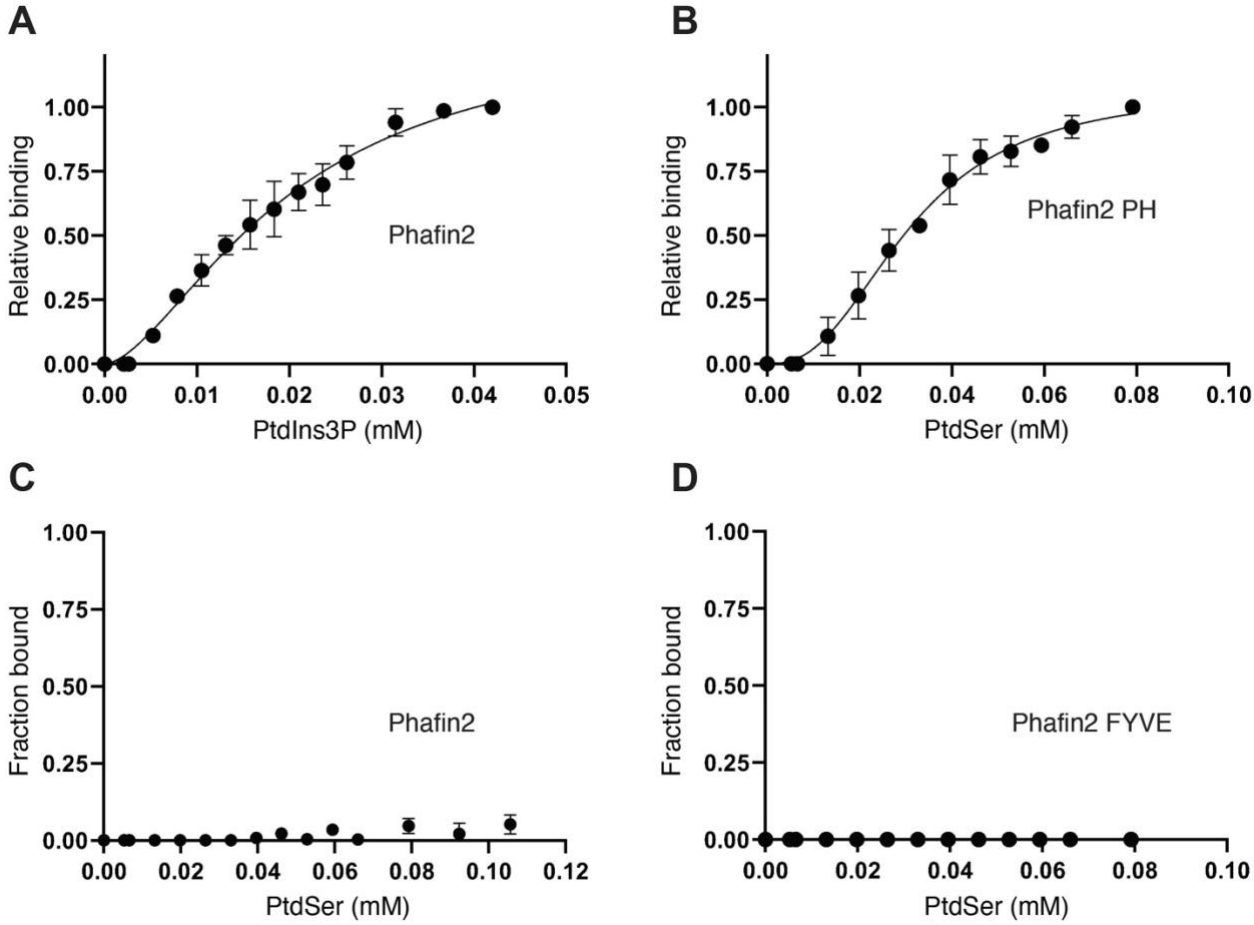

Supplementary Figure S3. Specificity and affinity of phospholipid binding using the liposome co-sedimentation assay. (A) Binding of Phafin2 to PtdIns3P liposomes. Bound Phafin2 is plotted as a function of the PtdIns3P concentration of the outer leaflet of the liposomes. (B) Binding of the Phafin2 PH domain to PtdSer liposomes. Bound Phafin2 PH domain is plotted as a function of the PtdSer concentration of the outer leaflet of the liposomes. (C) Binding of Phafin2 to PtdSer liposomes. Percentage of bound Phafin2 is plotted as a function of the PtdSer concentration of the outer leaflet of the liposomes. (D) Binding of Phafin2 FYVE domain to PtdSer liposomes. Percentage of bound Phafin2 FYVE domain is plotted as a function of the PtdSer concentration of the outer leaflet of the liposomes.

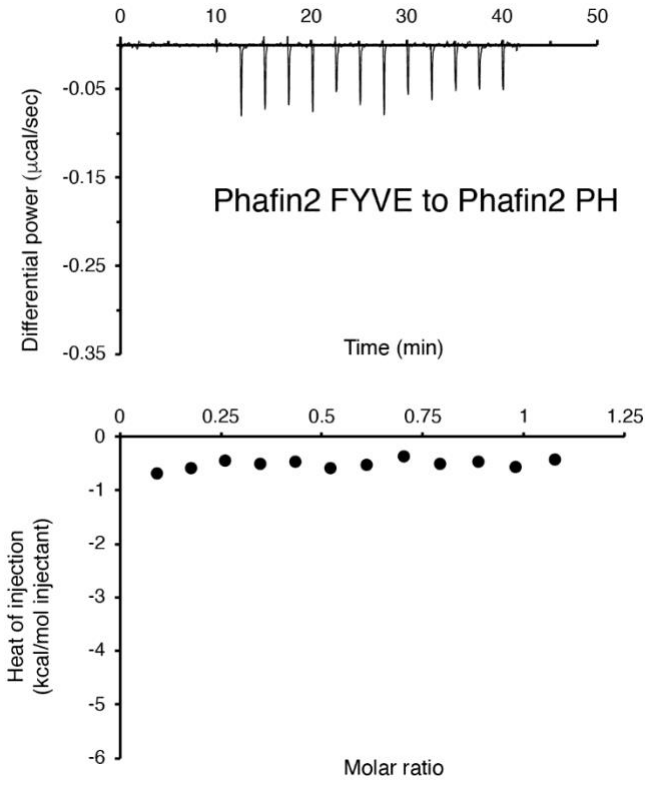

Supplementary Figure S4. Phafin2 FYVE domain does not interact with the Phafin2 PH domain. ITC analysis for Phafin2 FYVE domain injected to a solution containing Phafin2 PH domain.

Chapter 4 The C-terminal polyD motif of Phafin2 intramolecularly interacts with the PH domain

Tuo-Xian Tang and Daniel G. S. Capelluto

Abstract

The autoinhibition mechanism has been widely utilized in nature to regulate many protein functions, including kinase activity, transcription activation, and protein-ligand interactions. Phafin2 is a PH domain and FYVE domain-containing protein involved in endosomal cargo trafficking, macropinocytosis, and autophagy. Both Phafin2 PH and FYVE domains bind phosphatidylinositol 3-phosphate [PtdIns(3)P]. Phafin2 exhibits an intramolecular autoinhibition mechanism by which its C-terminal polyD motif blocks Phafin2 PH domain's PtdIns(3)P binding. Here, various biochemical and biophysical techniques were used to study interactions between the Phafin2 PH domain and a chemically synthesized polyD peptide. Phafin2 PH domain directly interacted with the polyD peptide with an estimated dissociation constant of ~4 μM. NMR studies showed that polyD peptide bound the Phafin2 PH domain, causing perturbations of a specific set of resonances on ^{1}H-^{15}N HSQC spectra. Phafin2 plays a role in autophagy, endosome fusion and tubulation of macropinosomes. We hypothesized that Phafin2 might induce membrane remodeling. Using negative-stain Transmission Electron Microscopy, we found Phafin2 caused membrane tubulation of PtdIns(3)P-containing liposomes. A PtdIns(3)P-interaction defective mutant of Phafin2, Phafin2 R53C/R171A/R172A, did not change the shape of PtdIns(3)P-containing liposomes, indicating that the tubulation activity is PtdIns(3)P-dependent. Future studies will focus on the role of Phafin2 PH and FYVE domains and potential regulatory functions of the polyD region in membrane tubulation.

1. Introduction

Autoinhibition plays an important role in regulating protein functions. Autoinhibitory mechanisms are found in many catalytic proteins (e.g., kinases) and non-catalytic proteins (e.g., adaptor proteins). Specifically, proteins utilize two molecular tricks to achieve autoinhibition: allosteric mechanism and direct blocking of active sites (catalytic or binding site). [1-2] Protein kinase B or Akt gives a prominent example of the first autoinhibitory mechanism. Structurally,

Akt has an N-terminal pleckstrin homology (PH) domain, a kinase domain (KD) in the middle, and a C-terminal hydrophobic motif (HM). In the inactive conformation, the PH domain negatively regulates Akt kinase activity by intramolecularly interacting with KD. Upon growth factor activation, PtdIns(3,4,5)P_3 levels increase on the plasma membrane, and Akt activation is initiated by association with PtdIns(3,4,5)P_3 via its PH domain. PtdIns(3,4,5)P_3 binding causes conformational changes in Akt, leading to its activation. Activated Akt is available for phosphorylation by two protein kinases, PDK1 (phosphoinositide-dependent protein kinase 1) and mTORC2 (mechanistic target of rapamycin complex 2), which phosphorylate Akt at Thr308 and Ser473, respectively. [3-5] The second autoinhibition mechanism is well represented by some transcription factors, such as the mitochondrial transcription factor 1 (Mtf1) and the transcription factor B2 mitochondrial (TFB2M). [6-7] Mtf1 and TFB2M have a flexible C-tail region comprising 16-20 amino acid residues. This C-tail motif autoinhibits the DNA binding activity of Mtf1 and TFB2M. Mtf1 deletion mutant lacking the entire C-tail region (residues 322-341) displays high DNA binding affinity. Structural analysis of TFB2M reveals that C-tail intramolecularly interacts with the DNA binding groove and abrogates its DNA binding activity. [6] Such autoinhibitory mechanisms provide a unique strategy to modulate protein functions. Autoinhibition can be relieved by several regulatory approaches, including post-translational modifications, binding to activating biomolecules, and irreversible proteolysis. Autoinhibitory mechanisms, in combination with their counteracting strategies, add one more dimension to the intracellular regulatory networks, which are essential for cell growth and homeostasis. In the pharmaceutical industry, autoinhibited proteins are potential targets for developing allosteric inhibitors. [1-2, 8]

Phafin2 is a PtdIns(3)P effector. It has two PtdIns(3)P binding domains, an N-terminal PH domain, followed by a central FYVE domain. Phafin2 serves as an adaptor protein in endosomal cargo trafficking [9], macropinocytosis [10-11], and autophagy [12]. PtdIns(3)P binding activity is critical to the recruitment of Phafin2 and its binding partners to a specific organelle. We have previously shown that the Phafin2 FYVE domain constitutively binds PtdIns(3)P, whereas the PH domain binding to PtdIns(3)P is blocked by the C-terminal polyD motif. [13] Intramolecular autoinhibition of PtdIns(3)P binding is possible in Phafin2 because of the following findings. First, Phafin2 is a monomeric protein, and it has a flexible C-terminal polyD tail. Second, Phafin2 has a large portion of random coil (~40%) in its structural elements [14], which might facilitate intramolecular interactions. This observation is consistent with that found in autoinhibited proteins, which are enriched in intrinsic disorder regions, especially in

their inhibitory domains. [15] Third, the negatively charged C-terminal polyD motif (eight aspartic acid and two serine residues) may electrostatically interact with the positively charged PtdIns(3)P-binding pocket in the PH domain. In this chapter, we describe the interactions between the Phafin2 PH domain and the C-terminal polyD motif by a variety of biophysical approaches. We found that the Phafin2 PH domain directly binds the Phafin2 polyD motif. We also explored the possibility that Phafin2 induces membrane remodeling. Phafin2 protein molecules promote the tubulation of PtdIns(3)P-embedded liposomes in a PtdIns(3)P dependent manner.

2. Materials and methods

2.1 Materials

The chemically synthesized polyD peptide from human Phafin2 (residues 240-DDDDDDDSSD-249) was purchased from Biomatik Corporation (Canada). Its identity was confirmed using Mass Spectroscopy (MS) and High Performance Liquid Chromatography (HPLC). The Formvar/Carbon (F/C) 200 mesh grids were obtained from Electron Microscopy Sciences (USA).

2.2 Protein expression and purification

The human full-length Phafin2 (residues 1-249) cDNA was cloned into a pGEX4T3 vector (Cytiva). Site-directed mutagenesis was used to generate the Phafin2 R53C/R171A/R172A mutant. cDNA encoding the Phafin2 PH domain (residues 1-135) was cloned into a pGEX6P1 vector, whereas the cDNA encoding the Phafin2 FYVE domain (residues 145-212) was cloned into a pGEX4T3 vector. Recombinant proteins were expressed in *Escherichia coli* (Rosetta; Stratagene) cells. The expression and purification procedures used in this chapter are similar to those previously reported. [13-14]

2.3 Tryptophan fluorescence

Intrinsic tryptophan fluorescence emission spectra of the Phafin2 PH domain (0.25 μM) were recorded at room temperature on a Jasco-815 spectropolarimeter. The prepared protein sample was in a buffer containing 5 mM sodium citrate and 50 mM KF (pH 7.3). Emission spectra with fluorescence excitation at 295 nm were scanned between 310 nm and 410 nm using a 10-mm quartz cuvette. Increasing concentrations of polyD peptide (2-30 μM) were titrated into the Phafin2 PH domain (0.25 μM). Data were analyzed using GraphPad Prism software,

version 8.

2.4 Isothermal titration calorimetry

Isothermal titration calorimetry (ITC) experiments were performed at 25 °C in 20 mM HEPES, pH 7.0, 100 mM NaCl, using a MicroCal PEAQ instrument (Malvern Panalytical Inc.). The polyD peptide was dissolved in the same buffer, and the resulting solution was adjusted to pH 7.0. The sample cell was filled with 45 μM Phafin2 PH or FYVE domains and titrated with 500 μM polyD peptide, which was placed in the syringe. A single injection of 0.4 μL of polyD peptide was followed by 12 injections of 3.0 μL each. The time interval between two successive injections was 120 s, and the stirring speed was 750 rpm. The raw titration results were adjusted by subtracting heat changes from the titrations of polyD peptide to buffer. The binding curve was fitted to a one-site binding model using the MicroCal PEAQ-ITC analysis software. The reported *K*d value was the average from three independent experiments.

2.5 Nuclear magnetic resonance spectroscopy

The ^{15}N-labeled Phafin2 PH domain (100 μM) was prepared in 90% H_2O, 10% D_2O, 20 mM d_{11}-Tris-HCl (pH 7.0), 100 mM NaCl, 1 mM d_{18}-DTT, and 1 mM NaN_3. NMR experiments were performed at 25 °C on a Bruker Avance III 600 MHz NMR spectrometer (Virginia Tech) equipped with a 5 mm z-gradient triple resonance probe. The polyD peptide was dissolved in the same buffer (stock concentration 2 mM) and adjusted to pH 7.0. ^{1}H-^{15}N HSQC (heteronuclear single quantum coherence) spectra were collected for the Phafin2 PH protein samples in the absence and presence of increasing concentrations of unlabeled Phafin2 polyD motif. Spectra were processed and analyzed using Mnova (Mestrelab Research).

2.6 Transmission electron microscopy

Liposomes were prepared as previously described. [13-14] The total lipid concentration was 0.2 mg/mL (95% DOPC (1, 2-dioleoyl-*sn*-glycero-3-phosphocholine)/5% PtdIns(3)P). The protein samples were prepared in the same buffer (20 mM HEPES, 100 mM NaCl, pH 7.0). For the negative-staining TEM grid preparation, equal volume (10 μL) of proteins (40 μM) and liposomes were incubated at room temperature for 10 min. Ten μL of the mixtures were subsequently placed on carbon-coated grids and stained with 2 % uranyl acetate for 1 min. The uranyl acetate solution was blotted by dry filter paper. The grids were examined using a JEM-2100 Electron Microscope (JEOL, Japan).

3. Results

3.1 Phafin2 PH domain binds the polyD motif

Phafin2 PH domain (135 amino acid residues) has two tryptophan residues (Trp100 and Trp122). Thus, it is a suitable candidate for intrinsic tryptophan fluorescence studies. Titrations of an increasing concentrations of the polyD peptide caused quenching of fluorescence emission in Phafin2 PH, Thus, one or both Trp residues become more exposed to the aqueous solution in the presence of the polyD peptide. (**Figure 1**) Fluorescence emission change reaches saturation as the concentration of polyD peptide increases, suggesting that the interaction is specific. The curve best fit to a one-site binding model with an estimated dissociation constant (K_D) of 4.21 ± 1.04 μM. Binding of Phafin2 PH to the polyD region was also investigated using ITC. Interactions between the Phafin2 PH domain and the polyD peptide were exothermic events. The enthalpy change (ΔH) for the binding of Phafin2 PH domain to polyD peptide was -3.25 kcal/mol. In agreement with the intrinsic tryptophan fluorescence data, the resulting isotherm best fits a one-site binding model with an estimated K_D of 4.14 ± 0.67 μM. (**Figure 2**) In contrast, the Phafin2 FYVE domain did not interact with the polyD region (**Figure 2**), indicating that this motif is specific for the PH domain. To identify the PH domain residues that interact with the polyD peptide, we initially titrated the ^{15}N-labeled Phafin2 PH domain with unlabeled polyD peptide and collected ^{1}H-^{15}N HSQC spectra for each peptide concentration. The overlay of ^{1}H-^{15}N HSQC spectra showed perturbations of some PH domain resonances. (**Figure 3**) Thus, using three independent methods, we show that the Phafin2 PH domain directly interacts with the polyD motif.

3.2 Phafin2 promotes liposomal tubulation in a PtdIns(3)P-dependent manner

Phafin2 is involved in endosome fusion and autophagy. We hypothesize that Phafin2 may cause changes in membrane shape, a pre-requisite for membrane fusion. We use extruded liposomes, which mimic lipid bilayers, of 100 nm composed by DOPC in the absence and presence of 5% PtdIns(3)P. Membrane interaction of Phafin2 was analyzed by transmission-electron microscopy (TEM) after incubating the protein with PtdIns(3)P-free (**data not shown**) or PtdIns(3)P liposomes (**Fig. 4A**). As opposed to that observed in PtdIns(3)P-free liposomes (**Fig. 4A**), data on PtdIns3P-embedded liposomes revealed that Phafin2 promotes the formation of ~250 nm tubules (**Fig. 4B-C**), consistent with the observed enlargement of endosomes induced by overexpression of Phafin2. [9] Proteins that promote membrane remodeling, such

as BAR domain-containing proteins, nuclear pore proteins, and clathrin adaptor proteins, form longer liposomal tubulations with lengths over the micrometer range under similar Phafin2 experimental conditions. [16] Thus, it is possible that additional contributions of ligand partners, such as AKT, might enhance the tubulation activity of Phafin2. In contrast, Phafin2 R53C/R171A/R172A mutant did not promote liposomal tubulation, indicating that this activity is PtdIns(3)P-dependent (**Fig. 4D**). Remarkably, individual Phafin2 PH domains simultaneously triggered many short projections throughout the surface of PtdIns(3)P liposomes (**Fig. 4E**), similar to those observed by the action of other unrelated proteins on liposomes. [17] Despite the fact that the individual Phafin2 FYVE domain did not show tubulation activity (**Fig. 4F**), data indicate that the FYVE domain, or other downstream regions in Phafin2, are required for tubulation activity.

4. Conclusions

In this chapter, we show that the polyD motif directly interacted with the Phafin2 PH domain. By using two independent methods, the measured affinity of binding was ~4.0 μM. Further evidence of direct binding of the polyD peptide to the Phafin2 PH domain is shown from NMR titrations, in which a set of resonances of the proteins was perturbed by the presence of the peptide. Future studies will focus on the resonance assignments of the Phafin2 PH domain, which will serve to identify the polyD binding site in the protein as well as to establish whether this site overlaps with that for PtdIns(3)P binding.

Our TEM experiments show that Phafin2 changed the shape of liposomes resulting in membrane tubulation in a PtdIns(3)P-dependent manner. Unlike FYVE domain, the isolated PH domain promoted short tubulations. We suspect that the PH domain is the driving force for Phafin2 to trigger changes in membrane shape, but it requires the integrity of the FYVE domain. The next step will be to establish the role of polyD motif in membrane tubulation and how much the serine/threonine kinase AKT contributes to this process.

References

[1] M. A. P. and B. J. Graves (2002). "Autoinhibitory Domains: Modular Effectors of Cellular Regulation." Annual Review of Cell and Developmental Biology 18(1): 421-462.

[2] Peterson, J. R. and E. A. Golemis (2004). "Autoinhibited proteins as promising drug

targets." Journal of Cellular Biochemistry 93(1): 68-73.
[3] Ebner, M., I. Lučić, T. A. Leonard and I. Yudushkin (2017). "PI(3,4,5)P3 Engagement Restricts Akt Activity to Cellular Membranes." Molecular Cell 65(3): 416-431.e416.
[4] Chu, N., A. L. Salguero, A. Z. Liu, Z. Chen, D. R. Dempsey, S. B. Ficarro, W. M. Alexander, J. A. Marto, Y. Li, L. M. Amzel, S. B. Gabelli and P. A. Cole (2018). "Akt Kinase Activation Mechanisms Revealed Using Protein Semisynthesis." Cell 174(4): 897-907.e814.
[5] Yudushkin, I. (2020). "Control of Akt activity and substrate phosphorylation in cells." IUBMB Life 72(6): 1115-1125.
[6] Basu, U., S.-W. Lee, A. Deshpande, J. Shen, B.-K. Sohn, H. Cho, H. Kim and S. S. Patel (2020). "The C-terminal tail of the yeast mitochondrial transcription factor Mtf1 coordinates template strand alignment, DNA scrunching and timely transition into elongation." Nucleic Acids Research 48(5): 2604-2620.
[7] Basu, U., N. Mishra, M. Farooqui, J. Shen, L. C. Johnson and S. S. Patel (2020). "The C-terminal tails of the mitochondrial transcription factors Mtf1 and TFB2M are part of an autoinhibitory mechanism that regulates DNA binding." Journal of Biological Chemistry 295(20): 6823-6830.
[8] Mol, C. D., D. R. Dougan, T. R. Schneider, R. J. Skene, M. L. Kraus, D. N. Scheibe, G. P. Snell, H. Zou, B.-C. Sang and K. P. Wilson (2004). "Structural Basis for the Autoinhibition and STI-571 Inhibition of c-Kit Tyrosine Kinase*." Journal of Biological Chemistry 279(30): 31655-31663.
[9] Pedersen, N. M., C. Raiborg, A. Brech, E. Skarpen, I. Roxrud, H. W. Platta, K. Liestøl and H. Stenmark (2012). "The PtdIns3P-Binding Protein Phafin 2 Mediates Epidermal Growth Factor Receptor Degradation by Promoting Endosome Fusion." Traffic 13(11): 1547-1563.
[10] Schink, K. O., K. W. Tan, H. Spangenberg, D. Martorana, M. Sneeggen, C. Campsteijn, C. Raiborg and H. Stenmark (2017). "The PtdIns3P-binding protein Phafin2 escorts macropinosomes through the cortical actin cytoskeleton." bioRxiv: 180760.
[11] Tan, K. W., V. Nähse, C. Campsteijn, A. Brech, K. O. Schink and H. Stenmark (2020). "JIP4 is recruited by the phosphoinositide-binding protein Phafin2 to promote recycling tubules on macropinosomes." bioRxiv: 2020.2009.2029.319111.
[12] Matsuda-Lennikov, M., F. Suizu, N. Hirata, M. Hashimoto, K. Kimura, T. Nagamine, Y. Fujioka, Y. Ohba, T. Iwanaga and M. Noguchi (2014). "Lysosomal Interaction of Akt with Phafin2: A Critical Step in the Induction of Autophagy." PLOS ONE 9(1): e79795.
[13] Tang, T.-X., C. V. Finkielstein and D. G. S. Capelluto (2020). "The C-terminal acidic motif of Phafin2 inhibits PH domain binding to phosphatidylinositol 3-phosphate." Biochimica

et Biophysica Acta (BBA) - Biomembranes 1862(6): 183230.
[14] Tang, T.-X., A. Jo, J. Deng, J. F. Ellena, I. M. Lazar, R. M. Davis and D. G. S. Capelluto (2017). "Structural, thermodynamic, and phosphatidylinositol 3-phosphate binding properties of Phafin2." Protein Science 26(4): 814-823.
[15] Trudeau, T., R. Nassar, A. Cumberworth, Eric T. C. Wong, G. Woollard and J. Gsponer (2013). "Structure and Intrinsic Disorder in Protein Autoinhibition." Structure 21(3): 332-341.
[16] Tanaka-Takiguchi, Y., T. Itoh, K. Tsujita, S. Yamada, M. Yanagisawa, K. Fujiwara, A. Yamamoto, M. Ichikawa and K. Takiguchi (2013). "Physicochemical Analysis from Real-Time Imaging of Liposome Tubulation Reveals the Characteristics of Individual F-BAR Domain Proteins." Langmuir 29(1): 328-336.
[17] Taneva, S. G., J. M. C. Lee and R. B. Cornell (2012). "The amphipathic helix of an enzyme that regulates phosphatidylcholine synthesis remodels membranes into highly curved nanotubules." Biochimica et Biophysica Acta (BBA) - Biomembranes 1818(5): 1173-1186.

Figures

Figure 1. Titrations of polyD peptide decreased fluorescence emissions of the Phafin2 PH domain. (**A**) Intrinsic tryptophan fluorescence emission spectra of Phafin2 PH domain in the absence and presence of increasing concentrations of the polyD peptide. (**B**) Quenching of the intrinsic tryptophan fluorescence as a function of ligand concentration for the polyD peptide.

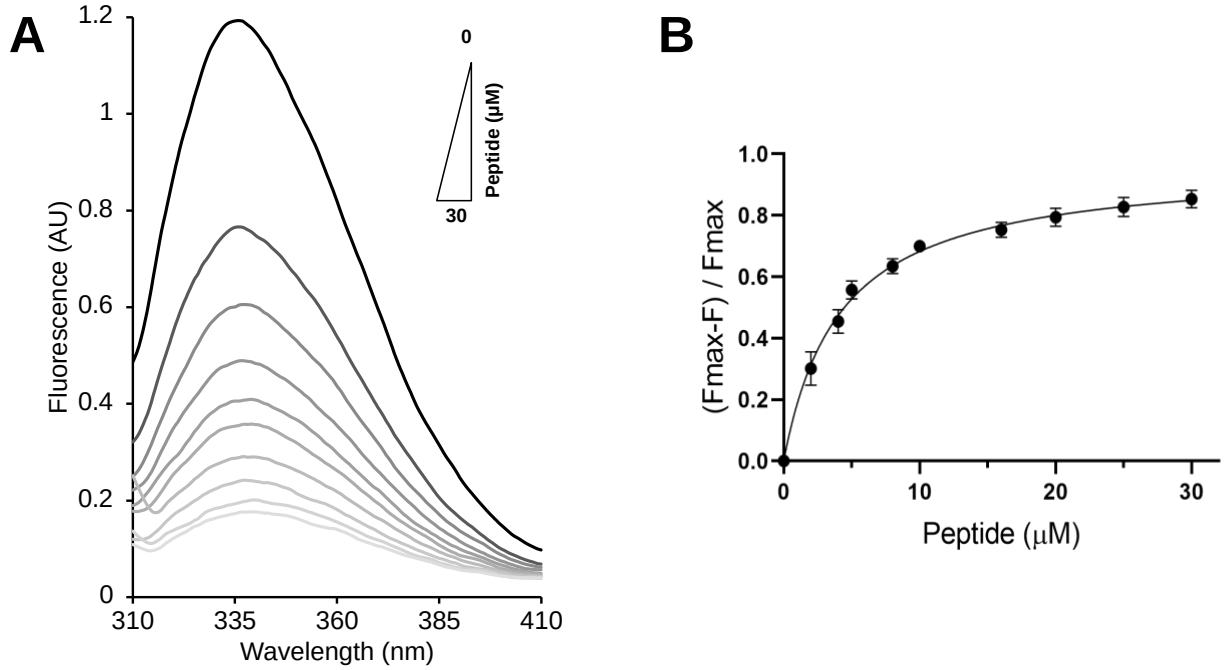

Figure 2. The Phafin2 polyD motif specifically interacts with the PH domain. The upper panel shows the ITC heat change upon serial injections of the polyD peptide into the Phafin2 PH and FYVE domains. The lower panel displays the integrated binding isotherm as a function of the polyD peptide/Phafin2 PH or Phafin2 FYVE domain ratio.

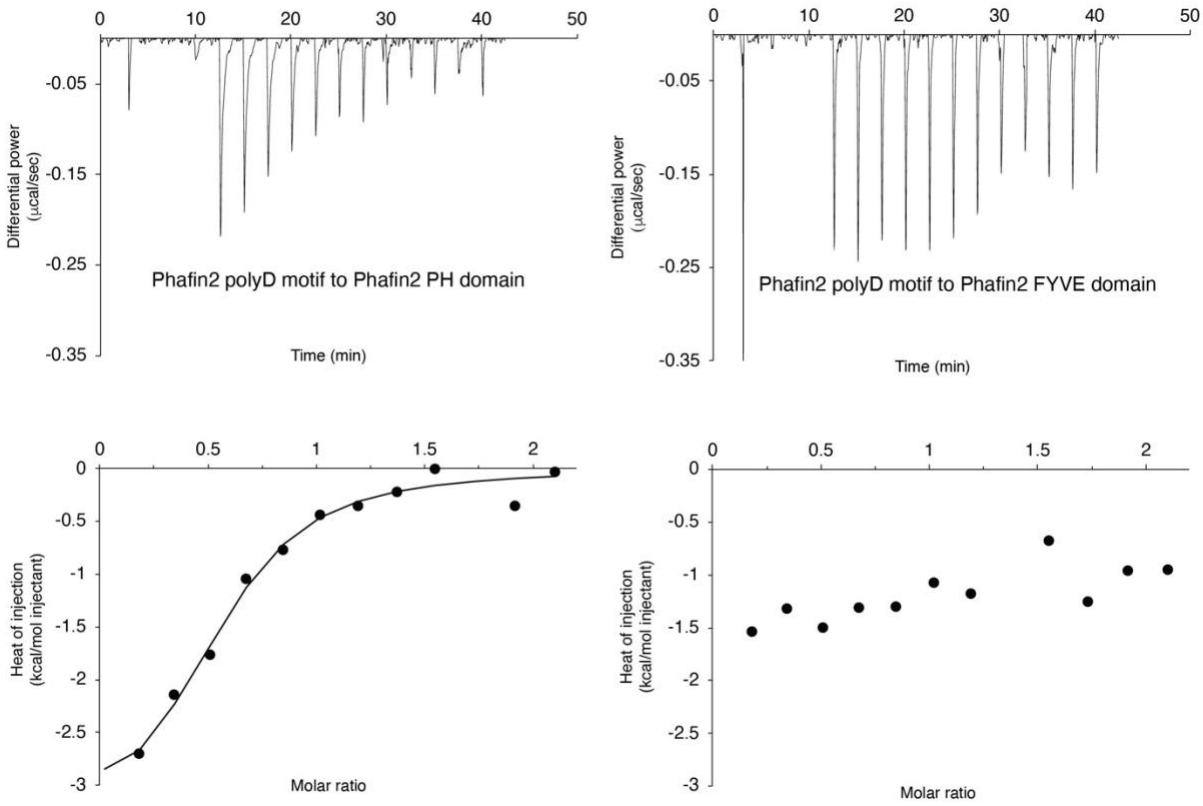

Figure 3. The superimposed ^{1}H-^{15}N HSQC spectra of the ^{15}N-labeled Phafin2 PH domain collected during step wise addition of the unlabeled polyD peptide. The spectra are color-coded: 100 μM ^{15}N-labeled Phafin2 PH domain (gray); addition of 200 μM polyD peptide (red); addition of 400 μM polyD peptide (green).

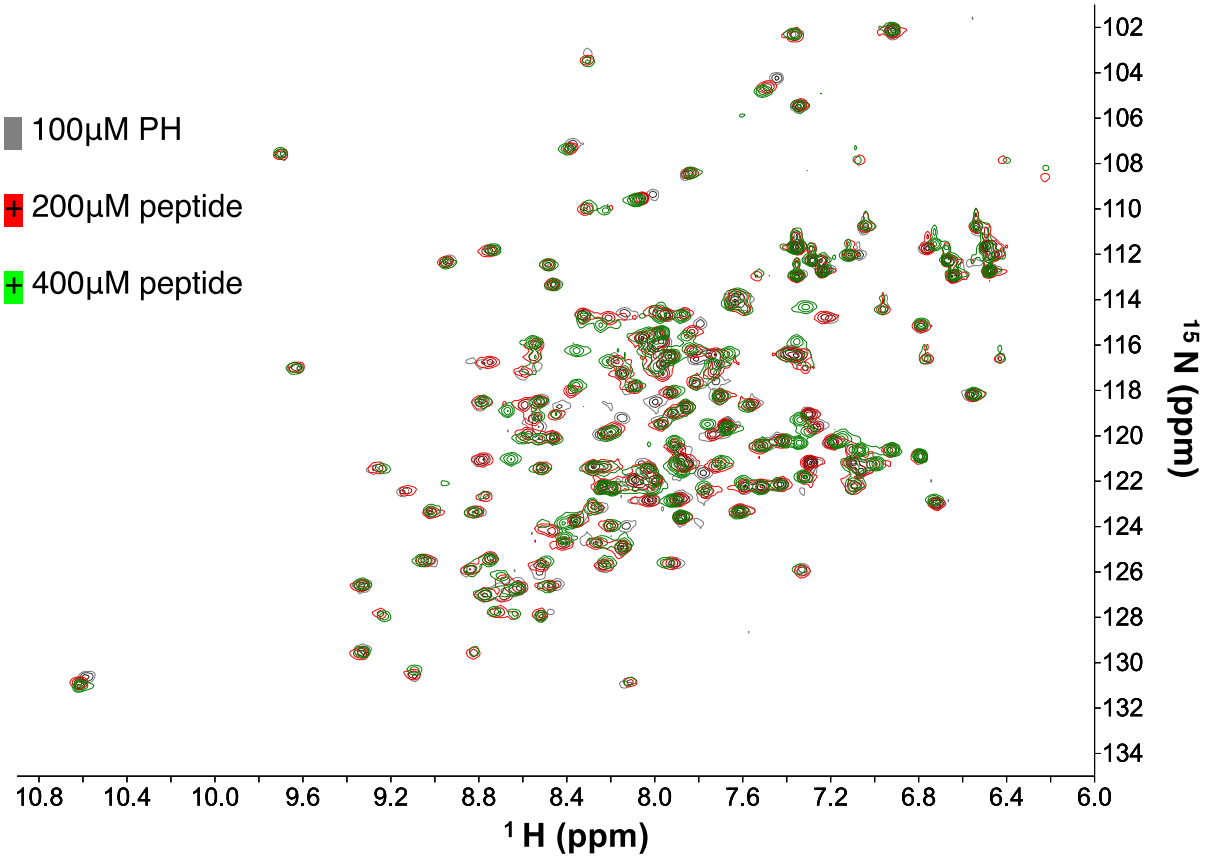

Figure 4. Phafin2 induces PtdIns(3)P-dependent liposomal tubulation. (**A**-**B**) TEM images of PtdIns(3)P-containing liposomes in the absence (**A**) and presence of 20 μM Phafin2 (**B**). (**C**) Zoom in of a region shown in (**B**). White arrowheads indicate the Phafin2-mediated tubulation of the liposomes. (**D**) TEM image of PtdIns(3)P-containing liposomes in the presence of 20 μM of the PtdIns(3)P-binding deficient mutant Phafin2 R53C/R171A/R172A. (**E**) TEM image of PtdIns(3)P-containing liposomes in the presence of 20 μM of the individual Phafin2 PH domain. White arrowheads show the presence of multiple short protrusions over the entire liposomal surface. Insets: Two zooms-ins of PH domain-mediated tubulations. (**F**) PtdIns(3)P-containing liposomes in the presence of 20 μM of the individual Phafin2 FYVE domain. Scale: 1 μm.

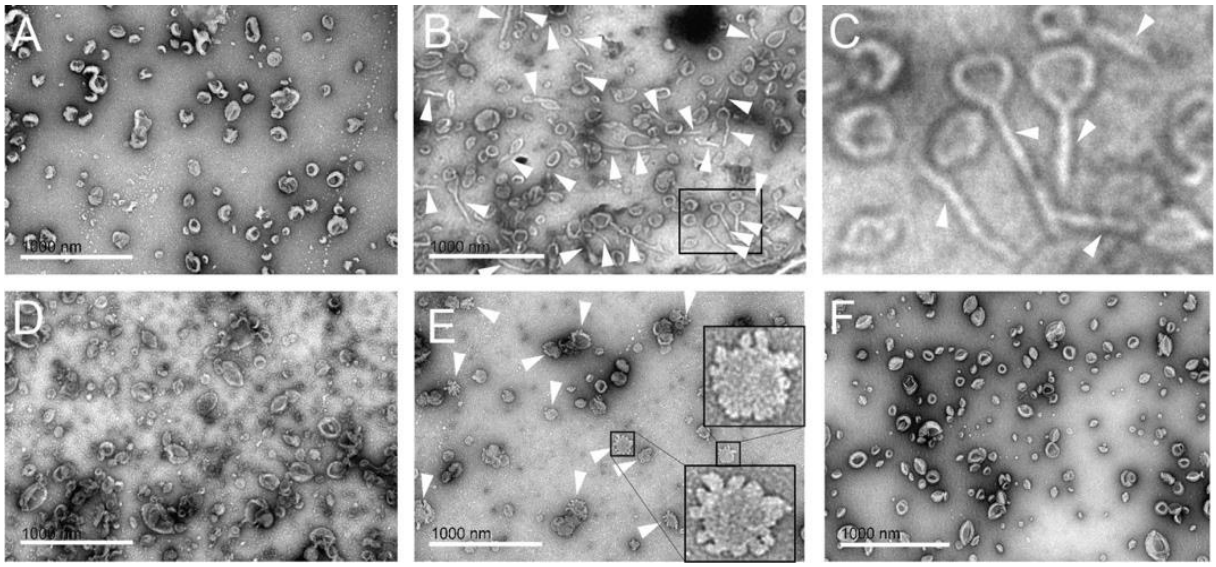

Chapter 5 Conclusions

In this dissertation, I show biophysical and biochemical studies of human Phafin2, a protein involved in many signaling pathways such as endosomal cargo trafficking, macropinocytosis, and autophagy. Phafin2 displays two PtdIns(3)P-binding domains, the PH and FYVE domains. I characterized structural features and biochemical properties of this protein and mainly focused on studying its interactions with PtdIns(3)P.

First, our structural analysis showed that monomeric Phafin2 is a typical α/β protein. It is predicted that a large portion of Phafin2 is random coil (~40%). Phafin2 preferentially binds PtdIns(3)P and weakly to PtdIns(4)P and PtdIns(5)P, which is presumably attributed to the PH domain. Titrations of dibutanoyl PtdIns(3)P did not influence the secondary structure of Phafin2 but cause local conformational changes in its tertiary structure. The estimated dissociation constant (K_D) PtdIns(3)P was 0.3 μM, which is comparable with other PtdIns(3)P-binding proteins and domains. [1-4] The structural modeling and sequence homology analysis showed conserved PtdIns(3)P binding motifs in the Phafin2 FYVE and PH domains. Based on these conserved binding sites, we designed a PtdIns(3)P-binding defective mutant, Phafin2 R53C/R171A/R172A (one mutation in the PH domain and two mutations in the FYVE domain), which reduced PtdIns(3)P binding without altering the overall structure of the protein.

Second, the Phafin2 FYVE and PH domains have different PtdIns(3)P binding properties. We found that the Phafin2 FYVE domain constitutively binds dibutanoyl PtdIns(3)P and PtdIns(3)P-containing liposomes. In contrast, the Phafin2 PH domain only binds PtdIns(3)P-containing liposomes. Initially, we studied PtdIns(3)P binding properties of each domain within the full-length Phafin2 and mutants. Surprisingly, the Phafin2 R171A/R172A mutant did not show PtdIns(3)P binding. In Phafin2, the R171A/R172A mutations completely abolished the FYVE domain's PtdIns(3)P binding ability, but the PH domain remained active. Therefore, we expected to observe a similar PtdIns(3)P binding strength with the Phafin2 PH domain. We then isolated the FYVE and PH domains, as well as their PtdIns(3)P-binding defective mutants. In ITC experiments, we were unable to detect binding signals when dibutanoyl PtdIns(3)P was titrated into the Phafin2 PH domain. It is possible that the Phafin2 PH domain cannot bind dibutanoyl PtdIns(3)P or binds dibutanoyl PtdIns(3)P with very low affinity because dibutanoyl PtdIns(3)P molecules are not organized in a lipid bilayer. Another possibility is that the Phafin2 PH domain binds dibutanoyl PtdIns(3)P, but their interactions

did not absorb or release heat. This result explains why the Phafin2 R171A/R172A mutant did not bind dibutanoyl PtdIns(3)P, but it did not answer why the Phafin2 R171A/R172A mutant did not bind PtdIns(3)P-containing liposomes. We then hypothesized that an internal region of Phafin2 might inhibit the binding of Phafin2 PH domain to PtdIns(3)P. We found a conserved C-terminal polyD motif in Phafin proteins, which may regulate the Phafin2 PH domain's PtdIns(3)P binding. This may explain why the Phafin2 R171A/R172A mutant did not bind PtdIns(3)P-containing liposomes. After the deletion of the C-terminal polyD tail (Phafin2 R171A/R172A ΔpolyD), Phafin2 PH domain's PtdIns(3)P binding ability was observed. Indeed, the Phafin2 R171A/R172A ΔpolyD showed a similar PtdIns(3)P binding strength to that measured for the Phafin2 PH domain. Analogously, the Phafin2 R53C/R171A/R172A ΔpolyD mutant mirrored the Phafin2 PH R53C's PtdIns(3)P binding strength.

Third, we demonstrated that the polyD peptide directly interacts with the Phafin2 PH domain. Intrinsic tryptophan fluorescence experiments showed that titrations of polyD peptide into the Phafin2 PH domain resulted in quenching of fluorescence emissions. The fluorescence changes reached saturation as the concentration of polyD peptides increased, indicating their specific interactions. Using ITC, the measured dissociation constant (K_D) is 4.0 μM, consistent with that measured using intrinsic tryptophan fluorescence. Titrations of polyD peptide into the ^{15}N-labeled Phafin2 PH domain gave rise to the resonance perturbations on the ^{1}H-^{15}N HSQC spectra, confirming their interactions. Ongoing research includes the backbone assignment of the Phafin2 PH domain with an aim to identify the amino acid residues that have direct interactions with the polyD peptide.

Moreover, we found that Phafin2 caused the membrane tubulation of PtdIns(3)P-containing liposomes. This membrane tubulation activity was a PtdIns(3)P-dependent event. Phafin2 did not change the shape of PtdIns(3)P-free liposomes, and the PtdIns(3)P-interaction defective mutant, Phafin2 R53C/R171A/R172A, failed to induce liposomal membrane remodeling. Compared with the full-length Phafin2, the isolated Phafin2 PH domain caused minor changes in the shape of PtdIns(3)P-containing liposomes. In contrast, the Phafin2 FYVE domain did not show the same effect. Therefore, we suspect that the Phafin2 PH domain displays membrane remodeling activity, which depends on other regions in the protein.

Our structural analysis and PtdIns(3)P binding studies of Phafin2 lay a solid foundation for future functional research on this protein. More importantly, the current study revealed that Phafin2 exhibits an autoinhibitory mechanism for PtdIns(3)P binding. This autoinhibitory mechanism may play a key role in regulating the functions of Phafin2 in several signaling pathways. It will be beneficial to identify which strategy the C-terminal polyD tail employs to intramolecularly autoinhibit the Phafin2 PH domain's PtdIns(3)P binding. The C-terminal polyD tail may directly interact and, consequently, compete with PtdIns(3)P for binding to the Phafin2 PH domain. Alternatively, the C-terminal polyD tail may exploit an allosteric mechanism by association to residues near the Phafin2 PH domain's PtdIns(3)P binding pocket, inducing local conformational changes and weakening PtdIns(3)P binding. Furthermore, it will an exciting research project to investigate how this autoinhibitory mechanism is relieved. Phosphorylation may be one of the strategies the cells utilize to counteract autoinhibition. Within the C-terminal polyD region, S248 is predicted to be a phosphorylation site. [5-6] Alternatively, activation of the Phafin2 PH domain by binding partners may be another mechanism to release the polyD region bound to the PH domain.

References

[1] Lawe, D. C., V. Patki, R. Heller-Harrison, D. Lambright and S. Corvera (2000). "The FYVE Domain of Early Endosome Antigen 1 Is Required for Both Phosphatidylinositol 3-Phosphate and Rab5 Binding: CRITICAL ROLE OF THIS DUAL INTERACTION FOR ENDOSOMAL LOCALIZATION*." Journal of Biological Chemistry 275(5): 3699-3705.

[2] Gaullier, J.-M., E. Rønning, D. J. Gillooly and H. Stenmark (2000). "Interaction of the EEA1 FYVE Finger with Phosphatidylinositol 3-Phosphate and Early Endosomes: ROLE OF CONSERVED RESIDUES*." Journal of Biological Chemistry 275(32): 24595-24600.

[3] Sun, F., S. D. Kale, H. F. Azurmendi, D. Li, B. M. Tyler and D. G. S. Capelluto (2013). "Structural Basis for Interactions of the Phytophthora sojae RxLR Effector Avh5 with Phosphatidylinositol 3-Phosphate and for Host Cell Entry." Molecular Plant-Microbe Interactions® 26(3): 330-344.

[4] Ridley, S. H., N. Ktistakis, K. Davidson, K. E. Anderson, M. Manifava, C. D. Ellson, P. Lipp, M. Bootman, J. Coadwell, A. Nazarian, H. Erdjument-Bromage, P. Tempst, M. A. Cooper, J. W. J. F. Thuring, Z. Y. Lim, A. B. Holmes, L. R. Stephens and P. T. Hawkins (2001).

"FENS-1 and DFCP1 are FYVE domain-containing proteins with distinct functions in the endosomal and Golgi compartments." Journal of Cell Science 114(22): 3991.

[5] Rigbolt, K. T. G., T. A. Prokhorova, V. Akimov, J. Henningsen, P. T. Johansen, I. Kratchmarova, M. Kassem, M. Mann, J. V. Olsen and B. Blagoev (2011). "System-Wide Temporal Characterization of the Proteome and Phosphoproteome of Human Embryonic Stem Cell Differentiation." Science Signaling 4(164): rs3.

[6] Olsen, J. V., M. Vermeulen, A. Santamaria, C. Kumar, M. L. Miller, L. J. Jensen, F. Gnad, J. Cox, T. S. Jensen, E. A. Nigg, S. Brunak and M. Mann (2010). "Quantitative Phosphoproteomics Reveals Widespread Full Phosphorylation Site Occupancy During Mitosis." Science Signaling 3(104): ra3.